

Cadmium Sulfide Solar Cells

A. G. STANLEY†

LINCOLN LABORATORY, MASSACHUSETTS INSTITUTE OF TECHNOLOGY
LEXINGTON, MASSACHUSETTS

I. Introduction	251
II. CdS-Cu _x S Photovoltaic Cell Structures	254
1. Single Crystal Photovoltaic Cells	254
2. Vapor Deposited Thin Film Photovoltaic Cells	255
3. Other Structures	265
III. Thin Film Solar Cell Technology	268
4. Vapor Deposition	268
5. Other Methods of Thin Film Preparation	281
6. Junction Formation	292
7. Counterelectrode	297
8. Lamination	298
IV. Properties of Cadmium Sulfide and Cuprous Sulfide Layers	299
9. Structure of Vapor Deposited CdS Films	299
10. Structure of Films Prepared by Other Techniques	308
11. Cuprous Sulfide Layer	313
V. Properties of CdS-Cu _x S Photovoltaic Cells	321
12. Spectral Response	321
13. Stability	326
14. Other Properties	332
VI. Mechanisms of the CdS-Cu _x S Photovoltaic Cell	336
VII. Other Photovoltaic Effects in CdS	340
15. Contact Photovoltage	340
16. Surface Photovoltage	346
17. Other Photovoltaic Devices	347
18. Anomalous Photovoltages	350
VIII. Conclusions	350
References	352

I. Introduction

Over the last two decades cadmium sulfide has found application as a semiconductor in many areas including photocells and other photoconduc-

† Present address: Jet Propulsion Laboratory of the California Institute of Technology, Pasadena, California.

tive devices, light amplifiers, image intensities, vidicons, phosphors and electroluminescent devices, radiation detectors, and more recently thin film transistors and diodes, piezoelectric ultrasonic transducers and amplifiers, piezoelectric acoustic resonators, and electron beam pumped lasers. This has stimulated an enormous interest in many laboratories throughout the world in the structural and electrooptical properties and in the overall physical chemistry of the material.

Important contributions in these areas were made at the Aerospace Research Laboratories (ARL) under the direction of D. C. Reynolds. The cadmium sulfide photovoltaic cell,^{1,2} which was discovered there in 1954, paved the way to the development of a practical thin film solar cell. The aim of such a device is to provide low cost, lightweight solar energy conversion with a potential for terrestrial applications. The weight advantage over silicon solar cells is mainly due to the ability to deposit the thin film onto a light, flexible substrate which can be self-deployed in space. Also, the devices are less susceptible to charged particle radiation damage and thus require less shielding. The lower weight of the semiconductor film itself is offset by decreased conversion efficiency.

The chief disadvantage in the utilization of silicon solar cells for terrestrial power generation is the high cost of silicon solar cell arrays, which includes not only the cost of cell fabrication, but also the expense of assembling large numbers of very small devices to cover a large area. It is, therefore, of interest to review other types of photovoltaic devices that might not suffer from these disadvantages.

It is evident that thin layer solar cells are superior to the standard silicon cells in this respect. They could be fabricated from cheaper polycrystalline materials, would require less semiconductor material, and could cover large areas, thus lowering the assembly costs. Also the production process would lend itself to automation. By this means it is hoped to realize substantial cost reductions in the manufacture of the arrays.

Such a system would require a flexible substrate to avoid breakage, a good match in the thermal expansion coefficients of the materials employed, and a stable transparent cover as protection. Conductors of large current carrying capacity are also needed.

Semiconductor materials must fulfill a number of requirements to qualify for thin film photoelectric applications. A large area film formed on a glassy or microcrystalline substrate is necessarily polycrystalline. This makes it impossible to produce p-n homojunctions of good quality due to preferential diffusion along the intercrystalline boundaries. One therefore has to revert either to heterojunctions or to surface barrier junctions. The former are more efficient, since electron-hole pairs generated by photons on either

TABLE I
COMPARISON OF PHOTOVOLTAIC CELLS*

	Single Crystal		Thin Film	
	Si	GaAs	CdS	CdTe
Type	IV	III-V	II-VI	II-VI
Band Gap	indirect	direct	direct	direct
Minimum Substrate Temp (°C)	1000	700-800	200-300	300-400
Junction	diffused p-n	surface barrier	heterojunction $\text{Cu}_2\text{S}-\text{CdS}$	surface barrier
Cutoff Wavelength (Å)	12,000	8750	10,500	8500
Short Circuit Current (mA/cm²)	34-40	21	34	24
Open Circuit Voltage (V)	0.57	0.50	0.50	0.58
Efficiency (%)	11.5	4.2	8.35	6.5
Fill Factor	0.78	0.57	0.69	0.65
Present Cost	\$60-80/watt bare cell	most expensive	\$45/watt	
Maximum Cell Area (cm²)	50	1	250	2

* Based on data by Crossley *et al.*³

side of the junction contribute to the cell output. Very good optical absorption is required, since the minority carrier lifetime in polycrystalline material is very short. The series resistance must be reduced to a minimum for large area cells. This usually presents a problem on the side of the junction facing the light. Finally, the deposition and subsequent processing temperatures should be low, so as to permit the use of plastic substrates.

It seems natural that the development of large area solar cell arrays would first of all be tried with silicon, the most successful photovoltaic material to date. However, the formation of single crystal layers requires very high substrate temperatures and slow growth rates, while polycrystalline material possesses very low conversion efficiencies.

Three other materials have also been investigated extensively as suitable for photovoltaic conversion of solar power. They are GaAs, CdS, and CdTe. All three materials have been used in the form of thin polycrystalline layers, and their most important properties are compared to those of silicon in Table I. GaAs was found to require an extremely complex technology, which made it very expensive to produce solar cells with reasonable efficiencies. CdTe solar cells possess a more complex structure than CdS while not showing any other advantages. Also, they are more unstable than the latter and suffer from contact problems. By a process of elimination CdS thus became the sole surviving thin film photovoltaic material.

Historically, the first photovoltaic effects in CdS related to the Becquerel effect and to contact photovoltages described in Section VII. Experiments by Reynolds¹ and others indicated that much larger photocurrents are generated at Cu-CdS contacts than with other metal systems. This resulted in the development of CdS-Cu₂S photovoltaic cells. Initially these were made using CdS single crystals. Subsequently ceramic and evaporated thin film cells were developed. All these structures are described in Section II. The thin film technology is outlined in Section III and the properties of the cadmium sulfide and cuprous sulfide layers in Section IV. The most important properties of CdS-Cu₂S photovoltaic cells are listed in Section V and mechanisms that have been proposed for their operation are reviewed in Section VI. The review concludes with an assessment of the prospects for future terrestrial applications in Section VIII.

II. CdS-Cu₂S Photovoltaic Cell Structures

1. SINGLE CRYSTAL PHOTOVOLTAIC CELLS

Reynolds^{1,2} discovered a strong photovoltaic response in CdS-Cu₂S rectifiers in May, 1954. A copper layer was electroplated onto an indium

doped, etched CdS crystal. The junction formation was completed by heating for 30 sec at 350°C. An efficiency of 1.5% was initially achieved.

After Reynolds' discovery work on the photovoltaic effect was initiated by ARL which included outside work at Harshaw Corporation. Hammond and Shirland⁴⁻⁶ were able to improve the efficiency beyond 5% by 1959. They investigated a number of methods of junction formation: (a) Cu electroplated and oxidized to Cu₂O, (b) deposition of Cu₂O from solvent slurry, (c) Cu evaporation and oxidation, (d) decomposition of copper acetate and oxidation to Cu₂O, and, (e) evaporation or solvent slurry of Cu₂S. All the initial cells were of the backwall construction, i.e., the light must penetrate the CdS crystal before reaching the junction. Hammond and Shirland constructed the first frontwall cells by etching away the excess Cu₂O material from the barrier, thus enabling the light to pass through the junction before the CdS.

Other single crystal constructions are listed in Table II. Williams and Bube¹³ made Cu-CdS cells with undiffused metal-semiconductor junctions. Bockemuehl¹⁴ diffused copper into photoconductive, dark insulating CdS. This produced two potential barriers, one at the surface and one in the bulk. This structure was unsuitable for photovoltaic effects.

Recent work on single crystal cells by Bube,^{21,26,27} Miya,²³ and Boer^{24,25} was carried out primarily to simplify the study of the photovoltaic properties of the CdS-Cu₂S system.

2. VAPOR DEPOSITED THIN FILM PHOTOVOLTAIC CELLS

The development of thin film CdS cells has been reviewed by Massie,²⁸ Shirland,^{29,30} Crossley *et al.*³ and by Perkins.³¹ The early history has been described by Komons.³²

The first polycrystalline CdS thin film photovoltaic cells were made by Carlson *et al.*^{33,34} at Clevite. Cells were constructed on glass and copper substrates in a frontwall and backwall configuration (see Table III). A thin film of Cu₂S was applied to the CdS film. Low temperature baking at 150 to 200°C was necessary to activate the barrier. The efficiency was less than 0.1% due to the high CdS bulk resistance. Attempts were made to reduce the resistance by heavy doping.

Gorski at Harshaw^{5,64} tried to reduce the series resistance by means of thicker vacuum deposited CdS films up to 100 μm. He adopted a silver paint grid to reduce the resistance of the Cu₂S layer. The barrier layer was formed by electroplated mossy copper that was air heated at 275°C.

The early cells suffered not only from a high series resistance. They also

TABLE II
SINGLE CRYSTAL CdS-Cu_xS PHOTOVOLTAIC CELLS

Reference	CdS Doping	Junction Formation	Ohmic Contact to CdS	Counter Electrode to Cu _x S	Efficiency	V _{oc} (V)	I _{sc} (mA/cm ²)	Construction
Reynolds ^{1,7-9}	In	electroplated Cu, diffused at 350 to 450°C	solder, Zn,Cu	Ag loaded epoxy	1.5 - 5%	0.4	15	backwall
Woods & Champion ¹⁰		Cu evap., heat at 600°C	In	Au		0.4	10	frontwall/backwall
Harshaw ⁴⁻⁶	In,Cl	Cu ₂ O, Cu electroplated* oxidation at 300-350°C	In,Zn,Rh	Ag paint, Cu,Au	5 - 7% 1 x 1 cm ²	0.5		backwall/frontwall
Avinor ¹¹	Ga	Cu evap., air heat at 400°C	In	Ag paste				
Ibuki ¹²	In	Cu, heat treatment	In			0.5	1	
Williams & Bubel ¹³	I	electroplated Cu, CuCl ₂ , CuSO ₄ , no heat	In			0.3	0.02	frontwall/backwall
Bockemuehl ¹⁴	photo-cond.	Cu evap., diffused at 400°C	In	Cu,Ag paint		0.2 - 0.6**	10 ⁻⁹ to 10 ⁻⁶ A	backwall
Paritskii ¹⁵		Cu plated, no heat						
Fabricius ¹⁶	Cu	Cu evap., heat at 300-400°C	In	Ag paste				
Grimmeiss ¹⁷	In,Ga	Cu evap., diffused at 600-700°C	Zn			0.63	8.5	frontwall

Clevite ¹⁸	Cu ₂ O slurry			7% 1.7 cm ²	0.5	
Duc Cuong ¹⁹	Cu evap.	In	Ag paint, Cu wire			
Selle ²⁰	evap. Cu ₂ S, 1 μm	In	Cu			backwall
Bube ²¹	CuCl dip, Cu ₂ S+NH ₄ OH, Cu in cyanide bath, heated at 250°C in air					
Shitaya ²²	electroplated Cu	In-Ga	Ag paint	0.42	3.2	backwall
Miya ²³	boiling CuCl	In	Au	S junction: 0.40-0.45 Cd junction: 0.50-0.60		
Boer ^{24, 25}	CuCl dip at 90°C	Ti/Al	Ag paint			frontwall/ backwall
Gill & Bube ²⁶ , Lindquist & Bube ²⁷	CuCl, hydroxylamine hydrochloride, KCl at 75°C	In	Au, Ag paint <3.6	0.45	4-6	frontwall

* A number of other methods, see text.

** Depends on wavelength.

TABLE
THIN FILM PHOTO

Year	Reference	Type	Substrate	Ohmic Contact to CdS	CdS Layer
a. Clevite					
1954-1958	Carlson ^{33,34}	frontwall	cond. glass	Ga,In	0.2-5 μm In doped
		backwall	Cu, oxidized	grid	0.2-10 μm
		backwall	cond. glass	SnO _x	0.2-10 μm
1963-1965	18,29,35-44	backwall	pyrex, H-film, 2 mil	metal film & mesh peripheral In contact	25-50 μm In doped
1965	29,43	backwall	H-film, 1 mil	Ag Pyr-M-L	50 μm In doped
1965	29,30,42,43	frontwall	Mo, 2 mil		25-50 μm, In doped
1965	29,43	frontwall	H-film, 1 mil	Ag Pyr-M-L, Zn	25-50 μm, In doped
1965	29,44,45	frontwall	Mo, 2 mil, Cu 1 mil		25-50 μm
1965	29,44,45	frontwall	H-film, 1 mil	Ag Pyr-M-L, Zn	25-50 μm
1965	46-48	frontwall	Mo, Cu	Zn plating	15-20 μm
1965	30,46-48	frontwall	H-film, 1 mil	Ag Pyr-M-L, Zn	15-20 μm
1966	49,50	frontwall	Mo,Cu	Zn plating	15-20 μm
1966	49,50	frontwall	H-film, 1 mil	Ag Pyr-M-L, Cr	15-20 μm
1966-1967	30,51-56	frontwall	Mo,Cu	Zn plating	15-20 μm
1966-1969	30,51-60	frontwall	H-film, 1 mil	Ag Pyr-M-L, Zn	15-20 μm
b. Harshaw					
1960-1962	5,61-64	backwall	glass	SnO _x , Ag, In	40-75 μm, InCl doped
1960-1962	62	frontwall	Mo foil, 1-5 mil		40-75 μm
1962-1965	65-73	frontwall	Mo foil, 1 mil	Zn	25 μm, undoped
1963-1965	70-72	frontwall	Ti, 1-2 mil	Ti	25-50 μm, undoped
1963-1965	70-72	frontwall	H-film, 1-2 mil	Au	25-50 μm, undoped
1965-1966	74,75	frontwall	Mo, 0.3 mil	Zn	20-25 μm, undoped
1967	76	frontwall	Mo, 0.3 mil	Zn	20-25 μm, undoped
c. RCA					
1960-1961	77-79	backwall	pyrex	SnO _x	<10 μm, In,Cl doped
1960-1962	100,189,3,30	backwall	H-film	Cr-Au, semitransp.	<10 μm
1960-1962	100,189,3,30	frontwall	H-film	Cr-Au, low resist.	<10 μm
1965	80	frontwall	H-film		
d. Others					
1958	Cabannes ⁸¹	backwall	Cu	In grid	2-10 μm
1961	Itek ^{82,83}	backwall/ frontwall	glass	SnO _x , Au	10-20 μm, 2 layers, donor, acceptor doped, air bake at 600°C
1962	Grimmeiss ⁸⁴	frontwall			Cu evap or Cu S, O ₂ anneal
1964	Drozdov ⁸⁵	backwall	Cu	Al	2-5 μm, In doped
1965	Pastel ^{86,87}	backwall	glass	SnO ₂	8-15 μm

III

VOLTAIC STRUCTURES

Barrier Formation	Counter Electrode to Cu ₂ S Material	Contact	Material	Adhesive	Efficiency	I _{sc}	V _{oc}
Cu ₂ O, Cu ₂ S air bake 200°C	SnO ₂				0.1%	10 ⁻⁵ -10 ⁻⁶ A	
Cu ₂ O, air bake					< 0.1%		
Cu ₂ S evap., air bake	In				< 0.1%		
Cu ₂ O slurry, bake at 250-300°C	evap. Ag, Au; Ag paint	pressure	Mylar, 1 mil	Capran Lamination	< 4% 3" x 3"		
Cu ₂ O slurry, bake at 250°C	Ag paint	pressure	Mylar, 1 mil	Capran Lamin.	< 3.5% 3" x 3"		
CuCl dip, heat at 250°C	electroformed Au mesh	pressure	Mylar, 1 mil	Capran Lamin.	3-5% 3" x 3"		
CuCl dip, heat at 250°C	electroformed Au mesh	pressure	Mylar, 1 mil	Capran Lamin.	2-3% 3" x 3"		
CuCl dip, heat at 250°C	electroformed Au mesh	Ag epoxy	Mylar, 1 mil	Capran Lamin.	5-7% 3" x 3"		
CuCl dip, heat at 250°C	electroformed Au mesh	Ag epoxy	Mylar, 1 mil	Capran Lamin.	4-7% 3" x 3"		
CuCl dip, heat at 250°C	electroformed Cu mesh	Ag epoxy	Mylar, 1 mil	Capran Lamin.	6-8% 3" x 3"	20-25 mA/cm ²	0.5V
CuCl dip, heat at 250°C	electroformed Cu mesh	Ag epoxy	Mylar, 1 mil	Capran Lamin.	4-7% 3" x 3"	175 mA/cm ²	0.5V
CuCl dip, heat at 250°C	electroformed Au mesh	Au epoxy	Mylar, 1 mil	Capran Lamin.	< 6.4% 3" x 3"		
CuCl dip, heat at 250°C	electroformed Au mesh	Au epoxy	Mylar, 1 mil	Capran Lamin.	3-4% 3" x 3"		
CuCl dip, heat at 250°C	Au plated Cu mesh	Au epoxy	Mylar, Kapton 1 mil	clear epoxy	4-6% 3" x 3"		
CuCl dip, heat at 250°C	Au plated Cu mesh	Au epoxy	Mylar, Kapton 1 mil	clear epoxy	4-6% 3" x 3"		
electroplated mossy Cu, air heat at 275°C	Ag paint				<1% to 4.95%	88 mA/cm ²	0.46V
1 cm ²							
electroplated mossy Cu, air heat at 275°C	Ag paint	pressure	Mylar, Kapton	Capran Lamin.	0.5 to 1.5%	3" x 3"	
CuCl dip, electrolytic Cu ₂ O, electroplated Cu	electroformed Au grid	pressure	Mylar, Kapton	Capran Lamin.	< 5% 3" x 3"		
CuCl dip, electroplated Cu	electroformed Au grid	pressure	Mylar	Capran Lamin.	< 3% 3" x 3"		
CuCl dip, electroplated Cu	electroformed Au grid	pressure	Mylar	Capran Lamin.	4.5% 3" x 3"		
CuCl dip, heat	electroformed Au grid	pressure	Mylar Kapton	Capran Lamin.	< 5% 3" x 3"	< 2.3% 3" x 3"	
CuCl dip, heat	Au plated Cu grid	Astrochem. cement	Mylar, Kapton 1 mil	epoxy	4% 3" x 3"		
Cu paint, heated to 300°C	Ag strips				<3.3% 1 cm ²	2.5-5 mA/cm ²	<0.5V
Cu paint, heated to 300°C	Ag paste				< 1%		
Cu treated layer	Ag paste				< 1%		
	electroformed grid				4.7-5.1%	10.8 cm ²	
Cu evap.&d.c. electric field	Cu				10 ⁻⁵ A		
Cu evap., 400°C air bake	evap. Au film						
Cu ₂ O, heated at 300°C	Cu				6 mA/cm ²	0.5V	
evap. Cu., 0.5-1 µm, heated at 300°C					2.5% 1-4 cm ²	2-8 mA/cm ²	

(continued)

TABLE

Year	Reference	Type	Substrate	Ohmic Contact to CdS	CdS Layer
1965	B.A.R.A. ⁸⁸	backwall	pyrex	SnO_x	
		frontwall	Al foil	Al	
		frontwall	H-film	Al, Au film, evap. Cr	
1965-1966	NCR ⁸⁹⁻⁹¹	backwall	glass	SnO_x	spray dep. 2 μm
		frontwall	plated steel, phosphor bronze, anodized Al	SnO_x	spray dep. 2 μm
1966	Balkanski & Choné ⁹²	frontwall	glass, Al foil, Kapton	Al, Au	20 μm
1966	Pavelet ⁹⁴ & Fedorus ⁹³	frontwall	Mo		sputtered, In & S doped
1967	Albrand ⁹⁴	frontwall	glass	In grid	5-10 μm
		backwall	glass		3-10 μm
1967-1970	S.A.T. ^{55,95-99}	frontwall	Kapton, 1,2 mil	Ag Pyr-M-L; Zn	25-35 μm
1968	Mytton ¹⁰⁰	frontwall	Mo		25 μm
1968	Egorova ¹⁰¹	frontwall/ backwall	cond. glass	SnO_x	15-15 μm
1968	Daspet ¹⁰²	frontwall	Kapton	metal	
1969	Anshon & Karpovich ¹⁰³	backwall/ frontwall	glass	CdO	1-3 μm
1970	David ¹⁰⁴	frontwall	Kapton	evap. Ag; Zn	20-30 μm
1970	AEG-Telefunken ^{105,106}	frontwall	Kapton, Mo	Ti-Pd-Ag; Zn	30-50 μm ; 30-60 $\Omega\text{-cm}$
1970	Clark, Ird. Co. ¹⁰⁷	frontwall	Kapton, 1 mil	Ag Pyr-M-L; Zn	15-20 μm
1970	Mickelsen ¹⁰⁸	frontwall	Kapton	NiCr-Cu-Cr, evap	> 25 μm
1973	U. of Delaware ^{109,110}	frontwall	Cu	Zn	

degraded on storage due to moisture and showed a lack of reproducibility in forming the active layer on the CdS and providing satisfactory electrical contacts. The subsequent development was carried out mainly by Harshaw and Clevite who maintained pilot lines, and initially by RCA as well (see table).

a. RCA

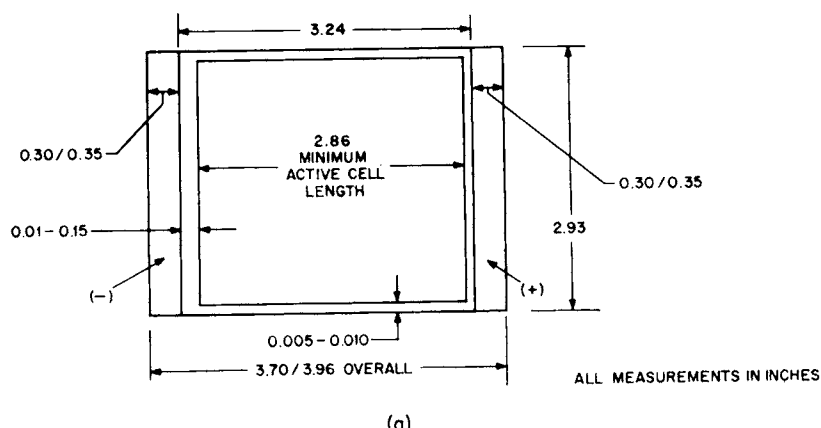
The most notable achievement of RCA⁷⁹ was to pioneer the use of Kapton in the form of H-film as a plastic substrate. This started the development of flexible, lightweight CdS solar cell arrays using frontwall illumination. Kapton is stable at higher temperatures and can, therefore, stand the deposition of CdS at an optimum temperature around 200°C.

III (continued)

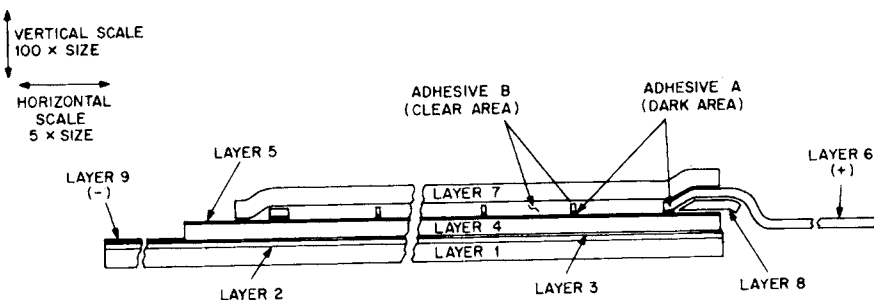
Barrier Formation	Counter Electrode to Cu ₂ S Material	Contact	Material	Adhesive	Efficiency	I _{sc}	V _{oc}
evap. Cu, 1500A + heat	Cu						
do	Au grid (Cr),				0.15-0.25%		
do	Cu grid	epoxy			0.10%		
spray deposited Cu ₂ S, 0.1 μm heat in air to 250° C					< 4% 1 cm ²		
do	Au plated Ni mesh, evap. Au grid				2% 1 cm ²		
evap. Cu & heat at 300°C (chloride)	evap Cu or Au grids		varnish		< 1.5%		
evap. Cu ₂ Cu ₂ S; no heat treatment							
CuCl					1%		
Cu or H ₂ S							
chemipl. CuCl at 90°C & heat	Au plated Cu grid	Au epoxy	Aclar	Kapton	7% 55 cm ² 5.1%		0.46V
chemipl. CuCl bake in air at 240°C	Cu grid					5-8mA/cm ²	0.4- 0.43V
chemipl. CuCl, heat							
chemipl.	metal grid	Ag epoxy			7%		
evap. Cu ₂ S, 0.1 μm	Cu				3% 1 cm ²		0.3-0.5V
chemipl. CuCl heat to 200°C, Cu ₂ S evap. & sputtered							
chemipl. CuCl	Au mesh, Au plated Cu grid		Teflon FEP		4-6% 4x4 cm ²		0.48-0.52V
Cu ion dip; 0.2 μm Cu ₂ S air bake at 250°C also CuCl evap.	Au plated Cu grid	Au epoxy	Kapton, Aclar				
vacuum dep. CuCl + 180°C air bake, also CuCl dip + 250°C bake	Au-Cr evap. grid	Kapton	silicone		2-2.4%		
evap. CuCl, heat in N ₂	Au grid				3%		
					5% 4 cm ²		

b. Harshaw

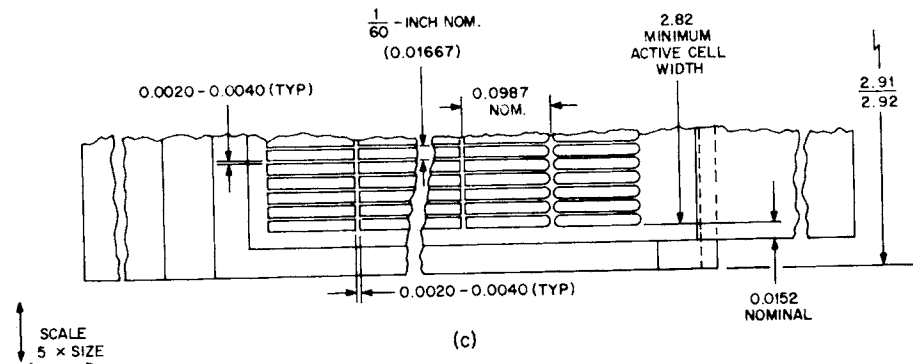
A frontwall cell on a molybdenum substrate was developed at Harshaw.⁶² Molybdenum is a good match for the thermal expansion coefficient of CdS. The cells were laminated between two plastic sheets, Mylar or Kapton, to inhibit curling using a nylon (Capran) adhesive. Griffin^{65,68} replaced the top contact of conductive silver paint by an electroformed fine metal mesh. This improved the cell efficiency by reducing the series resistance. Gold grids gave the best results.^{66,71} A pressure contact was formed between the metal grid and the Cu₂S layer during lamination. Evaporated grids were also tried, but they produced too high a series resistance. A 40-100 Å zinc layer between the molybdenum substrate and the CdS provided a better ohmic contact.⁶⁸ The molybdenum substrate was later re-



(a)



(b)



(c)

Fig. 1. Construction of cadmium sulfide thin film solar cell. (a) Overall cell dimensions. (b) Vertical cross section through cell (cut through X-axis). (c) Grid layer 6. Nominal array cell area = $2.93 \times 3.25 = 9.52$ sq in. or 0.0661 sq ft. Minimum active cell area = $2.82 \times 3.25 = 8.065$ sq in. or 0.0560 sq ft. Nominal closed area of grid = 19.6%. Overall thickness = 0.004 in. Adhesive "A" between layers 5 and 6 is a conducting epoxy. Adhesive "B" between layers 6 and 7 and 5 and 7 is clear epoxy trans-

duced from 2 to 0.3 mil by chemical milling to reduce the weight of the cell.^{71,74}

In the final work at Harshaw⁷⁶ the grid was changed from gold to gold-plated copper to reduce the cost. The grid was thermocompressed into the cell by passing through heated rollers. The nylon lamination was replaced by clear epoxy in order to increase the stability of the cell.

c. Clevite

Clevite³⁷ persevered with a backwall cell until 1965, using a Pyrex or H-film substrate, also copper foil. A peripheral indium contact to the CdS caused deterioration of the cell and was replaced by a metal film or mesh, and by evaporated gold stripes on H-film. The barrier layer was formed by means of a Cu₂O slurry followed by baking at 250 to 300°C. Formation by electroplating, vacuum evaporation, and thermal decomposition were also tried.^{18,44} The counterelectrode was formed by conducting silver paint or evaporated gold stripes. The H-film was laminated by Mylar plastic using a nylon adhesive to prevent curling. Water vapor caused the cells to deteriorate rapidly initially.

In 1965 Clevite^{29,43} switched to frontwall cells with molybdenum or Kapton substrates. The cell instability caused by contact deterioration at the grids was solved by means of conducting adhesive. Improvements in the barrier formation method by going to a CuCl dip resulted in efficiencies

parent to sunlight. Individual solar cell weight is 2.36×10^{-3} lb (1.608 g). Internal cell construction taken from Refs. 30 and 53. Construction of solar cell

Layer No.	Material	Thickness
1	Kapton, polyimide, H film	0.001 in.
2	Ag + polyimide varnish, 50% Ag by volume	0.0003 in.
3	Zinc plating	
4	CdS film, vacuum deposited fiber axis orientation—C axis perp. to substrate	0.0006 to 0.001 in.
5	p-type Cu ₂ S layer	
6	Au plated Cu grid	0.00045 in.
7	Kapton, polyimide, H film	0.001 in.
8	Kapton, polyimide, H film	0.0005 in.
9	Gold-plating	

Grid: 169 openings in width, 29 openings in length, 4901 openings total.

between 4 and 6% from a 50 cm² cell. A combined frontwall-backwall cell on a polyimide substrate showed substantially lower efficiencies and was difficult to reproduce.^{29,30,42,44}

In the final version of the Clevite cell⁵¹ nylon was replaced by clear epoxy resin to eliminate degradation in humid ambients. Copper or silver in contact with the barrier causes degradation to the cell output after high temperature exposure. The silver epoxy grid contact was therefore replaced by a gold pigmented epoxy. The electroformed gold metal mesh was replaced by a gold-plated copper mesh. Figure 1 shows a typical cell structure.

d. Other Developments

In 1958 Cabannes⁸¹ evaporated a layer of copper on top of a CdS film. Initially, there was a very high resistance and no photovoltaic effect. The application of a dc electric field caused a sudden decrease in the resistance and a photovoltaic response with a maximum in the red.

A frontwall-backwall cell was developed by Itek.^{82,83} The barrier layer was formed by copper evaporation followed by air baking for 15 min at 400°C. Copper evaporation was also employed by Pastel,^{86,87} by Balkanski and Choné,⁹² and by Anshon and Karpovich.¹⁰³

A major effort in the CdS thin film solar cell development was made by the S.A.T. Company in France.^{55,95-99} The construction of the cells is basically the same as in the final Clevite version (see Table III), except that Aclar as well as Kapton is used as cover material. By improvements in the different layers, gridding, and encapsulation the efficiency of the cell has increased from 3% in 1968 to 7% in 1970 at air mass zero.†⁹⁶ Similar cells have also been developed by the International Research and Development Company in England¹⁰⁷ and by AEG-Telefunken in Germany.^{105,106}

Mickelsen and Abbott of the Boeing Corporation¹⁰⁸ investigated a dry barrier formation process. Purified cuprous chloride was evaporated from a quartz crucible, followed by a two minute bake at 180°C in air or hydrogen. The efficiency was only 3% at air mass zero.† An attempt was made to carry out most of the fabrication steps by vacuum evaporation. The metallization of the Kapton substrate was changed to a NiCr-Cu-Cr layer. A number of materials were tested to encapsulate the cell. Silicone R63-488 gave the best adherence. CuCl evaporation was also attempted by experimenters at the University of Delaware.¹⁰⁹

† Air mass zero defines the solar illumination intensity just outside the earth's atmosphere.

3. OTHER STRUCTURES

a. *Sputtered Cells*

Photovoltaic cells from sputtered CdS films have been prepared by Pavelets and Fedorus⁹³ and by Yefremenkova *et al.*¹¹¹; see Table IV. Some attempts to fabricate such cells were also made by Albrand *et al.*⁹⁴

Pavelets and Fedorus⁹³ doped the sputtered CdS layer with In. This was followed by successive evaporations of sulfur and copper or Cu₂S. A heat treatment in sulfur doped cells was not required.

Yefremenkova *et al.*¹¹¹ prepared cathode sputtered films on substrates of conducting glass heated at 50° to 150°C. A more perfect structure at higher temperatures increased the open-circuit voltage.

b. *Spray Deposited Cells*

Chamberlin and Skarman^{89-91,112,113} prepared photovoltaic cells from spray deposited CdS films. The process is described in Section 5. The crystallinity increases with the substrate temperature. The optimum temperature was between 550° and 650°F.

Initially, backwall cells were made on conducting glass. An efficiency of 3.5% was reached over a region of 2 cm² (see Table IV). Frontwall cells on flexible metal substrates showed low efficiencies. The deposited materials underwent chemical reactions with Mo and Pt substrates. Other substrates tried were phosphor bronze, anodized aluminum, steel with an electroplated copper layer, and copper-cadmium alloys. Most of these were chosen to prevent deleterious reactions.

The barrier layer was also formed by a spray process. Copper sulfide in the form of digenite was spray deposited from a mixture of aqueous copper acetate and *N-N*,dimethyl thiourea at 250°F. A heat treatment in air or nitrogen at 250°–300°C for 2 to 10 min increased the efficiency. The spray deposited junction does not depend on interaction with the CdS, thus leading to a more abrupt junction.

Junction formation by chemiplating or electroplating requires a thicker CdS layer than that formed by the chemical spray process. On the other hand, spray deposition creates a thick Cu₂S layer with low efficiency for frontwall cells. Consequently, the effort to fabricate spray deposited cells was discontinued.

Earlier the Clevite^{18,35-37} group attempted to form junctions by spraying Cu₂O. The cells possessed efficiencies of less than 1%. Vojdani¹²⁵ made some cells using a spray deposited layer of CdS.

TABLE
CdS PHOTOVOLTAIC CELLS PREPARED

Reference	Type	Substrate	Ohmic Contact to CdS	CdS Layer
Pavelets & Fedorus ⁹³		Mo		In doped & S doped
Yefremenkova ¹¹¹	frontwall/ rearwall	cond. glass		cathode sputtered
Chamberlin & Skarman ^{89-91,112,113}	backwall	glass	SnO_x , In contact	1-2 μm undoped
	frontwall	phosphur-bronze, 1 mil Mo, Pt, Cu-Cd plated steel		1 μm undoped
RCA ^{114,115}	inter- digital & sandwich			5 μm
Kanev ^{116,117}			Sn, SnCdPb alloy	
Kanev ¹¹⁸			Sn	10 μm
Shiozawa ¹¹⁹⁻¹²¹				1 μm , In, Cu, Cl doped
Nakayama ^{122,123}			Ni plate	200 μm , 10 μm
Konstantinova & Kanev ¹²⁴			Sn	
Vojdani ¹²⁵		ceramic		20 μm
Te Velde ^{126,127}	gap & sandwich	plastic, 0.3 μm	Cd	40 μm grains

c. Sintered Cells

The first sintered CdS cells were made at RCA^{114,115} with interdigital and sandwich structures. The latter gave a greater output. The junction was made with copper paste. The porosity of the sintered layers limited the efficiency.

Kanev *et al.*¹¹⁶⁻¹¹⁸ used low resistivity sintered CdS films. The junction was formed by copper deposition and diffusion, and also by dipping into an aqueous solution of boiling copper sulfate.

Shiozawa¹¹⁹⁻¹²¹ developed a lateral construction to avoid shorting caused by pinholes. Heat treatment improved the properties of the cells, which were covered by Mylar. Indium-doped cells had a lower open-circuit voltage, but a higher short-circuit current than the undoped cells.

Nakayama^{122,123} prepared highly efficient ceramic CdS cells with an effective junction area more than 10 times the surface area. The junction

IV

BY OTHER METHODS

Barrier Formation	Counter Electrode to Cu ₂ S Material	Cover	Efficiency	I _{SC}	V _{OC}
<u>a. Sputtered CdS Layer</u>					
Cu or Cu ₂ S evaporation, no heat treatment					
electroplating, heat treatment	Cu			5-8 mA/cm ²	0.4 - 0.43
<u>b. Spray Deposited Films, N.C.R.</u>					
spray dep. 0.1 μm heat at 280-320°C	Cu grid	Mylar, 1 mil	< 4%	1 cm ²	
spray dep. 0.1 μm heat at 280-320°C	Cu grid, Au plated Ni mesh	Mylar, 1 mil	< 4% 0.56%	1 cm ² 3" x 3"	2 mA/cm ²
<u>c. Sintered Cells</u>					
Cu paste	Ag paste		> 0.1%	1-6 mA/cm ²	0.45
Cu evap or cathode sputtering heat at 550°C in Air	Cu			5 mA/cm ²	.25 - .4
CuSO ₄ dip, heat at 350°C	Cu mesh				
CuCl dip & heat			5-6%	0.68 cm ²	0.45 and
CuSO ₄ dip	Ag grid, painted		6-9%	3 x 3 cm ²	20-30 mA/cm ² 0.45
BiNO ₃ + Cu salt electroplated	Ag grid		3-5%		
<u>d. Silk Screening</u>					
CuCl dip at 87°C 2 mil heat at 300°C					0.7
<u>e. Micro-Grain Layers</u>					
hot cuprous ion solution	Au film	Plastic 0.3 μm	0.5%		

was formed by dipping in a copper sulfate solution after an HCl etch. A cathodic treatment produced a silver gray color.

Konstantinova and Kaney¹²⁴ prepared heterojunctions from ceramic CdS plates by electroplating in a saturated solution of bismuth nitrate containing a 0.05% saturated copper salt so as to reduce the excess copper concentration. The resulting cells had efficiencies of 3-5%, were insensitive to heat treatment to 200°C, and remained stable for more than 1000 working hours.

d. Silk-Screening

Vojdani *et al.*¹²⁵ prepared 20 μm CdS layers on a ceramic substrate by silk-screening an ink containing CdS, CdCl₂, ethyl cellulose, and 2-butoxy ethanol. The layers were dipped in a solution containing CuCl and HCl at

87°C, then baked for 2 min at 300°C. The cells possessed an open circuit voltage as high as 0.7 V, but had too high a series resistance.

e. *Monograin Layers*

TeVelde^{126,127} prepared sheets of CdS single crystal grains, 40 μm diam, in a plastic binder with electrical contacts on either side. The CdS was photoconductive, but the surface was made strongly n-type to provide good ohmic contact.

To prepare a solar cell the CdS powder was washed in a hot cuprous ion solution, so that each grain was covered with a Cu_xS layer. To form the monograin layer the plastic substrate was covered with glue and the treated CdS powder was then sprinkled onto the glue. After application of a thermosetting resin the top layer was etched off, the resin was hardened, the sheet was stripped from the substrate and the adhesive dissolved. The exposed Cu_xS layer was then etched away on one side by KCN. The efficiency of the cells was extremely low; it did not exceed 0.5%.

III. Thin Film Solar Cell Technology

4. VAPOR DEPOSITION

Thin films of cadmium sulfide can be deposited in many different ways. The best known method is vapor deposition, which is rather arbitrarily defined here to include both standard vacuum evaporation as well as those closed system procedures which allow a considerable buildup of molecules in the vapor phase, as long as no other gases, either inert or reactive, are present. Other methods are described in Section 5.

a. *Open Systems*

The vapor deposition of CdS has frequently been described in the literature, particularly during the last decade, as the result of the growing importance of CdS thin film devices. The majority of the depositions have been carried out in open systems, i.e., without separation of source and substrate from the main volume of the evaporator, so that the direct beam from the source impinges on the substrate. This causes contamination of the deposited film by impurities from the evaporator which is further enhanced by the following:

1. The CdS charge, usually in the form of a powder, has not been sufficiently purified and degassed.

2. Absorbed gases on the substrate are not removed before deposition by vacuum baking, ion bombardment, or glow discharge.

3. The residual gas pressure in the vacuum system cannot be reduced below 10^{-6} torr.

Aitchison¹²⁸ has shown that the effect of residual traces of oxygen during evaporation is extremely critical and affects both the spectral transmission and photoconductivity of the evaporated film. Miksic *et al.*¹²⁹ found that in the range 10^{-6} – 10^{-4} torr the higher oxygen pressures result in a marked increase in the CdS film resistivity, particularly at higher substrate temperatures (175°C). Hughes and Carter¹³⁰ found that an ultrahigh vacuum alone improves the reproducibility of the thin films, but that there is still a wide variation in the composition of the residual gases.

In a direct source arrangement the molecules evaporated at the source travel in a straight line from the source to the substrate, which is located approximately normal to the molecular beam, and whose temperature is usually higher than that of its surroundings (Fig. 2a). Above 220°C the deposited material is reevaporated causing a slowdown in the net condensation rate.^{131,132}

The splattering of solid particles during evaporation of CdS has led to the indirect source arrangement shown in Fig. 2b. The evaporated atoms or molecules arrive at the substrate after multiple reflections at the baffle and the cylindrical enclosure which is kept at a higher temperature than the substrate.^{133–135} The molecules now impinge on the substrate surface from all directions, resulting in a disorientation of the *c*-axis.

b. Enclosed Systems

(i) *Heated Inner Chamber.* A number of systems with a tightly enclosed source and substrate have been introduced to facilitate CdS deposition at elevated temperatures. The arrangement has the advantage that already at low source temperatures a sufficient density of CdS vapor is obtained above the substrate, so that at a given deposition rate the deviation from stoichiometry is lower than in the usual evaporation arrangement.¹³⁶

In the simplest arrangement the enclosure consists of a glass, quartz, or metal cylinder (Fig. 2c) which keeps out residual gases desorbed from the outer walls and from the heaters during evaporation.¹³⁷ During depositions at higher temperatures the cylinder is externally heated to a temperature intermediate between source and substrate temperature.^{79,138,139} This forces the deposition of all the evaporated material onto the substrate, which is surrounded by an appreciable concentration of CdS molecules.

One of the problems encountered in such a system is a significant tem-

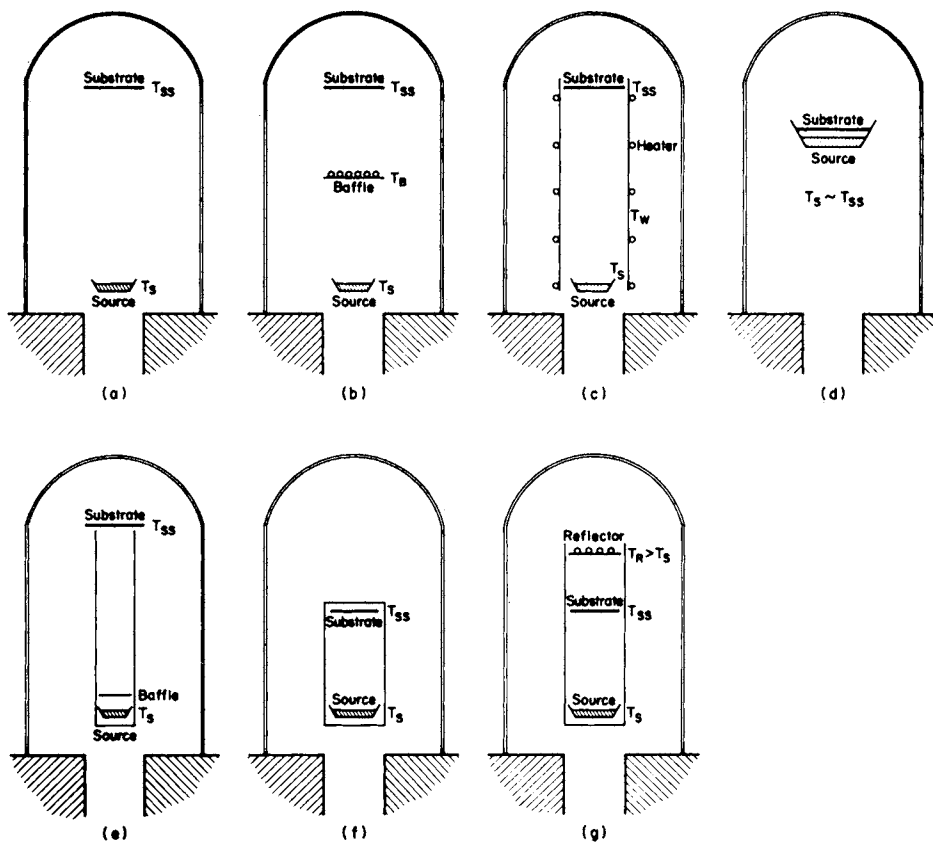


Fig. 2. Systems for vapor deposition of CdS. (a) Open system, direct source, molecular beam. (b) Open system, indirect source, heated glass wall. (c) Enclosed system, heated inner chamber. (d) Close space or sandwich system. (e) Knudsen source. (f) Closed crucible. (g) Thermal reflector. T_s , source temperature; T_{ss} , substrate temperature; T_B , baffle temperature; T_w , wall temperature; T_R , reflector temperature.

perature gradient across the substrate surface that can affect the structure of the deposited film. Bujatti¹⁴⁰ was able to modify this temperature gradient for a given substrate temperature by adjusting the length of the internal quartz tube by means of a telescopic arrangement. The film structure is also affected by the fact that the particles impinge upon the substrate from all directions. Many evaporation systems employ a heated inner chamber. Instead of a cylinder, the arrangement may also take the form of a completely closed crucible.^{141,142}

(ii) *Quasi-Equilibrium Vacuum Deposition.* Hudock¹⁴³ was able to

achieve CdS films with electronic properties approaching those of the source material by using an equilibrium deposition method in an ultrahigh vacuum (better than 10^{-9} torr). Similar methods were used by Kalinkin *et al.*^{142,144,145} and by Krasulin.¹⁴⁶ In vacuum growth under quasi-equilibrium conditions with supersaturation the growth rate is proportional to $\exp(-E/RT_{gr})$, where T_{gr} is the growth temperature and E , the activation energy of condensation of a monocrystalline layer, is equal to 12 kcal/mol.

In the close space or sandwich method shown in Fig. 2d, the substrate is located one or two millimeters above the source forming a closed box. The CdS sublimes from the source and condenses on the substrate under near isothermal conditions, i.e., the source and substrate temperatures are almost equal. Krasulin and Vanyukhov¹⁴⁶ obtained quasi equilibrium by means of the arrangement shown in Fig. 2g. Here the CdS molecules are prevented from escaping by means of a thermal reflector at a temperature greater than the source temperature.

c. Sources

The construction of the source is one of the most critical elements in the achievement of uniform and reproducible deposited films. The rate of evaporation and hence the deposition rate varies exponentially with the absolute temperature,¹⁴⁷ requiring a very steady and uniform heating of the charge which should be thoroughly degassed before evaporation. In particular, it is important to ensure that there are no temperature gradients within the source and that the temperature and evaporation rate are independent of the amount of charge present.

It is difficult to heat the CdS material gradually to the sublimation temperature without local overheating of some particles, which vaporize with explosive force causing the ejection of small particles onto the substrate. This phenomenon is referred to as "spattering" or "splattering."⁶²

The particles are loosely bound to the substrate and give rise to the following formations when viewed under a microscope¹⁴⁸: (1) "pinholes," narrow perforations extending through the film to the substrate; (2) bumps or protrusions caused by adherent particles of CdS which have been deposited at an early stage of the film formation and have been subsequently covered; (3) amorphous pits formed underneath particles that have subsequently become detached.

The effect is minimized by using coarse grained sintered CdS, by covering the substrate with a shutter on starting up the evaporation, and by covering the source with a quartz wool plug. These precautions are inadequate for large area devices such as solar cells, where a single short

produced by one pinhole may ruin the device, and where rapid evaporation rates are required. Also, the plug acts as a secondary evaporation source whose temperature cannot be adequately controlled. The same applies to baffles which are also used to reduce spattering. On the other hand, in an indirect source a shield at a much lower temperature than the source prevents the particles from following a direct path to the substrate.

Knudsen sources^{132,149-152} are constructed so as to prevent particles from leaving the source while still providing a molecular beam directed toward the substrate. However, they are not normally designed to give uniform coverage over a large substrate. In the Knudsen source arrangement the source is totally enclosed by a tube and the substrate is located a short distance from the end of the tube (Fig. 2e). Other indirect sources with a baffle located just above the crucible, such as the one designed by Galla,¹⁵³ may be more suitable for this purpose.

Several other sources described in the literature have been designed for evaporating CdS. Card and Galen¹⁵⁴ mix the charge with alumina crystals to reduce spattering and to provide a larger surface area for evaporation. In the source developed by Spriggs and Learn¹⁴⁷ the charge is placed in 144 holes in a molybdenum block whose large thermal mass keeps the temperature constant. A silica crucible with a hollow center yields a more uniform evaporation rate than cylindrical crucibles.¹⁵⁵ None of these sources eliminates spattering at rapid evaporation rates. A perforated tantalum chimney source developed by Drumheller^{129,156} is capable of producing very uniform evaporation rates while reducing streaming of particles from the source to a minimum.

Some care is required in the selection of the source construction material in contact with the CdS. Quartz is satisfactory, but molybdenum reacts with CdS forming a bluish scale of MoS¹⁵⁷ which may produce a sulfur deficiency in the deposited film. Tantalum is slowly attacked by CdS and sulfur vapor forming Ta₂S₄, a black crystalline powder stable below 1300°C, which causes embrittlement.^{75,76,158}

A number of systems employ electron beam heating to vaporize the charge.¹⁵⁹⁻¹⁶⁷ This greatly reduces the danger of contamination, since the container is not heated directly and may be water cooled. Sorbier *et al.*¹⁶³ have shown that deposition rates of several microns per minute may be achieved. The rate of evaporation varies with the crystal surface struck by the electron beam. For this reason lightly compacted powders produce a more uniform evaporation rate than polycrystalline material. The composition of the residue after electron beam evaporation is unchanged, unlike the residue from thermal evaporation. However, electron beam heating may cause considerable spattering of solid particles onto the substrate.¹⁶⁸

Flash evaporation has also been used in the vacuum deposition of CdS.^{86,88,169} The method makes it possible to deposit films of the same stoichiometry as the source material. It is not suitable for the deposition of thick films and the intense heat tends to damage organic substrates. Also, it is difficult to control and requires frequent cleaning of the evaporator.

d. *Doping and Coevaporation*

The methods so far described are not suitable for varying the stoichiometry of the deposited films or for introducing dopants in a controlled manner. Since CdS dissociates completely in the vapor phase the stoichiometry of the deposited film depends not only on the stoichiometry of the source material, but also on many other parameters. Three methods have been adopted for doping CdS thin films: (1) deposition of dopant onto completed thin films followed by indiffusion; (2) CdS charge in source contains dopant; (3) coevaporation of CdS and dopant using separate sources.

(i) *Evaporation of Doped CdS Charge.* Diffusion of dopants into the completed film has been used extensively to activate photoconductors and to induce recrystallization. Many attempts have also been made to produce doped films by incorporating a known amount of dopant into the CdS charge. In general, the dopant concentration in the film is different from that in the source material.¹⁷⁰ This is to be expected if the dopant and the dissociated Cd and S₂ vapors possess widely different vapor pressures. Moreover, the evaporation rates are time dependent.

Shirland *et al.*⁴³ evaporated a series of films onto glass substrates from a CdS charge which contained a variable amount of indium up to 1 mole %. The indium was presintered into the charge. They obtained an essentially linear relationship in the log-log plot of resistivity versus indium concentration in the charge for dopings up to 0.1 mole % (see Fig. 3). At higher doping levels the resistivity plot deviated from linearity, possibly because a smaller proportion of the total indium content carried over into the deposited film. The dopant also caused a change in the optical transmission of the film which varied linearly with the doping level up to 0.1 mole %.

Schaefer *et al.*^{75,76} evaporated CdS doped with different concentrations of In, Al, Cu, Ag, and Au under a number of different experimental conditions including open and enclosed systems as well as close space vapor transport. They were unable to find a correlation between the doping level and the carrier concentration of the deposited film which they obtained from the Hall coefficient.

Hudock¹⁴³ was able to prepare CdS films by close space equilibrium vapor

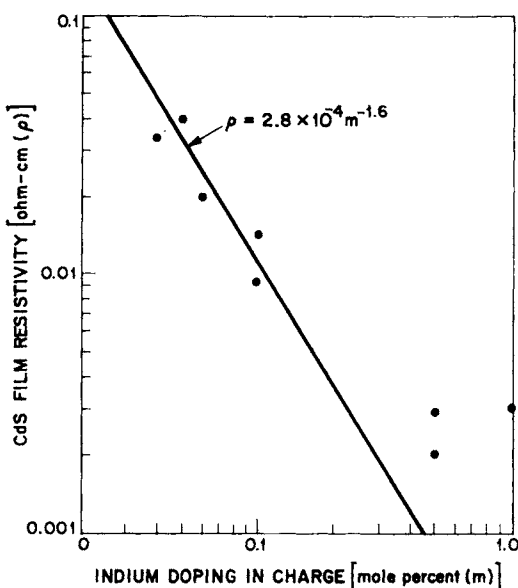


Fig. 3. Effect of indium doping on CdS film resistivity. (From Shirland *et al.*⁴³)

deposition whose resistivity was comparable to the resistivity of the source material over a range of four orders of magnitude (up to 4×10^4 ohm-cm). The source material could be in the form of a powder, provided that the latter was presublimed at 700°C in vacuum at 10^{-7} torr to remove volatile impurities.

Indium, the most common dopant, is usually introduced into the charge as chloride or sulfide. An attempt to deposit CdCl₂ mixed with a CdS charge onto a preevaporated CdS film caused the latter to be attacked by chlorine.⁵⁴ It proved impossible to deposit CdS films doped with Al by doping the charge with AlCl₃. This is believed to be due to conversion of AlCl₃ to Al₂S₃, which has a very low vapor pressure.^{75,76}

Avignon *et al.*¹⁷⁰ used an electron beam method to evaporate I, In, Ag, and Cu doped source material. Radioactive tracer, colorimetric, and spectrophotometric methods were employed to measure the dopant concentration in the film.

The ease of doping with different impurities is obviously related to the diffusion coefficient of the dopant. Thus Cusano¹⁷¹ states that chlorine and bromine produce heavily doped films of low conductivity, whereas iodine which has a low diffusion coefficient is not easily incorporated and forms photoconductive films of high resistivity.

(ii) *Coevaporation.* By simultaneous deposition of the elements onto a heated substrate it is possible to control the stoichiometry of the film by adjusting the temperature of each source as well as the substrate temperature. The introduction of dopants can then be accomplished by means of additional sources. Molecular beams of cadmium and sulfur focused onto a substrate produce very uneven deposits in the form of globules, spiroidals, ribbons, and needles depending on the CdS ratio and the degree of supersaturation.^{168,172} Günther¹⁷³ describes a system with two concentric evaporation furnaces resulting in a more homogeneous beam. Indirect sources^{133,174} produce more homogeneous films and more flexible operation by independent control of four temperatures: two sources, the substrate, and the walls reflecting the molecular beams.

Beecham¹⁷⁵ has developed a double coaxial isothermal source for coevaporation of Cd and S for the vapor deposition of films used as electro-acoustic transducers. The requirements for this purpose are a high resistivity film, despite the vastly different substrate accommodation coefficients for Cd and S, and c-axis growth in a specific direction with respect to the substrate. The double coaxial construction allows the variation of the substrate angle with respect to both sources. Under excess sulfur evaporation conditions the film growth rate is determined by the cadmium arrival rate, and hence high resistivity films may be achieved.

Cd and S coevaporation has been criticized by Aitkhozhin *et al.*¹⁷⁶ in that it requires fine control of the sulfur source, produces significant amounts of cubic CdS, and is a slow process.

Lind *et al.*¹⁷⁷ have considered some of the problems encountered in controlling the evaporation rates of two or more sources. Special care is also required in the construction of the source to prevent reactions between the source material and constituents of the vapor phase, which may lead to fracture or plugging up of the source.¹⁵⁸

Some systems for the preparation of stoichiometric CdS films consist of a CdS source and an additional source of sulfur, the more volatile element. Both direct¹⁷⁸⁻¹⁸² and indirect¹³³ sources have been employed. The direct sources usually operate in an enclosed system. DeKlerk and Kelley,^{133,134,183} using the indirect method, obtained more reproducible results from coevaporation of the elements than from the CdS, S system. S condenses at temperatures below 50°C while Cd condenses above 200°C, so that only stoichiometric CdS is formed in the intermediate temperature range at the deposition rate of the lower of the two vapor pressures. CdS films have also been doped with copper, silver, and indium by coevaporation.^{33,178-180,184-186}

Nadjakov *et al.*¹⁸⁷ have prepared CdS films several micrometers thick on

a glass substrate by successively evaporating sulfur and cadmium followed by heating for 10 to 20 min in air at 400°–460°C.

e. *Vapor Deposition of CdS for Photovoltaic Cells*

The different methods used to deposit films of CdS for the production of photovoltaic cells are listed in Table V. For the most part open systems with direct single sources have been used. Fairly thick films require rapid deposition rates. Experimental depositions on many different substrates have been carried out, but the structure of the resulting films has usually not been investigated. In many evaporations the CdS charge contained donor or acceptor dopants.

The important characteristics of the films are that they be adherent to the substrate and reasonably free of pinholes or similar types of physical imperfections. The cleanliness and uniformity of the substrate are essential, and substrate temperatures in excess of 180°C have generally been required.⁵⁰ Special problems are encountered in the deposition of large areas.⁵⁷ Spattering of solid powder particles of CdS from the sources to the substrate must be avoided.

The thickness of the CdS film is a function of the relative perfection of the film. The better structured the film and the fewer flaws present, the thinner the film can be. Most high efficiency cells have been made from films 10–30 μm thick and with a resistivity of 10–100 ohm-cm.^{50,97,193} The short-circuit current increases steeply with the substrate temperature up to 220°C, peaks between 220° and 240°C, and then decreases. The open-circuit voltage is also an optimum there. The short-circuit current is slightly influenced by the deposition rate. The best results have been obtained at 1 μm/min. The open-circuit voltage is independent of the deposition rate.^{97,193}

Doping of CdS films to achieve good photovoltaic response has proved tricky. Early CdS cells produced at Clevite^{29,48,49} were In doped and gave reasonable efficiencies, as long as their thickness was greater than 5 μm. Thinner films tended to produce short circuits. Doping by CuCl lowers the efficiency due to loss of open-circuit voltage. The red response is increased, and the blue response is lowered.⁹⁸ Doping with Zn improves the ohmic contact, but also lowers the efficiency. Similar results were seen at Harshaw.⁷⁶ On the other hand, David *et al.*¹⁰⁴ state that doping with CuCl and CdCl₂ decreases the series resistance and improves the photovoltaic response.

The open-circuit voltage increases with resistivity, but so does the series resistance. An attempt was therefore made to deposit a low resistivity In doped layer followed by a high resistivity undoped layer.^{29,48,49} Unfortu-

nately, the efficiency was lower than that of a standard cell. The same result was obtained on doping the surface region of the CdS layer by Cu or Cu₂S.

Recently Palz *et al.*^{98,99} have used an unspecified doping technique to improve the high temperature stability by reducing copper diffusion. Konstantinova and Kanev¹²⁴ have used doping by Bi ions in ceramic cells for the same purpose.

An attempt was made at RCA⁷⁹ to improve the cell performance by reducing the number of grain boundaries by recrystallization of the CdS layer using the method of Gilles and van Cakenbergh^{194,195} (see Section 9). The cells showed low efficiencies due partly to shorting of the active junction by silver precipitation and partly due to nonuniform barrier formation.

f. *Substrate*

Vacuum deposition of CdS films is normally carried out at elevated temperatures to achieve the desired crystal structure and stoichiometry. Under these conditions reactions can occur between the CdS film and the substrate material that affect the properties of the electrical contact.

Up to 1961 the substrate of thin film CdS cells was mainly glass, though some other materials had also been used. Two mil ribbon glass was tested at Harshaw,^{62,65} but the strain was too great. Schaefer^{71,73} showed that polished quartz possessed good adhesion to CdS if the substrate is cooled slowly. There was poor adhesion on rapid cooling due to the difference in expansion coefficients.

Early work at Harshaw^{62,65} indicated that molybdenum is the best suited substrate for frontwall cells, because the thermal expansion coefficients of CdS and Mo match. At a later stage Harshaw^{71,74} developed a method for reducing the Mo thickness from 2 to 0.3 mil by etching after cell formation. At higher deposition temperatures molybdenum possesses poor adhesion due to the formation of surface coatings. Molybdenum is susceptible to oxidation by oxygen, sulfur, and water vapor.

The expense and weight of molybdenum led to a search for substitute metals (see Table VI). In many cases the adhesion was poor, as a result of chemical reactions or a mismatch in the thermal expansion coefficients. Aluminum is a very poor thermal match and produced flaky CdS deposits.⁶⁵ Initial experiments on titanium and zirconium were unsuccessful. The metals could not be adequately cleaned before deposition and yielded cells with poorer efficiency and more shorts.⁶⁵ Better results were obtained on titanium at a higher deposition temperature and also on tantalum at a

TABLE V
VACUUM DEPOSITION OF CdS FOR PHOTOVOLTAIC CELLS

Year	Reference	Method	CdS	Charge	Dopant	Source Material	Temp °C	Substrate Material	Temp °C	Vacuum During Evap. torr	Rate of Deposition (μm/min)	Film Thickness (μm)	Post Treatment
<u>a. Clevite</u>													
1954-1958	33, 34	coevaporation	luminous grade pwdr	2-4% In_2S_3		cond. glass, Cu_2O , Cu_2O on glass				10^{-4} - 10^{-5}		0.1-0.5	Air Bake
1963-1965	18, 36-39, 42		CdS chips, sintered pwdr	In_2S_3	quartz	< 1200	pyrex, H-film		200		1.25-10	25-60	
1964	41	hot wall, closed chamber	sintered pwdr	In_2S_3	quartz		H-film, glass, silicone-glass laminate	200		10^{-6}	4-18	15-60	
1964-1965	29, 42, 43, 48, 188	dble. layer, doped & undoped	sintered pwdr	In, CuCl	quartz	1000	H-film, glass, Mo	200-300			0.6 -10	25-60	
1965	44		sintered, luminous grade pwdr				Mo	200		10^{-5}	1.8-2.4	18-24	
1965	43	open		none			Vycor, Mo		220-570			0.5-20	
1965	43	hot wall, closed chamber		none	quartz	1085	Mo		400-600			7-250	
1965-1966	29, 47, 51	open	purified sintered pwdr	none	Ta	1050-1100	Mo, H-film	200-250		10^{-5} - 10^{-6}	1.2-1.8	15-20	
1965	29, 48	hot wall, closed chamber		In_2S_3			Mo	600				1-2.7	
1965-1966	29, 48, 49	open		In			Mo	350				5-11.4	
1968	57	open	purified sintered pwdr	none	quartz		H-film, Ag Pyr-M-L	220		10^{-5}	0.6-1.2	20-25	
<u>b. Harshaw</u>													
1960-1962	5, 62, 63, 65	open	crystal chips, purified $InCl_3$ & sintered pwdr.			cond. glass, mylar, teflon, mica, ribbon glass, glass laminate, Mo, Ta, Ti, Zr, Al	75-350			10^{-4}	3	12.5-200	
1963-1965	66, 68, 69, 71-73, 189, 190	open	sintered pwdr, crystal chips	undoped	Ta	1000-1100	Mo, glass, quartz, SnO_2 on glass, Ti, Au on H-film	140-260		10^{-5} - 10^{-6}	1.5	12.5-50	
1964	71, 73	hot wall				900	Mo, quartz, Ta, Si, CdF_2 , Invar, Ti, Cu, Cu_2S on Cu	50-650		10^{-4} - 10^{-5}	0.03-10	1-400	
1964	71		sintered pwdr	$InCl_3$			glass, Mo	600			1	< 100	
1966-1967	75, 76	close space	sintered pwdr	none, In_2S_3 , Ta, quartz	600-900		Mo, Cu, steel, Invar, brass, Zr, Ti	50-800				12-25	
				$InCl_3$, $AlCl_3$, Cu, Ag, Au							-32-		

c. RCA										
1960	77,78			InCl ₃		cond. glass	150-200	10 ⁻⁵		1-2
1962	79	enclosed	pellets, luminescent grade	In,Ga,Cl		cond. Pyrex	150	up to 10 ⁻²	0.07-0.5	7-10
1958	81		commercial pwdr			d. Other			0.1	2-10
1961	82	2-layer, donor & acceptor doped	powder	donor & acceptor	Mo	Cu ₂ O on Cu		5x10 ⁻⁶ - 10 ⁻⁵		10-20
				In	quartz	950	300	5 x 10 ⁻⁶		air bake at 600°C between layers
1965	85					SnO ₂ on Pyrex		10 ⁻⁵		2-5
1965	86,87	flash evap.				SnO ₂ on Pyrex				10-15
1965	191		pure pwdr.		quartz	750-200	glass, Al on glass	150-350	2 to 3x10 ⁻⁶	0.1 to 0.25
1965	88	flash evap.				Kapton, Al	160-170	< 10 ⁻⁵		15
1967	55		pure pwdr.	Ta	1050-1100	plastic + Ag + Zn	220	10 ⁻⁶	1.2-1.8	15
1967	100		pwdr., luminescent grade			Mo	200	10 ⁻⁵	1.2	25
1967	94			Ta	850-1000	glass	130-200		0.15-0.45	5-10 heat treatment
1970	192	open			quartz	890-1360	Cu, Mo	180-300		0.06-1.8 2.8 to 21.1
1970	97		high purity pwdr.		quartz		Kapton, Ag Pyr ML	220	1	30-35
1973	193	enclosed, hot wall	crushed crystals		quartz		glass	220	< 10 ⁻⁵	< 6 20

TABLE VI
PROPERTIES OF SUBSTRATE METALS FOR CdS FILMS

Metal	Thermal Expansion (°C × 10 ⁻⁶)	Adhesion	Chemical Reactions	Other Properties	Density (g/cm ³)	Reference
Cu		some problems	Cu ₂ S			Clevite ^{44, 45, 47, 57} Harshaw ⁷⁸
Ag	20.2			soft & durable	10.5	Clevite ^{44, 45, 47} Harshaw ⁶⁸
Zn	34-39			good ohmic contact to CdS, soft & durable	7.7	Harshaw ⁶⁸
Al		poor, flaking				Harshaw ⁶⁵
In			deteriorates cell	good ohmic contact to CdS		Clevite ^{29, 41}
Ti	9-4	poor good	dark gray interface	embrittled by acid etch & sandblasting	4.5	Harshaw ^{65, 68, 74} Harshaw ^{71, 73}
Zr	6.1	poor		cannot remove surface film	6.5	Harshaw ^{65, 68}
Nb	7.5	poor			8.6	Harshaw ⁶⁸
Ta	6.6	poor good		cannot remove surface film	16.6	Harshaw ⁶⁸ Harshaw ^{71, 73}
Mo	4.7-5.8	good		expensive	10.2	Harshaw ^{62, 65, 71, 73}
W	4.6	good			19.3	Harshaw ⁶⁸
steel		poor				Harshaw ⁷⁶
Invar	1.2-4.9	poor	yellowish powder	erratic etch	8.1	Harshaw ^{68, 71, 73, 74, 76}
Kovar		poor		erratic etch		Harshaw ⁶⁸

A. G. STANLEY

later stage.^{71,73} Copper substrates have been extensively used in place of molybdenum. However, some difficulty was experienced with adhesion.⁵⁷

Polyimide in the form of H-film was first used by RCA in 1962,⁷⁹ making possible the development of flexible arrays. H-film requires a metallic interlayer that makes good ohmic contact to CdS and possesses a low series resistance. Evaporated layers of gold were initially used for this purpose,^{29,42} but were found to have too high a series resistance. This was replaced by a conductive polyimide varnish loaded with silver, which was cured and then coated with a thin layer of zinc.^{44,45,47} The varnish provided good adhesion to the substrate, and the CdS layer adhered strongly to the zinc, simultaneously forming a low resistance contact. Experiments showed that a suitable intermediate layer is necessary, since silver does not make an ohmic low resistance contact to CdS.⁵¹

Experiments by Shiozawa¹²⁰ indicate that the zinc reacts with the silver forming high resistivity intermetallics and may also partially evaporate during CdS deposition and contaminate the CdS film. This has led to the search for a more stable substrate system. Chromium has been used as a substitute for zinc, but cells formed in this manner showed low efficiencies.^{50,51,57} Aluminum interlayers produced cells with poorer efficiencies,⁵⁷ and brass undercoatings gave very poor adherence of CdS.⁵¹

Mickelsen and Abbott¹⁰⁸ developed a completely vacuum deposited metallization system for Kapton. Sequential depositions of Cr-Cu-Cr were subsequently changed to NiCr-Cu-Cr to prevent delamination. Unfortunately, the cells showed low efficiencies.

Plastic materials other than Kapton were tried, but either melted or proved otherwise unsuitable. The materials included Mylar, Teflon, and composites of glass-paper, Teflon-glass, and paper laminates.^{62,65}

5. OTHER METHODS OF THIN FILM PREPARATION

Many other methods have been employed for the preparation of cadmium sulfide thin films. For most applications certain minimum requirements regarding adhesion and crystallinity must be met. For some photoconductive devices it is sufficient to embed an activated powder in plastics like ethyl cellulose or polystyrene.¹⁹⁶⁻¹⁹⁸ Layers 2-10 mils thick can be fabricated in this manner, but the interparticle barriers give rise to nonlinear and often nonreproducible current-voltage characteristics.^{195a} An interesting method has recently been developed at the Philips Research Laboratories¹²⁶ that does not suffer from this drawback. Single crystal grains of about 40 μm dimensions are embedded in plastic to form sheets of monograin layers about 30 μm thick. Contact is made to conducting

layers on both surfaces of the sheet; there is no contact between individual grains.

Polycrystalline films are built up either on the molecular level as in vapor phase deposition, or by recrystallization of thicker deposits as in the sintering process with cadmium chloride. The crystallinity of the first type of film invariably improves with increased substrate temperature. At ambient temperatures the films are either amorphous or microcrystalline. This presents a special problem for plastic and thin metallic substrates. Plastic substrates cannot be heated to too high a temperature and are attacked by alkaline solutions that could otherwise be used to deposit films at ambient temperatures. Many metals are attacked by CdS at higher temperatures. Sometimes the reaction product adheres well to the substrate, more often it flakes off.

Most methods employing deposition from the vapor phase are capable of producing good polycrystalline films under the right conditions. Vapor transport by a nonreactive gas is rather slow and requires a high source temperature; chemical reactions introduce impurities into the film and are most difficult to control; sputtering is very slow. Deposition from the liquid phase is limited to film thicknesses of a few microns. These methods will now be considered in more detail.

a. *Vapor Phase Deposition*

The classification of the vapor phase methods is somewhat arbitrary.¹⁷¹ No gases other than Cd and S₂ vapor are present in the vapor deposition described in Section 4. Vapor transport requires an inert carrier gas. A reversible chemical reaction takes place in chemical transport. All these methods start with a CdS source. In a vapor reaction cadmium is evaporated and reacted with H₂S or sulfur vapor.

Each of the methods listed above may be further divided into static and dynamic methods. In the dynamic method a carrier gas flows continuously through the apparatus. In the two-zone arrangement, the CdS charge and the substrate are located in two separate heated zones through which the gas passes sequentially. In the static method, transport takes place by diffusion through the gas phase. In the close space technique,^{199,200} the substrate is located a short distance above the source forming a closed box. The method differs from the close space quasi-equilibrium method described in Section 4, by the presence of a carrier gas.

The dynamic methods described in this section were originally developed for growing single crystals. They can be used for depositing microcrystalline films on amorphous substrates as well as for depositing epitaxial films on single crystals. They are dynamic methods requiring careful control of

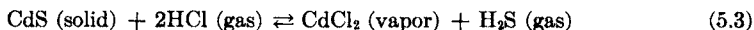
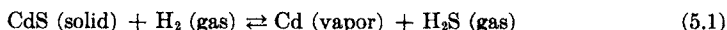
partial pressures and flow rates to achieve reproducible films of good quality. Dopants like halogens, gallium, and indium are readily introduced in the vapor phase.

(i) *Vapor Transport.* Dynamic vapor transport was used by Kroger *et al.*,²⁰¹ Ibuki,^{202,203} and Fuchs²⁰⁴ to grow single crystals of cadmium sulfide. They used hydrogen sulfide, nitrogen, or argon as the carrier gas. The method is very suitable for the growth of epitaxial films.^{205,206} The advantages over vacuum deposition may be found in the kinetics of the gas phase. The direction of the particles impinging on the substrate is randomly distributed, so that there are always some particles incident in the optimum direction for epitaxial growth. Also the particles are less likely to be reflected by the substrate, since they possess lower energies. The substrate may be heated to higher temperatures without fear of reevaporation, since the gas pressure employed is usually close to atmospheric. A considerably higher source temperature (1000° to 1150°C) is required than for vacuum deposition.

In close space vapor transport a considerable vapor pressure is built up from the evaporating source. The addition of small amounts of inert gas^{190,207} does not seem to offer any advantage, while at higher pressures the source temperature must be raised. Certain intermediate conditions of temperature and vapor pressure lead to whisker growth⁷⁸ particularly at higher evaporation rates,²⁰⁸ but still higher vapor pressures favor plate-shaped crystals.²⁰²

(ii) *Chemical Transport.* In the chemical transport method the source material is vaporized by forming volatile chemical intermediates by means of a reversible chemical reaction. The volatile constituents are transported to the substrate which is kept at a lower temperature. There the temperature dependence of the chemical equilibrium causes the film to be deposited by reversing the reaction.

For the deposition of CdS the following reactions have been used:^{200,209,210}



The source material can be doped. Hydrogen transport is capable of achieving a fast deposition rate, but films thicker than 20 μm show poor adhesion to a glass substrate. Iodine transport requires an inert carrier gas and the deposition rate is one order of magnitude slower. Bube²¹¹ also investigated the use of methyl mercaptan as a transport agent.

The dynamic technique has been used to obtain epitaxial growth on a number of single crystal substrates. Nicoll¹⁹⁹ and Hegyi²⁰⁰ developed the

close space method for depositing polycrystalline films on glass substrates. They obtained randomly oriented films using iodine transport, whereas hydrogen transported films were oriented in the usual way (*c*-axis of hexagonal crystallites normal to the substrate surface).

Chemical transport requires lower source temperatures than an inert carrier gas. This is of considerable advantage in the close space technique where the substrate temperature can be similarly reduced. However, a price has to be paid by the incorporation of the reactant gas into the film structure, 10^{-4} parts of iodine by weight.²¹² It is not possible to remove the iodine from single crystals formed by this method.²¹³

(iii) *Vapor Reaction.* Frerichs²¹⁴ obtained small single crystals of CdS by reacting cadmium vapor with H₂S. Cadmium metal was heated to a temperature in the range 800°–1000°C in a quartz tube. A slow stream of hydrogen at atmospheric pressure drove the cadmium vapor to a second zone where it could react with a slow stream of H₂S. The rate of evaporation of the Cd metal is difficult to control. Schossberger²¹⁵ has designed a special furnace for this purpose. Volkov and Kotelyanskii²¹⁶ considered the thermodynamics of the reaction.

Jacobs and Hart²¹⁷ applied the same reaction at low pressures (a few torr) to deposit 5–20 μm CdS films on glass substrates with areas up to 10 in.² The films were deposited at 600°C and showed good adhesion. Capella and Heyraud²¹⁸ prepared epitaxial layers of CdS on single crystal substrates by passing H₂S over red-hot CdCl₂.

b. *Sputtering*

The deposition of thin films by cathode sputtering has been reviewed by Berry *et al.*²¹⁹ and by Maissel.²²⁰ In the most commonly used method a glow discharge is set up in a purified inert gas with large atomic mass like argon. The CdS source acts as the cathode and the substrate is kept at anode potential. The source does not require any heating, so that crucible contamination is avoided. No chemical carriers are required, but contaminant gases such as oxygen have a major effect, since the ionized gas is very reactive. The glow discharge removes impurities from the substrate surface.

Wehner²²¹ has shown that sputtering takes place by momentum transfer. The sputtering yield depends on many parameters including the mass of the positive ions, the accelerating voltage, the gas pressure, and the angle of incidence. The ejected particles are atomic in nature and only about 1% are charged. Their velocities exceed the thermal velocities from an evaporation source by at least one order of magnitude.

A very important advantage of the sputtering process is the fact that the

chemical composition of the sputtered film is usually the same as that of the cathode. Both Cd and S atoms are deposited in equal numbers from a stoichiometric source, so that films with good stoichiometry can be formed, as long as S desorption is not significant. It is also claimed that sputtered films are denser and possess better adhesion than evaporated films.

A number of experiments to deposit CdS by sputtering are reported in the literature. These are listed in Table VII.

CdS thin films are also formed by reactive sputtering from a Cd cathode in a mixed H₂S–Ar atmosphere. This sputtering process corresponds to the vapor reactions described above. The H₂S–Ar dissociates in the flow discharge, and the sulfur ions react with the cadmium atoms at the substrate surface.²³⁴ In this method the stoichiometry of the resultant films can be varied over a wide range by varying the partial pressure of H₂S and the sputtering conditions. Moisture entrapped in the H₂S may cause poor adherence of the film to the substrate.²³² Albrand *et al.*⁹⁴ have attempted to sputter cadmium in a sulfur atmosphere generated by evaporating sulfur. Fraser and Melchior²³¹ produced insulating, photoconductive films by sputtering CdS in an Ar–H₂S atmosphere.

c. *Conversion of Films of Cd or Cd Salts by Heterogeneous Reactions*

A film of cadmium metal or of a suitable cadmium salt is first deposited on the substrate. It is then converted to cadmium sulfide by heating in an atmosphere of H₂S or S vapor.

Weissmantel^{235,236} baked evaporated cadmium films on glass and mica in sulfur vapor. The reaction was very slow, but could be carried out at relatively low temperatures.

Lawrance²³⁷ applied a variety of techniques to obtain photoconductive CdS layers. In one method reactive sputtering in air^{238–241} was used to obtain CdO films on glass, which were then converted by heating in H₂S at 500°C. There was some difficulty in obtaining complete conversion of thicker films. Other films were prepared by spraying solutions of cadmium salts and also by melting anhydrous cadmium chloride.

d. *Deposition from Alkaline Thiourea Solution*

Mokrushin and Tkachev²⁴² first prepared very thin films of CdS by deposition from aqueous alkaline solutions by thiourea. Since then the deposition mechanism has been studied in some detail and is fairly well understood.^{36,38,243–247} The dissociation of thiourea in an alkaline medium and the precipitation of the sulfide ions is catalyzed by a solid phase.²⁴⁶ Initially, the latter is provided by Cd(OH)₂ which induces nucleation on

TABLE VII
DEPOSITION OF CdS FILMS BY SPUTTERING

Reference	Cathode	Voltage (kV)	Current Density (mA/cm ²)	Substrate Material	(Anode) Temperature (°C)	Gas	Pressure (Torr)	Rate of Deposition (Å/Min)	Film Thickness (μm)	Application
<u>Sputtering of CdS in Ar or Ne</u>										
Brincourt ²²²	pure compressed powder	3		quartz	170	Ar	3×10^{-2}	50	1.5	electr. and optical prop.
Yefremen'kova ^{111,223,224}	sintered powder, In Cl ₃ or CdI ₂ doped ³	0.5-3	0.2-3.3	glass, SiO ₂ , conduct. glass, mica, NaCl, ruby	50-450	Ar	10^{-1} to 10^{-2}	30 to 600	<0.1 to 5	structure, photovoltaic devices
Yurasova ²²⁵ Gerasimov ²²⁶	sintered powder	1.5-3	0.3	rocksalt pyrophyllite, mica		Ne	8×10^{-2}	18-60	<0.1	epitaxy
Lagnado ²²⁷ , Lichtensteiger ²²⁸	sintered powder	RF		glass, CdS	170, <350	Ar	5×10^{-4}	600-9602	<10	structure
Honda ²²⁹		RF			220-340	Ar		40-50	0.1 to 1	photoconductor
Leighton ²³⁰		DC & RF		glass, quartz	20	Ar	2×10^{-2}	200		electr. prop.

Sputtering of CdS in H₂S-Ar Mixture

Fraser & 231
Melchior
glass, SnO₂, In 200-320 H₂S-Ar 0.05 170 3 photoconductor

Reactive Sputtering of Cd in H₂S-Ar Mixture

Helwig²³² Cd 1 glass ambient to >600 H₂S-Ar 10⁻¹ to 10⁻² photo-conductivity
 Dresner & 131
Shallcross²³¹ Cd glass 20 to 200 H₂S-Ar structure,
 Lakshmanan &
Mitchell²³³ Cd, Cu and In
alloys glass H₂S-Ar 0.5 photoconduc-
 Pompei²³⁴ 2-3 0.3 H₂S-Ar 60 0.175 tive & photo-
 voltaic prop.
 sputtering
 technique

Reactive Sputtering of Cd in S-Ar Mixture

Albrand⁹⁴ Cd glass S-Ar 0.1

the substrate. An optimal value of the $[\text{OH}^-]:[\text{NH}_3]^3$ ratio is 1.65×10^{-2} at 25°C. Continued presence of the solid $\text{Cd}(\text{OH})_2$ after nucleation is unnecessary, since the CdS layer formed now acts as the catalyst, and undesirable, since it causes most of the CdS to precipitate in the bulk of the reaction vessel. By now adding excess ammonia or an ammonium salt, the hydroxide is dissolved and the cadmium is complexed as cadmium tetrammine. The latter is converted to CdS only at the substrate.

Nagao and Watanabe²⁴⁸ essentially used this method to deposit films of up to 2.2 μm on glass and single crystals of zinc sulfide. They added aqueous solutions of $\text{Cd}(\text{NO}_3)_2$, NaOH , NH_4NO_3 , and thiourea successively to deionized water. Just sufficient NH_4NO_3 was added to redissolve all the $\text{Cd}(\text{OH})_2$ precipitated by the NaOH in order to obtain films of optimum thickness.

Deshotels *et al.*³⁸ added NH_4OH to a cadmium salt solution, preferably CdSO_4 , until the precipitated $\text{Cd}(\text{OH})_2$ was redissolved. Then the solution of the sulfur releasing agent was added in slight stoichiometric excess. Both thiourea and thiosinamine formed CdS at a reasonably slow rate; thioacetamide precipitated CdS almost instantaneously and cystine did not produce any CdS . Previous attempts using caustic soda and complexing agents (EDTA) instead of ammonia to keep the Cd in solution resulted in thin, powdery, nonadherent films.³⁶ The method cannot be applied to H-film substrates, since these are attacked by ammonia and caustic soda. Films several micrometers thick may be built up by repeated deposition.

The films possess a very small grain size and are at least partly cubic in structure with the *c*-axis mainly perpendicular to the surface.^{38, 248} They can be doped by adding dopants soluble in alkaline solutions.^{36, 248, 249}

Films of Cd metal or Cd salts may be converted into CdS films by prolonged treatment in solutions of thiourea, thioacetamide, or ammonium sulfide.³⁶ This provides a low temperature alternative to the treatment in H_2S or S vapor described in Section 6.c.

e. Chemical Spray Reactions

The method consists of mixing reagents in aqueous solution and spraying them onto a heated substrate.⁹¹ The reagents consist of cadmium salts and sulfo-organic compounds as in the case of the chemical deposition described in the preceding section, but in this case the reaction is by pyrolytic decomposition at the substrate of the soluble complex formed on mixing the reagents. The decomposition is endothermic, requiring a minimum substrate temperature depending on the composition, and produces a CdS film and volatile biproducts.

Chamberlin and Skarman⁹¹ used 0.001–0.05 M concentrations of cad-

mium chloride and thiourea to deposit CdS films. The choice of the cadmium salt determines the crystallinity of the film. Cadmium acetate produces an amorphous film (crystallites smaller than 400 Å) on an amorphous substrate, whereas cadmium chloride produces a film whose structure depends on the substrate material and temperature and whose orientation varies with the anion-cation ratio. This should be 1:1 to obtain films with the *c*-axis oriented perpendicular to the substrate. The method was also used by Micheletti and Mark.^{250,251}

Metallic substrates produce amorphous deposits, unless the surface of the metal is changed by a chemical reaction.²⁵² Platinum and copper produce layers of PtS and CuO, respectively, on which a crystalline deposit can be formed. Crystalline films on other metals may be obtained either by first depositing a thin amorphous film at a low temperature followed by deposition of a crystalline film at a higher temperature or by coating the metal with a CdCu alloy.¹¹² Deposited films on glass and ceramics show an inverse relationship between the crystallinity of the film and that of the substrate. Crystalline surfaces provide a large number of nucleation sites, whereas in amorphous substrates there are only a few such sites enabling the deposited CdS crystallites to grow laterally as well as vertically.

The reagents can be doped, as long as the dopant does not react chemically. For example, if a cadmium sulfide film is to be doped with copper, *N,N*-dimethyl thiourea is needed to prevent the precipitation of copper hydroxide on adding copper acetate to the solution.⁹¹

Deshotels *et al.*^{18,86} used several modifications of the spray process. In one method two separate spray guns containing cadmium chloride and ammonium sulfide, respectively, were focused on the substrate which was heated to a temperature of 400°–600°C. It is believed that the films were sintered at these temperatures, the cadmium chloride acting as a flux (see below). Nitrogen was used as carrier gas. A more convenient method employed a single spray gun operating on H₂S gas and cadmium chloride. It was important to exclude oxygen, which produced CdO. For this reason cadmium nitrate was not a satisfactory substitute for cadmium chloride. The films could be doped with indium or gallium by adding a chloride or nitrate of these metals to the solution.

Wu, Feigelson, and Bube²⁵³ spray deposited a mixture of CdCl₂ and thiourea on glass at 450°C in air. The film was subsequently heated at 650°C for 60 min with CdCl₂ and CuCl₂.

f. *Sintered Layers*

Sintered layers of cadmium sulfide are widely used as photoconductors. In a typical process cadmium sulfide powder is mixed in a slurry with

TABLE VIII: PREPARATION OF SINTERED FILMS

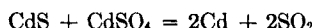
Reference	Pre-sintered	<u>Suspension</u>			Application to Substrate	Substrate Material	Time min.	<u>Sintering Temp.</u> °C	Gas	Film Thickness μm
		Dopant	Binder	Vehicle						
Thomsen ^{198,254} Hadley ²⁵⁵ Nicol ¹¹⁵	no	Cu salt		water	spray	glass	5	600	limited air	5 to 25
Thomas ²⁵⁶	yes	CuCl ₂ or basic copper carbonate	ethyl cellulose	xylene	spray, flow-on	Pyrex	10	550	air	50 to 125
Billups ²⁵⁷	yes	CuCl ₂	polystyrene or ethyl cellulose	xylene	spray, settling	Pyrex	10	535	air	40 to 225
Kitamura ²⁵⁸⁻²⁶⁰	no	CuCl ₂		water	spray	glass, quartz, ceramics	5-20	600	N ₂ , N ₂ +H ₂ S cool in air	5 to 10
Sihvonen ²⁶¹	yes		ethyl cellulose	butyl cellosolve	screen	alumina		570	limited air	2 to 25
Hill ²⁶²		CuCl ₂		water	spray	conducting glass, Mo	5	600	air	100
Micheletti ²⁶³		CuCl ₂				Al ₂ O ₃		600		3 to 5
Deshotels ^{36,37}	yes	InCl ₃ , In ₂ S ₃		water, methanol	brush, screen, spray, roll	Pyrex, copper foil	5-30	600	argon, nitrogen	
Griffin ⁷⁴				water, methanol	spray	Pyrex, Mo, tin coated steel	30	500-800	argon	

cadmium chloride and other dopants and presintered. The material is then ball-milled to produce a fine particle powder. The latter is suspended in a slurry using either water or an organic solvent. Often an organic binder is added. The slurry is applied to the substrate most commonly by spraying, but a variety of other techniques have also been used. After drying the substrate is heated to a temperature from 500 to 600°C. Different variants of this method are listed in Table VIII.

The use of cadmium chloride, which acts as a flux, is essential to the process. CdCl₂ melts at 568°C and CdS dissolves in molten CdCl₂. The sintering process promotes particle fusion and granule regrowth at a relatively low temperature, so that sintered films resemble single crystals in many of their properties. Chlorine also acts as a donor in CdS, which is undesirable for some applications. However, CdCl₂ volatilizes above 400°C and at 600°C the volatilization is complete, whereas that of CdS is negligible. The chloride may also be leached out.²⁶¹

The films are frequently sintered in air for use as photoconductors. This leads to the formation of cadmium oxide.²⁵⁸ Glass, quartz, and ceramics make good substrates for sintered films, but the sintering temperature is too high for plastics, and many metals undergo chemical reactions. The films flake off tin-coated stainless steel; and copper tends to migrate into the film.^{37,38}

Sintering of CdS layers deposited without CdCl₂ is not very successful, since higher temperatures are required, which causes the CdS to evaporate. Photoconductors have been made by compressing activated CdS powder into tablets and then sintering the material.^{264,265} Kanev *et al.*¹¹⁷ compressed the powder under a pressure of several hundred kilograms per square centimeter followed by heating in argon at 850°–950°C. During sintering the cadmium sulfide reacts with cadmium sulfate present as an impurity



The cadmium liberated increases the conductivity. Gombay *et al.*^{266,267} compressed CdS powder followed by slow heating to 520°C. Wendland²⁶⁸ developed a method in which a mixture of CdS, CdCl₂, and CuCl₂ is first fired at 600°C in air, mixed with acrylic powder as binder, and then molded at 8000 psi at 250°C. It is claimed that this provides a mechanically stronger layer, while retaining the desirable electrical qualities of sintered layers.

Schaefer *et al.*^{66,73} attempted to deposit CdS by electrophoresis of a colloidal suspension of CdS in isopropyl alcohol onto molybdenum substrates. Before sintering the films possessed no adhesion. On prolonged sintering in argon at temperatures from 750° to 900°C the films evaporated. At lower temperatures the adhesion improved, but the films remained amorphous.

6. JUNCTION FORMATION

a. *Electroplating*

In the first single crystal CdS solar cells made by Reynolds^{1,8} the junction was formed by electroplating copper from copper sulfate solution followed by oxidation and heat treatment. A strongly acidic plating bath produced a layer of finely divided copper particles.

Williams and Bube¹³ obtained the best results by omitting the heat treatment and using a copper cyanide plating solution. A copper sulfate solution gave a different spectral response. The diffusion of copper into the CdS under heat treatment greatly lowered the photovoltaic response and changed the spectral distribution due to the generation of a high resistance photoconducting layer of CdS next to the junction.

In the early thin film solar cell program both at Harshaw^{62,65,71} and at Clevite^{18,35-37} junctions were fabricated by the electrodeposition of mossy black copper followed by oxidation. The cells possessed relatively low efficiencies. Electroplated cells have poor diode characteristics due to high shunt losses.²⁵

b. *Evaporation*

The application of the copper by evaporation followed by oxidation and heating was attempted at Harshaw^{269,271} in 1957 on single crystals. A similar method was used by Woods and Champion¹⁰ and by Fabricius.¹⁶ The latter noted that the photocurrent increased by three orders of magnitude on heating. He attributed this either to the removal of Cu₂O which acts as a grey light filter or to the removal of surface states. The heat treatment causes the diffusion of copper impurities into the depletion region and the formation of S vacancies due to outgassing.

It was attempted at Clevite to apply Cu₂S by vacuum deposition. Initially this was done on backwall cells. The Cu₂S was evaporated onto a glass substrate followed by the CdS layer.^{33,34} At a much later stage it was attempted to form the junction by vacuum deposition of Cu₂S, followed by immersion in Na₂S. In another variation copper was vacuum deposited followed by immersion in a solution of sulfur in benzene. None of these attempts was successful in making efficient solar cells.³

David *et al.*¹⁰⁴ employed flash evaporation of Cu₂S. The thickness of the Cu₂S layer was 0.25 μm. Clark *et al.*¹⁰⁷ and Mickelsen and Abbott¹⁰⁸ evaporated purified cuprous chloride from a quartz crucible, followed by an air bake. The dry process was intended to minimize the formation of Cu₂S in pinholes and cracks. However, the cells showed a much lower efficiency.

Mickelsen and Abbott were able to improve the efficiency somewhat by applying an HCl etch before deposition and by subsequent heating in hydrogen.

c. *Brushing*

In early work at RCA, Moss^{77,79} found that the electrodeposition of copper leads to unevenness on polycrystalline CdS. He applied a paste of finely divided metallic copper by brushing or silk-screening, followed by heat treatment.

In early work at Harshaw^{4,269} Cu₂O or Cu₂S was deposited from a slurry, followed by heating. During 1964, the barrier-formation process in use at Clevite^{37,41} involved the application of a cuprous oxide suspension in water with a brush at a temperature of 90°–100°C. After drying the excess Cu₂O was wiped off, and the cell was heated to 200°C for a few minutes. This method was applied to backwall cells.

d. *CuCl Dip*

In this method the CdS layer is dipped for a period of a few seconds into a suspension of CuCl in water at 90°–100°C. This is followed by a heat treatment at 250°C for about 2 min.

The chemiplating technique was described by Cusano²⁷⁰ in 1962 for the formation of photovoltaic Cu₂S/CdS junctions. The procedure was first used for the fabrication of solar cells by the Harshaw group⁷¹ in 1964. In the following year the Clevite group also went over to the cuprous chloride dip process and a striking improvement in cell efficiency was obtained.^{29,44,45,47} Although many alternative processes have since been tried, none has given better results.

The process is known to form a layer of cuprous sulfide on the cell surface, probably by the ion-exchange reaction:



Hill and Keramidas^{272–274} have suggested that this reaction stops before equilibrium is reached and that the concentration gradient results in a very slow diffusion of all components.

An HCl etch is necessary before the chemiplating operation to achieve a high solar cell efficiency. The CdS layer must be sufficiently thick to prevent shorts caused by etching. Etching in aqueous HCl causes preferential etching at grain boundaries and surface roughness.⁶⁰ The short-circuit current is markedly increased.⁹⁶ The etch is critical for optimizing the shunt resistance at low light levels.²⁷⁵

Shiozawa^{119,276} measured the thickness of the Cu₂S layer as a function of the dipping time for oriented CdS plates by an interferometric method. The thickness increased linearly with time, but varied with the crystallographic orientation of the CdS crystal. Shiozawa⁶⁰ obtained a revised value of 0.35 μm for the thickness in a high efficiency thin film solar cell allowing for grain-boundary penetration. Van Aerschot²⁷⁷ and Fabbricotti²⁷⁸ obtained values from 0.10 to 0.15 μm from an electron microprobe analysis of the Cu₂S barrier layer and proton damage experiments. Egorova¹⁰¹ found the value to be on the order of several hundred angstroms. Values from 1 to 5 μm were obtained by Gill and Bube^{279,280} and by Shitaya and Sato²² on single crystal CdS. Very thin layers from 0.1 to 0.5 μm were obtained by Gill and Bube²⁶ in a CuCl and hydroxylamine solution with 1–5 min dips.

Shitaya and Sato²² and Shiozawa⁶⁰ point out that a highly nonplanar structure is essential to obtain a high efficiency cell. Rough junction surfaces result in effectively large junction areas due to multiple reflections of light. Nakayama¹²² made a ceramic cell in which the maximum penetration depth of the Cu₂S was 60 μm, thus greatly improving the light absorption efficiency.

As the thickness of the Cu₂S layer increases the open-circuit voltage is constant at first and then decreases.^{95,96} The short-circuit current for long wavelengths increases initially with the thickness of the Cu₂S layer, but that produced by short wavelengths decreases.^{97,101} Thicker Cu₂S layers have a poor shunt resistance.⁹⁶ The short-circuit current decreases as the thickness exceeds the diffusion length of electrons in Cu₂S^{60,120}. The optimum thickness is less in undoped ceramic cells than in In doped cells. Mytton¹⁰⁰ has shown that these phenomena are caused by shorting of Cu ions across vertical grain boundaries and by the isolation of crystallites.

Care must be taken to exclude cupric ions from the solution. Gill and Bube^{26,27} employed a saturated solution of CuCl and hydroxylamine to ensure the reduction of Cu to Cu⁺. The growth had a linear time dependence, suggesting that the growth rate is controlled by an interface reaction. The Cu₂S layer grew more rapidly on the Cd (0001) face than on the S (0001̄) face. Van Aerschot and Reinhartz²⁸¹ utilized a CuCl–NH₄Cl solution with varying copper concentrations to achieve thermodynamic equilibrium. The formation rate of the Cu₂S layer was proportional to the square root of the time and increased slowly with the total copper concentration. The short-circuit current, efficiency, and the red spectral response were dependent on both free Cu⁺ and Cl⁻ concentrations. Also the electrochemical potential of the solar cell during plating is an important parameter influencing the efficiency.

e. *Other Chemiplating Processes*

Cells with efficiencies exceeding 8% were prepared at Clevite²⁹ by replacing HCl by HBr or HI in the prebarrier etch step. However, the cell output was maintained for only a few hours. The replacement of CuCl by CuBr for the dip solution was less effective. Dipping the films in Na₂S or CdCl₂ solutions prior to barrier formation was not effective. Kanev *et al.*^{11a} formed a junction in sintered CdS by dipping into an aqueous solution of boiling copper sulfate followed by heating for 30 sec at 350°C.

It was thought that the elimination of water from the processing cycle would improve the stability. Organic solutions for the dip process were originally used by the RCA group during early work.³ Good results were obtained at Harshaw⁷⁶ in 1967 with a mixture of lithium and cuprous iodides in ethylene glycol. Clevite experimented with a solution of CuCl in acetone. At Harshaw⁷⁶ it was also attempted to use molten salt baths consisting of eutectic mixtures of cuprous salts with other salts in the temperature range from 120° to 300°C. However, the high temperatures led to reactions so rapid that they could not be accurately controlled.

f. *Heat Treatment*

An essential step in the junction formation process is a short heat treatment after the copper deposition, which causes some copper diffusion into the CdS. Williams and Bube¹³ heated the cell to 380°C for 15 sec, and this produced a deleterious effect on the photovoltaic response. Hill and Keramidas²⁷²⁻²⁷⁴ concluded that heating at 300°C increases the Cu⁺ concentration inside the cell and the Cd²⁺ concentration near the surface. Prolonged heating reduced the photovoltaic conversion efficiency. Van Aerschot²⁷⁷ and Palz⁹⁵ suggest that the heat treatment also removes residual traces of Cl and Cd from the Cu₂S layer.

Egorova¹⁰¹ observed the photovoltaic effect immediately after formation only if the CdS film was doped by acceptors or prepared at high substrate temperatures. Those films with high donor impurities required additional heat treatment to show the effect. The same result was obtained by Palz *et al.*⁹⁵ A cell with a 300 ohm-cm CdS layer showed no change in output on heating. Bube *et al.*^{26,282} prepared high efficiency single crystal photovoltaic cells by dipping in warm CuCl without subsequent heat treatment.

Hill and Keramidas²⁷⁴ concluded that it was necessary to heat the cell in air or oxygen, which increased the resistance of Cu₂S by one order of magnitude. The effect took place more slowly on standing in air. The majority of acceptors in Cu₂S were oxygen atoms. Heating in air causes the oxygen acceptor concentration to rise to a level determined by the atmos-

pheric oxygen concentration. If, on the other hand, the cells are heated in vacuum, nitrogen, or argon the resistance of the Cu₂S layer increases, as the acceptors in the Cu₂S diffuse into the bulk CdS.

The Clevite group^{57,278,283,284} also considered that exposure to oxygen in the form of oxygen, air, or hydrogen peroxide is required either during or prior to the 250°C heat treatment to obtain an observable photovoltaic effect. Exposure to argon alone did not produce an effect. The oven treatment serves a secondary purpose in removing water from the barrier layer. Boer²⁵ considered the reaction to form Cu₂S (djurleite) to be more rapid in air due to the oxidation of Cu.

The heat treatment improves the photovoltaic properties by decreasing the shunt losses. Bube^{21,26,279,285} found that heating in air at 250°C increases the open-circuit voltage. Boer²⁵ and Bogus¹⁰⁶ showed that the open-circuit voltage under low intensity blue and red illumination increases with the heat treatment time and then saturates. The short-circuit current decreases monotonically with time on heating at 250°C.²¹ The short-circuit current decreases rapidly under red light and less rapidly under blue light.²⁵ Kanev, Fahrenbruch, and Bube^{26,282,286-288} concluded that the degradation is not due to thermal diffusion, but mainly due to a photochemical change in the heat treated junction associated with the presence of a high concentration of excess copper. The degradation was not present at 77°K and could be removed by heat treatment above 100°C.

The variation in open-circuit voltage and short-circuit current causes the maximum power to go through a maximum after 7 min of heating in air at 250°C.²¹ The fill factor is also improved by heat treatment,⁹⁷ but decreases under prolonged heat treatment, suggesting a diode shunt effect.¹⁰⁶ The diode *A* factor† passes through a minimum and then increases with heat treatment under red light and in the dark; it decreases steadily under blue light. The saturation current goes through a minimum and then increases under red light and in the dark; it remains constant under blue illumination. Gill and Bube^{26,279,285} showed that the forward dark current decreases by five orders of magnitude after heating for 1 min. The heat treatment causes a crossover of the forward light and dark current-voltage characteristics.

† The output current *I* of a solar cell is given by the equation^{288a}

$$I = I_o \left\{ \exp \left[\frac{q}{AkT} \left(V - IR_s \right) \right] - 1 \right\} - I_l + \frac{V}{R_{sh}} - \frac{IR_s}{R_{sh}}$$

where *V* is the output voltage, *I_l* the light-generated current, *I_o* the reverse saturation current of the diode, *R_s* the series resistance, *R_{sh}* the shunt resistance, *k* is Boltzmann's constant, *q* the electronic charge, and *T* the absolute temperature. In this equation the diode *A* factor is a dimensionless constant between 1 and 5.

The heat treatment alters the spectral response; see Section 12. The copper diffusion forms a narrow region of highly compensated CdS at the CdS-Cu₂S interface which is affected by the illumination and exhibits deep trapping effects.^{26,285} The thickness of this layer in CdS single crystals is 0.5 to 0.8 μm.^{60,279,289,290} Shiozawa⁶⁰ suggests that in thin film cells the thickness is 1-2 μm.

Gill and Bube^{280,285} observed a light-induced breakdown effect under reverse bias before the heat treatment, which they attributed to tunneling from the Cu₂S valence band to the CdS conduction band at high field points along the junction. The reverse breakdown effect could be correlated with visible defects in the junction. Gill and Bube considered the forward current to be tunneling limited also, and reduced by heat treatment.

7. COUNTERELECTRODE

a. Metal Mesh by Pressure Contact

Griffin,^{62,65} at Harshaw, solved the series resistance problem by applying a metal mesh to the Cu₂S layer of front wall cells. The grid was attached by lamination. The first metal grids used 70 lines/in. and had 85% transmission. In 1966 Clevite switched to 60 × 10 lines/in. with 1 mil lines (91% transmission). Experiments at the University of Delaware¹⁰⁹ indicate that large area cells are improved by increasing the line spacing and also increasing either the linewidth or the thickness.

Cu₂S is so degenerate that contact with any metal including gold should be ohmic. Copper grids showed a low open-circuit voltage, since copper reacts with Cu₂S forming CuS.⁷⁶ Silver and nickel also showed a short-term degradation.²⁹ For this reason a gold mesh was used, which was subsequently replaced by a gold-plated copper mesh for economy reasons.

b. Attachment by Conducting Epoxy

Laminated gold grids with mechanical contact to the Cu₂S layer caused degradation under temperature cycling due to short-circuiting or an increase in the series resistance caused by a relaxation in the pressure contact.²⁹ On relamination a degraded cell could be restored to its original efficiency.

An attempt was made to solve this problem by attaching copper grids with silver loaded epoxy.²⁹ Degradation occurred due to loss of adhesion. The copper grid was replaced by a silver-plated copper grid, but this did not solve the problem. It was postulated that stresses caused by differential thermal expansion between the grid and the CdS layer caused a

buildup of work damage in the CdS, resulting in loss of V_{oc} . It is also possible that the silver caused changes in the crystallographic structure of the CdS in contact with the epoxy.³ Stable cells were finally achieved by cementing gold or gold-plated copper grids with gold loaded epoxy.⁵¹

c. *Electroplated Grids*

Electroplated grids were developed at Harshaw.^{71,74-76} Although these grids produced low efficiency cells, they also showed exceptional stability. The electroplating was carried out through apertures in photoresist masks. The plating process requires fairly high current densities, which may be deleterious to the cell performance. Also plating times had to be minimized to prevent water from the bath degrading the cell. Copper cannot be plated directly onto Cu₂S without causing degradation.

d. *Vacuum Deposition*

The vacuum deposition process can lead to low efficiency cells, because of leakage across the junction. Also evaporated grids possess a limited current carrying capacity resulting in a series resistance. Gold layers thicker than 1 μm showed poor adhesion.^{29,57} Clevite developed a cell using evaporated gold grids overlaid with a standard gold-plated copper mesh and conducting epoxy. These cells showed the same efficiencies as a standard cell.

8. LAMINATION

Lamination was first investigated at Harshaw^{62,65} in 1961–1962. Lamination was carried out between plastic sheets to avoid curling, provide protection, and to facilitate connection into arrays, using thermoplastic films together with layers of release agents to prevent the thermoplastic from sticking to the die. Nylon film (Capran) was used as the thermoplastic despite its hygroscopic properties.

Mylar and Kapton were the commonly used cover materials. Mylar possesses excellent transmission properties, but darkens under ultraviolet radiation.^{71,74} Kapton has poorer transmission, but is far more resistant to ultraviolet, electron, and proton radiation. The deposition of glass layers by rf plasma sputtering was investigated at Harshaw,²⁹¹ but the adhesion was inadequate.

The hygroscopic nylon adhesive layer was replaced by clear epoxy.^{51,76} Humidity tests showed that this improved the cell stability.

IV. Properties of Cadmium Sulfide and Cuprous Sulfide Layers

9. STRUCTURE OF VAPOR DEPOSITED CdS FILMS

Films obtained by deposition from the vapor onto neutral substrates usually possess a textured polycrystalline structure, consisting of crystallites which are randomly oriented in azimuth with one principal face parallel to the substrate. Neutral substrates include glassy and amorphous substrates, as well as randomly oriented thin metal films. Epitaxial CdS films deposited on oriented substrates have found no application in large area CdS solar cells and are, therefore, outside the scope of this review.

a. *Structures*

The hexagonal wurtzite phase always predominates in CdS thin films. The presence of the cubic sphalerite phase is strongly temperature dependent, and is difficult to detect by x-ray analysis. It can be more readily detected by electron diffraction. The occurrence of the sphalerite phase also depends on the nature of the substrate, the presence of impurities, and the rate of deposition.¹⁴¹

(i) *Temperature Dependence.* The structure of vapor deposited CdS films may be divided into three temperature regions: at low temperatures the films possess a defective hexagonal structure, at intermediate temperatures both hexagonal and sphalerite phases are present, and at high temperatures the films are purely hexagonal. Shalimova²⁹² found that hexagonal structures with stacking faults were characteristic for deposits from -150° to 100°C . Andrushko²⁹³ obtained identical x-ray patterns from CdS powders precipitated from aqueous solutions or by annealing amorphous CdS. The degree of perfection increases with the temperature. Wendland²⁹⁴ obtained powder patterns indicating mixed microcrystalline hexagonal and sphalerite phases as well as an amorphous phase in the range from 50° to 100°C . The amorphous phase increased by lowering the substrate temperature and by increasing the deposition rate.

(ii) *Two-Phase Structure.* Shalimova *et al.*^{292,295} observed that the temperature range of the two-phase structure (sphalerite and hexagonal) extended to 250°C for glass substrates and up to 350°C for gold films on glass, demonstrating the influence of the substrate. Palatnik²⁹⁶ observed a two-phase structure in films deposited on a substrate with a temperature gradient over the temperature range from 50° to 180°C . Only hexagonal CdS was seen above 200°C . Bujatti^{140,297} noted the two-phase structure in the range from 150° to 250°C and ascribed them to an unknown impurity.

Palatnik²⁹⁶ suggested that a decrease in the number of sulfur vacancies promotes the formation of cubic CdS. In the two-phase structure larger hexagonal crystallites, <0.1 to 1 μm , are accompanied by much smaller cubic and hexagonal crystallites which give sharp lines in electron diffraction, but which cannot be detected by x-rays.²⁹² Also the cubic (111) plane cannot be distinguished from the hexagonal (0001) plane in oriented films.

(iii) *Stacking Faults.* Kazmerski, Berry, and Allen²⁹⁸⁻³⁰⁰ observed a two-phase structure for substrate temperatures between 120° and 300°C. The cubic phase reached a maximum at 220°C. Electron diffraction indicated that 30% of the material was faulted at this temperature.

Kazmerski *et al.* concluded that the cubic phase is due to highly faulted hexagonal grains in the polycrystalline films. The fault stacking is cubic, while the planes above and below are hexagonal. CdS possesses a very low stacking fault energy. Fault formation takes place during deposition and is also caused by plastic deformation due to the difference in thermal expansion coefficients between film and substrate. Hence the critical dependence of the cubic phase on the substrate temperature.

(iv) *Enclosed and Open Systems.* It may be significant that the phase structure at intermediate temperatures has been observed largely in enclosed vapor deposition systems. Foster¹⁷⁸ made a very thorough examination of thin films deposited on glass and thin metal films in the temperature range from 100° to 230°C. He was unable to identify the cubic phase either by transmission or reflection electron diffraction or by x-ray analysis. In a standard open evaporator the incident beam is highly directional, whereas in an enclosed system there may be a significant number of particles reflected from the enclosure. Also the vapor pressure is usually higher. These differences may have a significant effect on the structure of the thin film, but have not so far been investigated. Shallerross³⁰¹ and others found evidence of needlelike prismatic growth using an enclosed system.

Galkin, Troitskaya, and Ivanov¹⁴¹ obtained a mixture of hexagonal α -CdS and a cubic NaCl phase with a lattice parameter $a = 5.72 \text{ \AA}$, using a close crucible method with a source temperature of 550°–600°C. At lower temperatures a finely dispersed phase was produced. The NaCl phase was also obtained by the sandwich method.

(v) *Thin Films.* Very thin films on neutral substrates are often found to be amorphous, particularly at low substrate temperatures and at high deposition rates.^{157,160,294} Palatnik^{302,303} states that, in the initial stages of deposition on an amorphous substrate at 60°–80°C, a two-phase system is found consisting of hexagonal CdS and excess Cd. This applies to films below 800 Å.

(vi) *Lattice Spacing.* Reflection electron diffraction with 50 keV electrons has shown appreciable deviation from normal line spacings.¹⁶⁰ This may be due to surface conditions. In some films a slight extension, 0.5%, of the interatomic distance of the crystallites in the *c*-direction was observed by Bujatti.¹⁴⁰ Doping by different impurities also produces this effect. Escoffery¹⁴⁹ attributed a change in spacing from 3.357 to 3.38 in films deposited on molybdenum at 175°C to indium doping.

b. Orientation

Thin films deposited from the vapor phase onto a smooth amorphous or inactive crystalline substrate tend to grow with a close packed lattice plane parallel to the substrate surface. This single axis orientation originates from the tendency of atoms, whose mobility is sufficient on the substrate at the condensation temperature, to aggregate first in plane sheets of close packing. In hexagonal films the (0001) basal plane and in cubic films the (111) octahedral plane lies parallel to the surface of the substrate.^{304,305} If there exists a preferred growth direction in the crystallites (along the *c*-axis), then as growth continues those crystallites which initially were oriented with this fast growth direction nearly perpendicular to the substrate begin to predominate, and the thicker films consist of a thin layer of randomly oriented crystallites covered by a thicker layer of highly oriented crystallites.¹³⁹

CdS films more than 1 μm thick and deposited at temperatures above 150°C are found to be highly oriented with the hexagonal *c*-axis perpendicular to the substrate. In general, there is single axis orientation with random orientation in azimuthal directions. Griffin *et al.*⁷⁴ claim to have observed one degree of biaxial orientation on some samples on glass substrates with the *a*-axis more frequent in particular directions in the plane of the film.

The orientation of the (0001) plane is not perfect but assumes a range of angles with respect to the substrate. The result of x-ray pole figure analysis^{18,37,66,189} shows that on glass substrates the most frequent tilt of the (00.2) planes on the substrate side is at an angle of several degrees from the substrate plane. Schaefer *et al.*^{66,189} suggested that the growth they observed by pole figure analysis corresponds to Type II orientation described by Reynolds and Greene^{306,307} in CdS single crystals. A similar orientation was observed by Rozgonyi and Foster³⁰⁸ on thin gold films on quartz. Foster¹⁷⁸ noted that films deposited on glass substrates were oriented at approximately 20° corresponding to a predominant (10.5) reflection. He explained this in terms of a growth habit in which the axes of the crystallites are aligned in a cone about the film normal with a half-angle of ~20 deg. The spread in orientation was from 0 to 35 deg.

From etching experiments Vecht *et al.*³⁰⁹ concluded that in recrystallized CdS films the (0001) S surface is bonded to a glass substrate and that the top surface is (0001) Cd.

(i) *Effect of Film Thickness.* Many measurements have shown that using thin films (<1000 Å) on neutral substrates, the layers consist of small randomly oriented crystallites. This also applies to the layer next to the substrate in thicker films and is independent of the direction of the incident beam, suggesting that this is the initial condensation condition. Foster^{178,179} found some degree of preferred *c*-axis orientation using an open system, and considers that the lack of directivity of the beam in an enclosed system contributes to the randomness of the critical layer.

The degree of preferred orientation increases with the film thickness. Shallicross³⁰¹ describes the effect of increasing the film thickness on a typical CdS film deposited on glass at a temperature of 180°C at a deposition rate of 75 Å/sec. Very thin films, 0.2 μm thick, were randomly oriented. On increasing the thickness, the upper part of the film exhibited an increasing orientation of the *c*-axis perpendicular to the substrate. The degree of preferred orientation changed rapidly in the range 0.5 to 1 μm, very slowly beyond 3 μm. The *a*-axis remained randomly oriented. This applies to all films deposited at normal incidence, or where there is no well-defined beam direction.¹³⁹ The surface roughness remains fairly constant up to 3 μm thickness.³⁰¹

(ii) *Effect of Temperature and Rate of Deposition.* It is evident that the degree of preferred orientation is a function of the substrate temperature. At low temperatures the mobility is low and the orientation is poor. Shalimova *et al.*²⁹² found that for films deposited between -100° and -150°C the only lines clearly visible in a Debye-Scherrer powder camera were those corresponding to the (0002), (11̄20), (11̄22), (11̄24), and (30̄30) planes.

At higher temperatures the crystallites are oriented on the average with respect to the substrate, but there is a spread from the mean. Decreasing the deposition rate also produces an increase in the degree of preferred orientation,¹³³ but the effect of the substrate temperature is dominant.³⁰¹ Pressure bursts from the CdS source give rise to a sudden increase in the deposition rate which causes random orientation.⁷⁴ Doi and Ogawa³¹⁰ found fluctuations of the *c*-axis to be a function of the deposition rate with an optimum at 200–300 Å/min. Wilson and Woods¹⁹³ observed more highly oriented films at slower deposition rates.

Changes in the orientation of CdS films at high substrate temperatures have been observed in enclosed evaporation systems. Terasaki *et al.*³¹¹ noted an inclination of the *c*-axis away from the normal on quartz sub-

strates. Shalimova *et al.*^{292,295} found that layers deposited on the gold films above 350°C were not oriented. These phenomena appear to be associated with recrystallization effects (see Section 9, e).

Bujatti¹⁴⁰ investigated the effect of temperature gradients in the substrate in an enclosed system. The orientation was measured by the ratio of the intensities of the (00.2) and (10.1) lines, the latter being the most intense line in a randomly oriented sample. Below 280°C the temperature gradient had no effect. In the temperature range from 280° to 400°C a temperature gradient of 50°C/cm reduced the preferential orientation by a factor of more than 3.

(iii) *Effect of Doping.* The effect of doping on orientation was investigated by Terasaki *et al.*³¹¹ in an enclosed system. Indium, copper, and gallium doping have little effect, nor do silver and sulfur,¹⁷⁸ but chlorine doping destroys the preferred orientation of the *c*-axis. This is a recrystallization effect that has been observed on heating CdS films in the presence of halogens and also in the deposition of films by chemical transport employing halides. Recrystallization effects are also produced by silver doping at higher temperatures. They are discussed in Section 9, e.

c. Crystallite Size

The crystallite size of CdS films on neutral substrates depends on the film thickness, the substrate temperature, and the deposition rate. A microphotograph of a cross section through a typical CdS film is shown in Fig. 4. The layer next to the substrate consists of very small randomly

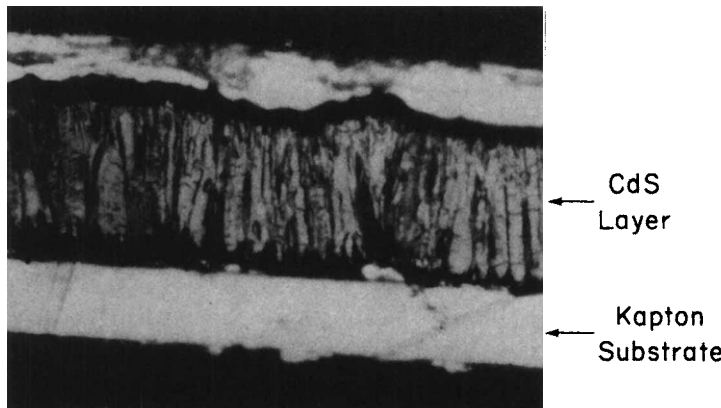


Fig. 4. Microphotograph of cross section through CdS thin film photovoltaic cell. 750 × magnification.

oriented crystallites. As the film thickness increases there are fewer but larger crystallites. Preferential growth normal to the *c*-axis hinders crystallites with an inclined *c*-axis from further growth, and thus results in a more oriented film with larger crystallites and fewer grain boundaries. The preferential growth is due to growth processes that minimize the grain boundary energy and a nucleation that is primarily limited to the substrate interface.¹³⁷ Transmission diffraction data confirm that the crystallite size is larger on the top surface than on the substrate surface.³⁰¹

The crystallite size increases with the substrate temperature and depends inversely on the rate of deposition. Shallerross³⁰¹ found a marked increase in grain size with substrate temperature, especially above 100°C at a deposition rate of 56 Å/sec. On reducing the deposition rate by a factor of 10 the crystallite size increased 50%. Films deposited at low temperature have a high density of initial nuclei and a resultant small grain size. When the substrate temperature is high the density of nuclei is small and the resulting crystallites are larger.

Measured values of crystallite size under different evaporation conditions vary from less than 0.01 to more than 10 μm. The vast discrepancies in these values are primarily due to measurement problems. While electron micrographs give accurately the dimensions of the top surface, the broadening of the x-ray diffraction peaks appears to be primarily due to defects or strain, so that the dimensions derived from such measurements are far too small. This has been verified directly in a number of instances. Deshotels *et al.*³⁷ found that an apparent crystallite size of 41 Å obtained by x-ray methods corresponds to a top surface dimension of 1–5 μm obtained by electron microscopy and produces 0.5 μm etch pits on etching with HCl. Conragan and Muller³¹² obtained a grain size from 500 Å to 5 μm by transmission x-ray diffraction, a grain size of 0.1–1 μm by metallurgical phase contrast microscopy, and HCl vapor etch structures about 10–50 μm across. The last dimension was explained by the formation of CdCl₂ crystallites by the etchant.

In an enclosed system the combination of high substrate temperature and high vapor pressure produces films of highly ordered, relatively large size microcrystallites of dimensions of the order of but somewhat smaller than the film thickness.^{79,139} Zuleeg and Senkovits¹³² were able to obtain surprisingly large crystallites up to 100 μm using a Knudsen source.

The surface roughness is very dependent on evaporation conditions. Aponick¹⁵⁷ used an exhausting source which caused a decay in the deposition rate with time and reduced the surface roughness. Equilibration with the substrate brought about by larger condensation times and higher mobility enlarges the grain size and fills in the asperities. On the other

hand, in an enclosed system the crystallites were bounded by well-defined crystallographic planes as in bulk crystals giving rise to sharp angular boundaries, ridges, and valleys at the surface.^{79,139}

d. *Effect of Heat Treatment*

Heat treatment of cadmium sulfide thin films in different ambients may bring about one or more of the following:

1. Changes in film stoichiometry by out-diffusion of excess material in a suitable ambient or incorporation of material from the atmosphere.
2. Annealing at higher temperatures promotes an increase in crystallite size, changes in film stress, and reduction in the defect density.
3. Films oriented with the basal plane parallel to the substrate undergo a tilting of the *c*-axis at higher temperatures resulting in less oriented films.
4. Recrystallization of the film takes place in a suitable flux (see below).

Annealing in air appears to have a considerably greater effect on the film structure than annealing in vacuum or in an inert gas. Many investigators have shown that heating in air produces CdO. Larger CdO crystallites may in fact have been confused with recrystallized cadmium sulfide. Kahle and Berger¹¹³ and Bujatti and Muller¹⁹¹ noted CdO lines by x-ray diffraction. (100) is the strongest, there is some (111), and the (110) reflection interferes with the (004) reflection of CdS. No cadmium sulfate could be detected. Kitamura²⁵⁸ heated a sintered CdS:Cl:Cu film in oxygen. The surface was examined by an electron microscope using a replica technique. Small surface particles were noted at 300°C. These increased on raising the temperature, and at 600°C the entire surface was covered. X-Ray measurements indicated that at 650°C 20% of the CdS had been converted to CdO.

The cubic phase formed by vapor deposition in an enclosed system at temperatures above 100°C is unstable on annealing in air.^{295,314} The cubic phase disappears completely only at temperatures higher than 500°C. The transition from the cubic to the hexagonal phase produces stacking faults in the superposition of the atomic layers.

Annealing at higher temperatures increases the crystallite size. Schaefer *et al.*⁶⁶ investigated the following techniques for promoting grain growth in cadmium sulfide:

1. Annealing films on molybdenum, glass, quartz, and tin oxide substrates by rapidly heating in a Bunsen burner at 800 to 1100°C.
2. Current was passed through molybdenum substrates for several

hours, heating the films to 550 to 600°C. This resulted in larger grains, dendrites, and faceting. An oxide was formed when the method was attempted in air at higher temperatures.

3. Films were annealed in a high vacuum using a heating tape or other heat source.

e. Recrystallization

(i) *Methods.* When cadmium sulfide films are heated in contact with certain metals above a certain critical temperature, they undergo recrystallization with the formation of larger crystallites and change in orientation. Gilles and van Cakenberghe,^{194,195} who first observed the phenomenon in cadmium sulfide, found that recrystallization with silver and copper produced very large crystallites, while lead, indium, aluminum, bismuth, zinc, and zinc sulfide form smaller crystallites. Addiss¹⁹⁹ was unable to obtain recrystallization with indium and lead.

A number of techniques have been developed for recrystallization. In the method originally described by Gilles and van Cakenberghe a thin layer of the activator, about 100 Å thick, is deposited on top of the cadmium sulfide film, which is then annealed in an inert atmosphere above a critical temperature below which no recrystallization takes place. Variants of this method consist in depositing the cadmium sulfide layer on a substrate coated with the activator, or by coevaporating cadmium sulfide and the activator onto the substrate.

In the embedding or microcrystallization technique³¹⁵ the film is embedded in CdS powder doped with copper or silver (acceptors) and with gallium or chlorine (donors) and heated in air or argon. Organometallic techniques³¹⁶ have also been developed in which the cadmium sulfide film is placed in a hot inert organic liquid containing traces of an organometallic compound. Diethyl dithiocarbamate complexes of copper or silver have been used with a coactivator or paradichlorobenzene in a medium of silicone fluid M.S. 704 or dinonylphthalate.

All growth promoting metals form sulfides partly soluble in cadmium sulfide. The amount of activator above a minimum, 0.16 at.%, is not critical. It is possible that an association of one of these metals with sulfur or with a halogen will reduce the surface free energy sufficiently to nucleate crystal growth.³¹⁴ The process is strongly affected by impurities, which decrease the activation energy. On increasing the indium content the critical temperature is raised from 500° to 600°C. Addiss¹⁹⁹ found that 10% of oxygen lowers the critical temperature, but decreases the crystallite size. Kahle and Berger¹⁹⁶ state that oxygen and CdS vapor inhibit recrys-

tallization. On the other hand, Behringer and Corrsin³¹⁷ and Boer^{318,319} observed an increase in crystallite size with oxygen. Kahle and Berger³¹⁶ showed that recrystallization may be achieved in vacuum or argon at 700°C in the absence of any impurities, and also that the recrystallization is influenced by evaporation parameters.

(ii) *Recrystallization Mechanism.* Addiss³¹⁹ made a detailed study of the recrystallization process, which consists of the formation of a nucleus followed by its extended growth across the film. Some of the silver, or other activator, is transported along with the growth front. Nucleation takes place at sites along the edge of the silvered area, at the edge of the film, at film inhomogeneities, and at sharp corners. A strain gradient is present at these sites. Vapor deposited films are under stress, which is relieved only when the activator is present, but before recrystallization occurs. The critical temperature depends on boundary conditions as well as on impurity content.

The incorporation of some of the activator into the crystal lattice results in the formation of a transition phase—a microcrystalline matrix of cadmium sulfide and the activator. It is a highly disordered phase containing a high concentration of defects—vacancies, interstitials, and clusters. The atoms in this phase are highly mobile, resulting in rapid diffusion and strain relaxation. The recrystallized region grows from this phase by deposition of the mobile atoms onto the growing crystallites. An important function of the activator is to provide for a sufficiently low activation energy so that a relatively fast growth rate, 0.1–0.5 μm/sec, occurs.

Recrystallization does not depend on the nature of the substrate. Crystalline and amorphous substrates are equally suitable. Randomly oriented very thin films, less than 1000 Å, will not recrystallize.

(iii) *Structural Changes.* Recrystallized films are always hexagonal in phase. Partly cubic films are converted to wholly hexagonal films by recrystallization.

The van Cakenberghe technique using a silver film is capable of producing crystallites several centimeters in size. Embedding and organometallic techniques can be applied at far lower temperatures, down to 250°C, but the crystallites do not exceed 10 μm.

Recrystallization is accompanied by an average tilting of the *c*-axis of up to 30° from the substrate normal. In embedding the preferred orientation is similar, but with a broader distribution of crystal orientation.³¹⁵

Larger crystals contain many small-angle grain boundaries. Uniform subgrains up to 1 mm give rise to a feathering appearance between crossed polarizers. In the organometallic technique a high activator concentration results in rapid growth of feathering crystals, while a low activator con-

centration produces plate crystals.³¹⁶ The feathers dissolve on etching for 1 sec in cold nitric acid. The etched recrystallized layers show inclusions, growth steps, and tension lines.³⁰⁹

Kazmerski, Berry, and Allen³⁰⁰ recrystallized evaporated CdS films on the hot stage of an electron microscope. Faulted films could be recrystallized into cubic CdS. Recrystallized films had a crystallite size of 1–2 μm and a misorientation of 17 deg from the substrate normal.

10. STRUCTURE OF FILMS PREPARED BY OTHER TECHNIQUES

a. *Vapor Phase Deposition*

Vapor phase deposition has been primarily employed to grow epitaxial films of cadmium sulfide on single crystal substrates. Films prepared in evaporators in an inert gas at low pressures possess the same structure as films deposited in vacuum under the same conditions. Relatively few investigations have been made of the structure of cadmium sulfide films deposited on amorphous substrates by vapor phase deposition and sputtering. These are listed in Table IX. The undoped cadmium sulfide films prepared by iodine transport are randomly oriented.²⁰⁰ The effect of halogens to induce random orientation has been noted by Behringer and Corrsin³¹⁷ and appears to be related to the temporary attachment of the halogen atoms to Cd surface atoms.

b. *Sputtering*

Yefremenkova^{111,223,224} has made a thorough study of the structure of sputtered CdS films on glass as well as on single crystal substrates. The orientation and dimensions of the crystallites increase with thickness from 500 Å to 5 μm . The thicker films have good one-dimensional orientation with grain dimensions on the order of 1 μm . The phase composition of the thicker films varies as a function of temperature and deposition rate in the same manner as on single crystal substrates. Cathode sputtering produces compact films, similar to vacuum evaporation in the presence of a transverse electric field.^{321,322} At a temperature of 80°–150°C there is distinct faceting of the crystallites on amorphous substrates.

Lagnado and Lichtensteiger²²⁷ succeeded in depositing single crystal CdS films on glass substrates by rf sputtering. The films were highly oriented with the *c*-axis perpendicular to the substrate. The orientation improved at deposition temperatures above 90°C and at deposition rates greater than 300 Å/min.

Dresner and Shallcross¹⁸¹ compared the structure of CdS films prepared

TABLE IX
STRUCTURE OF FILMS PREPARED BY VAPOR PHASE DEPOSITION AND SPUTTERING

Reference	Substrate	Gas Ambient	Temperature (°C)	Deposition Rate (μm/min)	Thickness (μm)	Measure- ment*	Structure	Preferred Ori- entation Parallel to Substrate	Crystallite Size (μm)
1. Vapor Phase Deposition									
a. Vapor Transport									
Shalimova ²⁹²	glass	Ar & H ₂ , 0.1-1 torr	> 200		0.5 - 0.6	x	hexagonal	(00.1)	
Gross ³²⁰	glass, quartz	10 ⁻² torr	ambient-600	1.8	0.04 - 1.2	e.d., e.m.	hexagonal		0.1
b. Chemical Transport (close space)									
Hegyi ²⁰⁰	glass	H ₂	380 - 500	0.1 - 0.3	> 1	x	hexagonal	(00.1), strongly oriented	crystallite size = film thickness
		I ₂ , In or Cd doped	480	0.01 - 0.03	0.3		hexagonal	(00.1), oriented	0.1
		I ₂ , undoped	480	0.01 - 0.03	0.3		hexagonal	random	
2. Sputtering									
Fraser & Melchior ²³¹	glass, SnO ₂		< 320			x, SEM	hexagonal	(00.1)	1
Brincourt ²²²	quartz		170	0.005	1.5	x	hexagonal	(00.1)	
Yefremenkova ^{111, 223}	SnO ₂ on glass, glass, amorphous SiO ₂		50 - 160		< 0.1	e.m., e.d.	polycrystalline		micro-granules
					0.2 - 0.5			more oriented	0.5
					1 - 5			(00.1), well oriented	1
				0.003 - 0.006	1 - 5		hexagonal	(00.1)	
				0.012 - 0.018			hex., cubic	(00.1); (100)	
				0.03 - 0.06			mainly hex.	(00.1)	
			300 - 450	0.018 - 0.036			hex., cubic	(00.1); (100)	
Lagnado ²²⁷	glass	Ar	90 - 350	0.03 - 0.1		x, e.d.	hexagonal	(00.1); epitax.	

* x = x-ray diffraction, e.d. = electron diffraction, e.m. = electron microscope.

TABLE X
STRUCTURE OF FILMS DEPOSITED BY CHEMICAL SPRAY REACTIONS*

Substrate	Crystallinity	Preferred Orientation Major	Minor	Crystal- lite Size (μm)	Reference
1. Glasses and Ceramic Substrates					
Glass	highly crystalline	(00.1), some films random	(10.1),(10.0)	> 0.1	91,113,252, 323
				1-10	18
Pyroceram	highly crystalline	(00.1)			113
Devitrified glass		(10.1),(00.1), (10.0)			252
Glass covered metal		(10.1)	(00.1),(10.0)		252
Ceramic	reduced crystallinity			0.1	91,250,250
Sintered alumina		random			252
2. Metal Substrates					
Mo,Cd	amorphous				113
Al,W,Ta	poor crystallinity				113
Pt	PtS formed	poor crystallinity			252

Cu	$\text{CuO}, \text{Cu}_2\text{S}$ formed			252
Pb-Sn		fair crystallinity	(00.1), (10.1) (10.0)	113
Cd-phosphor bronze alloy	CdS, CdO formed	crystalline	(00.1) (10.1), (10.0)	112, 252
Double deposition on Mo	< 500 Å amorphous layer at low temperature, followed by crystalline layer at higher temperature.			113, 252, 324
			(00.1) (10.1), (10.0)	

3. Effect of Cation-Anion Ratio

Glass	S:Cd = 1:1	(00.1)	91
	S:Cd = 2:1	(00.1), (10.1) (10.0)	
	S:Cd = 1:2	(10.1), (00.1) (10.0)	

4. Effect of Doping

Glass	1% Ga	(00.1)	highly oriented	113
	10 ppm In	(00.1)	(11.2), (10.1)	

* CdCl_2 + thiourea, film thickness $\sim 1 \mu\text{m}$, all crystalline deposits hexagonal.

by cathodic sputtering and by reactive sputtering of cadmium in an H₂S–argon mixture to films prepared by vacuum evaporation. The crystallite sizes were comparable, but the sputtered films showed less preferred orientation.

c. *Chemical Spray Reactions*

CdS films formed by chemical spray reactions usually possess a hexagonal structure or else they are amorphous to x-ray diffraction analysis. The crystalline films are either randomly oriented or they possess 1 deg orientation with the (0001) plane or the (10̄11) plane parallel to the substrate. The structure of the films depends on the nature of the substrate, the temperature, the cadmium salt, the cation–anion ratio and on dopants in the spray mixture.^{91,251}

Table X shows that the structure is strongly dependent on the nature of the substrate. In glasses and ceramics there is an inverse relationship between the crystallinity of the substrate and that of the deposited film. Films deposited on metals are usually amorphous, because the spray mixture reacts chemically with the substrate to form an amorphous deposit. Two methods have been developed for depositing crystalline films on metal substrates. In one method the film is deposited on steel clad with a cadmium phosphor bronze alloy. The formation of CdO or CdS provides a surface for the deposition of a crystalline layer. In the other method a thin amorphous film of CdS, less than 500 Å thick, is first deposited at a low temperature on a suitable metal such as molybdenum. A crystalline layer is then deposited on the first layer at a higher temperature.^{113,252}

When a solution of cadmium chloride and thiourea is sprayed onto an amorphous substrate, the film is highly crystalline and the crystallinity improves with temperature. The ratio of the sulfur to cadmium ion concentration in the solution affects the orientation (see Table X). A 1:1 ratio produces the most highly oriented films. The orientation is also influenced by doping. Relatively large amounts of gallium, which enter the lattice interstitially, produce highly oriented films, while small amounts of indium, which enter the lattice substitutionally, reduce the degree of preferred orientation. When cadmium chloride is replaced by cadmium acetate, the films become amorphous with a crystallite size of less than 400 Å.

d. *Sintered Layers*

Kitamura *et al.*²⁵³ measured the crystallite size of sintered films prepared by the cadmium chloride flux method with an electron microscope. The crystallites were about 1 μm in size. X-Ray diffraction measurements of

doubtful accuracy gave values below 0.1 μm .³⁶ The crystallites are randomly oriented.⁷⁴ The crystallite size of films prepared by compression sintering is 10–100 μm .²⁶⁵

e. *Deposition from Alkaline Thiourea Solution*

Pavaskar³²⁶ studied the structure of 1 μm films deposited from alkaline thiourea solution by means of reflection electron diffraction. The deposits were polycrystalline in nature and consisted of a mixture of the hexagonal and cubic forms.

11. CUPROUS SULFIDE LAYER

a. *Phases of Cuprous Sulfide*

The copper–sulfur phase diagram has been extensively reviewed by Cook *et al.*^{49,276,326,327} The most important structural properties of the predominant cuprous sulfide phases are shown in Table XI. It may be noted that all phases undergo transitions at relatively low temperatures.

The defect structure of Cu_2S consists of a highly ordered S sublattice and a disordered Cu lattice with two Cu^+ ions associated with each S^{2-} ion.^{24,327} Such a structure had been proposed by Rau³³⁵ for high temperature $\text{Cu}_{2-\alpha}\text{S}$. The djurleite phase, $\text{Cu}_{1.96}\text{S}$, is more stable than Cu_2S but is formed only in the presence of Cu^{2+} ions.²⁴

b. *Phases and Stoichiometry of Cuprous Sulfide Barrier Layer*

From the mass change of chemiplated films on chemiplating and etching in KCN it was concluded by the Harshaw group⁷⁵ that the Cu is in the form of digenite, $\text{Cu}_{1.8}\text{S}$. A similar analysis at Clevite^{56,276} indicated a stoichiometry of $\text{Cu}_{2.0025}\text{S}$ and suggested the presence of the chalcocite form.

The layer produced by cuprous ion treatment of doped or undoped CdS films was identified by Cusano²⁷⁰ with the aid of electron diffraction to be Cu_2S , but generally with departure toward excess sulfur, $\text{Cu}_{2-\alpha}\text{S}$. The digenite modification, $\text{Cu}_{1.8}\text{S}$, was sometimes observed. Spakowski *et al.*^{336,337} examined the cuprous sulfide layer on CdS single crystals by means of electron diffraction. Thin layers showed the high temperature hexagonal modification of chalcocite, Cu_2S , whose lattice structure matches that of CdS closely. X-Ray examination of thicker films indicated the orthorhombic room temperature modification of chalcocite. The orthorhombic form was also identified by Potter and Schalla^{338,339} on evaporated CdS films and by

TABLE XI
PREDOMINANT PHASES OF CUPROUS SULFIDE

Phase	Composition	Structure	Lattice Constants			Reference	Phase Transition		Reference
			a_0 (Å)	b_0 (Å)	c_0 (Å)		Temp.	High Temp. Structure	
Chalcocite	Cu_2S	orthorhombic	11.8	26.9	13.4	Rahlf ³²⁸	103.5°C	hexagonal	Djurle ³³⁰ , Roseboom ³³²
		pseudohexagonal	11.90	27.28	13.41	Burger ³²⁹	110°C		Posnjak ³³³
			11.881	27.323	13.491	Djurle ³³⁰	435°C	cubic	Jost ³³⁴
	layers grown on CdS	11.848	27.330	13.497	Cook ^{327,119}				
		11.88		13.49	Singer ³³¹				
		11.82	27. 0	13.45	Palz ⁹⁵				
Djurleite	$Cu_{1.96}S$	orthorhombic	15.71	13.50	26.84	Roseboom ³³²	93°C	hexagonal	Roseboom ³³²
Digenite	$Cu_{1.8}S$	pseudocubic	5.56			Djurle ³³⁰	~ 80°C	cubic	Cook ³²⁷

Singer and Faeth³³¹ and Shiozawa⁵⁶ on single crystal CdS by means of x-ray analysis. In later experiments Cook, Shiozawa, and Augustine³²⁷ observed both chalcocite and djurleite by x-ray diffraction of single crystals that had been dipped in CuCl.

Nakayama¹²² carried out x-ray analysis of the cuprous sulfide layer of ceramic cells after barrier formation by means of copper sulfate. Chalcocite, djurleite, and digenite were identified depending on the treatment.

Electron microprobe analysis of the barrier layer in CdS thin film solar cells by Fabbricotti²⁷⁸ and van Aerschot³⁴⁰ indicated a constant copper concentration in the bulk of thicker Cu_{2-x}S layers. A slightly copper doped region extended into the CdS and a slight Cd doped region exists in the Cu_2S near the interface. Cl was also found near the interface.

c. Junction Formation

The copper solution treatment causes the precipitation of the cuprous sulfide onto external or internal surfaces and along grain boundaries or dislocations.²⁷⁰ On chemically polished CdS surfaces, the film forms immediately and appears continuous after a few seconds.⁵⁶ The sides of the hexagonal etch pits of deeply etched surfaces require several minutes before they are covered by the cuprous sulfide film.

In ceramic cells cuprous sulfide is formed along grain boundaries over a range of 10 μm of surface layer.¹²² x-Ray microanalysis showed that the Cu ions were localized around the grains of the CdS ceramic.

Cook *et al.*³²⁷ showed that CdS can be converted directly to djurleite, $\text{Cu}_{1.96}\text{S}$, by dipping. Boer^{24,25} suggested that $\text{Cu}_{1.96}\text{S}$ forms initially on CdS as an interlayer before chalcocite starts to grow. Small amounts of Cu^{2+} ions in solution favor the formation of djurleite. After they are used up Cu^+ ions produce chalcocite. Different experimenters may have djurleite layers of different thickness resulting in variations in the spectral response. Gill and Bube²⁶ consider high efficiency cells to possess a thin djurleite layer. Chamberlin⁹⁰ obtained cells by chemically spraying a djurleite layer.

Another hypothesis is that the heat treatment after barrier layer formation produces the djurleite interlayer.^{25,122} Longer exposures at high temperatures produce cell degradation caused by phase transformations. These are described in Section 13.

d. Epitaxy and Crack Formation

Shiozawa^{56,119,276} and Singer and Faeth³³¹ showed that the Cu_2S layer grows epitaxially on CdS. The misorientation of the lattice is less than 10'. Each Cu_2S axis is equivalent to only one CdS direction according to

Shiozawa.^{119,276,327} Lattice constants of the epitaxial layer were measured by Singer and Faeth,³³¹ Shiozawa *et al.*,^{119,327} and by Palz⁹⁵; they are shown in Table XI.

The perfection of the Cu₂S lattice is poor, as indicated by a lack of line sharpness in the x-ray diffraction pattern.^{119,276} The misfit with the CdS lattice along the *a*, *b*, and *c* axes is 4.5%, 4.8%, and 0.4%, respectively.

Shiozawa^{56,60,119} showed that the formation of Cu₂S on a CdS single crystal causes fine cracks in the Cu₂S film due to a 9% volume mismatch; cracks appear also in the underlying CdS. The adhesion between the Cu₂S and the CdS substrate remains strong at all times. The cracks are perpendicular to the interface and occur in areas where the copper concentration is very high. The cracks contain Cu and Cd. They were also observed by Fabbricotti²⁷⁸ and by Palz.⁹⁵

Shiozawa^{119,341,342} considered thin film photovoltaic cells to be subject to the same kind of fine cracks. The irregular geometry of the thin film cell would therefore appear as shown in Fig. 5. The grains of the epitaxially oriented film average a micron across. There are many of these into which the Cu₂S penetrates from 2 to 5 μm deep during the dipping process. Shiozawa postulated that additional crack formation to relieve the built-up tension in the film during thermal cycling might lead to cell degradation, due to an increase in the effective sheet resistance of the Cu₂S layer and ultimately due to the formation of islands of Cu₂S that are isolated from the grid network.

e. Junction Profile

Hill and Keramidas²⁷³ assumed that the diffusion of reactants during junction formation would result in a graded junction in which Cu⁺ ions and Cu₂S extend into the CdS, while Cu²⁺ ions and CdS extend into the

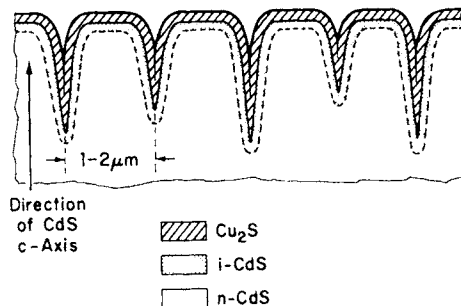


Fig. 5. Structure of epitaxial Cu₂S film. (From Shiozawa *et al.*³⁴²)

Cu_2S layer. Crossley *et al.*³ considered this to be a major reason for the high collection efficiency for the minority carriers generated on either side of the junction. The solution growth process operates close to equilibrium causing the epitaxial formation of Cu_2S . The implications are that it will be difficult to find a better alternative to the dip process since equilibrium vacuum deposition processes take place at much higher temperatures, which would lead to undesirable reactions between the deposited material and the substrate.

Nakayama¹²² prepared ceramic cells with three different types of junction profiles. A steep junction was initially formed after dipping in copper sulfate solution. Prolonged heating produced a graded junction due to copper diffusion into the CdS . The formation of a 2 μm insulating CdS layer on longer heating resulted in a Mott barrier. The junction profile was deduced from capacitance measurements.

Miya²³ obtained a graded junction on the Cd plane of CdS single crystals and an abrupt junction on the S plane. The Cu_2S layer on the Cd plane was thicker than the corresponding layer on the S plane and had a different appearance. Microprobe analysis indicated a Cu_2S layer on the Cd plane and a $\text{Cu}_{1.96}\text{S}$ layer on the S plane. Miya concluded that the Cd atoms dissolve more in solution at the Cd plane, so that the Cu ions diffuse deeper at the Cd junction.

f. Optical Properties of Cuprous Sulfide

The optical properties of cuprous sulfide have been measured by a number of experimenters (see Table XII). Figure 6 taken from Shiozawa⁵⁶ indicates that Cu_2S possesses an exceptionally high absorptivity in the visible region of the spectrum and a high transmission in the infrared.

The first detailed absorption measurements on cuprous sulfide films of different stoichiometric composition indicate the presence of band edges at 1.2 and 1.8 eV. Bube, Lind, and Dreeben³⁴⁴ carried out absorption measurements in heavily copper doped CdS . An absorption edge at 1.21 eV, in agreement with Eisenmann's³⁴³ results, indicated the presence of a second phase of Cu_2S distributed throughout the crystal.

Cusano²⁷⁰ observed a rise in the absorption at 1.8 eV. Marshall and Mitra³⁴⁵ confirmed the presence of an indirect bandgap at 1.21 eV. Sorokin³⁴⁶ measured the photoconductivity and optical absorption of evaporated Cu_2S films; he postulated the existence of a direct bandgap at 1.9 eV. Shiozawa^{56,353} concluded from an analysis of the above data that Cu_2S possesses absorption edges at 1.2 and at 1.8 eV. Finally, Ramoin *et al.*³⁵¹ concluded from absorption measurements on evaporated films that Cu_2S

TABLE XII: OPTICAL PROPERTIES OF CUPROUS SULFIDE

Reference	Structure	Stoichiometry	Measurements	Band Gap
Eisenmann ³⁴³	evap. film	Cu_xS $1 \leq x \leq 2$	absorption, reflection	
Bube ³⁴⁴	Cu doped CdS	Cu_2S ppted. 2nd phase	transmission	1.21
Cusano ²⁷¹	CdS film dipped in CuCl	Cu_{2-x}S	absorption	
Harshaw ⁷¹	CdS crystal with electropol. Cu_xS layer	Cu_2S	reflectivity, transmission	
Marshall & Mitra ³⁴⁵	polycrystals	Cu_2S	absorption, reflection	1.21 at 300°K 1.26 at 80°K
Sorokin ³⁴⁶	evap. film	Cu_2S	absorption	1.84
			photoconductivity	1.93
Ellis ³⁴⁷	flash evap. film	$\text{Cu}_{1.8}\text{S}$	transmission	
Shiozawa ⁵⁶	evap. film and CdS crystal dipped in CuCl	Cu_{2-x}S	transmission, reflection, refractive index	1.21, 1.83
Kryzhanovskii ³⁴⁸	evap. film	$\text{Cu}_{2-x}^{1+x}\text{S}$	reflection	
Selle & Maege ³⁴⁹	evap. film		absorption, refractive index	1.22 at 300°K 1.25 at 90°K
Egorova ¹⁰¹	CdS film dipped in CuCl	Cu_2S	transmission	
Nakayama ^{122,350}	evap. film	$\text{Cu}_{1.8}\text{S}$	transmission & reflection	2.3
		Cu_2S		1.0
		$\text{Cu}_{1.96}\text{S}$		1.5
Ramoin ³⁵¹	evap. film	Cu_2S	absorption	1.7, 1.05
Gustavino ³⁵²	evap. film	$\text{Cu}_{1.8}\text{S}$	transmission, reflection	2.6

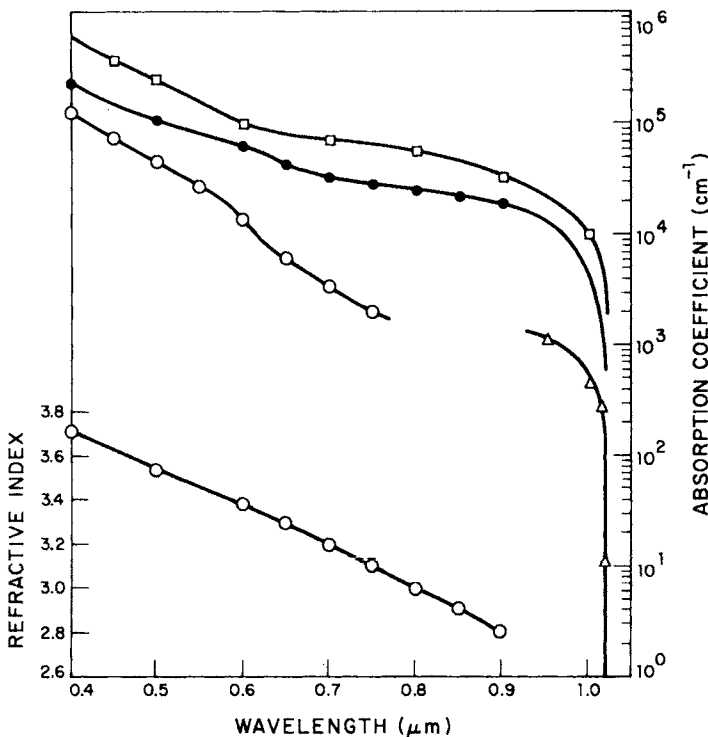


Fig. 6. Absorption coefficient and refractive index of vacuum evaporated Cu_2S thin films. □, Eisenmann,³⁴³ ●, Shiozawa,⁵⁶ ○, Sorokin,³⁴⁶ △, Marshall and Mitra.³⁴⁵ (From Shiozawa *et al.*⁵⁶.)

possesses a direct bandgap at 1.7 eV and an indirect bandgap at 1.05 eV. They also observed an impurity absorption band between 1.3 and 2 μm .

Table XII indicates some unconfirmed values for the bandgaps in $\text{Cu}_{1.8}\text{S}$ and $\text{Cu}_{1.96}\text{S}$.

g. Electrical and Thermal Properties of Cuprous Sulfide

Hirahara³⁵⁴⁻³⁵⁷ measured the electrical conductivity, the thermal expansion, heat capacity, specific heats, thermal emf, and Hall effect in cuprous sulfide from room temperature to 600°C. Cu_2S exists in three phases with transition points at 110° and 470°C. Anomalies in the electrical and thermal properties were observed at the transition points.

Cuprous sulfide is a *p*-type defect semiconductor. The beta phase between 110° and 470°C exhibits ionic conductivity which was first measured by Tubandt *et al.*³⁵⁸ at 220°C. Eisenmann³⁴³ measured the temperature dependence of the conductivity over a wide temperature range and as a

TABLE XIII
ELECTRICAL PROPERTIES

Reference	Structure	Stoichiometry	Temp. Range	Activation Energy	Resistivity ($\Omega\text{-cm}$)	Hall Mobility ($\text{cm}^2/\text{V sec}$)	Carrier Conc. (cm^{-3})	Thermal EMF
Hirahara ³⁵⁴⁻³⁵⁷	single crystal	Cu_2S	25 ~ 600°C			12	$10^{19}-10^{21}$	
Eisenmann ³⁴³	evap. film	Cu_xS $1 \leq x \leq 2$	-263-+350°C		$10^{-3}-10^{-2}$			
Cusano ²⁷¹	CdS film dipped in CuCl	Cu_{2-x}S			$10^{-2}-10^{-3}$	2	$>10^{20}$	
Marshaw ²⁷⁴	CdS film dipped in CuCl				$10^{-1}-10^{-2}$		$10^{18}-10^{19}$	
Potter & Schalla ^{338,339}	CdS crystal dipped in CuCl					1 - 10	$10^{20}-10^{21}$	
Ellis ³⁴⁷	100A evap. film	$\text{Cu}_{1.8}\text{S}$			6 - 65			
Abdullaev ³⁵⁹	single crystal	Cu_2S	20 - 600°C	0.064		25	7.4×10^{19}	90 mV/deg
Selle & Maege ³⁴⁹	evap. film	Cu_2S		0.43	2	7	4×10^{15}	200 $\mu\text{V}/\text{deg}$
Nakayama ^{122,350}	evap. film	$\text{Cu}_{1.8}\text{S}$			4.3×10^{-3}	0.51	2.8×10^{21}	
		$\text{Cu}_{1.96}\text{S}$			2.8×10^{-2}	10^{-2}	$\sim 10^{22}$	
		Cu_2S			6.7×10^{-2}	3.6	2.6×10^{19}	
Gustavino ³⁵²	evap. film	$\text{Cu}_{1.8}\text{S}$			$2-3 \times 10^{-3}$	1.75	1.6×10^{21}	
Martinuzzi ³⁶⁰	thin film	Cu_2S	200 - 700°K	0.05	$10^{-1}-10^{-2}$	1.5	10^{20}	
Bougnat ³⁶¹	single crystal	Cu_2S	77 - 900°K	0.11, 1.8	5×10^{-2}			
		$\text{Cu}_{1.94}\text{S}$		0.01, 0.06, 0.42	2×10^{-3}	7	4×10^{20}	
		$\text{Cu}_{1.85}\text{S}$			7×10^{-4}	5	1.8×10^{21}	
					1.8>700°K			

function of the stoichiometry. Cu₂S shows a room temperature resistivity of 100 ohm-cm. There is a decrease by about four orders of magnitude on going from Cu₂S to Cu_{1.8}S. In the higher resistivity range evaporated films are strongly affected by exposure to oxygen.

Table XIII lists the electrical properties of cuprous sulfide. The very high carrier concentrations shown indicate that cuprous sulfide layers are extremely degenerate.

The electron diffusion length in Cu₂S layers was measured by Shiozawa,¹²⁰ Gill and Bube²⁸⁰ and Mulder.³⁶² The last two experimenters utilized light microprobes. Shiozawa and Bube obtained diffusion lengths from less than 0.1 to 0.4 μm. Mulder³⁶² obtained a diffusion length of 0.7–0.8 μm.

A literature search on the properties of cuprous sulfide and cuprous sulfide–cadmium sulfide heterojunctions has been carried out by Neuberger.³⁶³

V. Properties of CdS–Cu_xS Photovoltaic Cells

12. SPECTRAL RESPONSE

a. Spectral Response of Backwall and Frontwall Photovoltaic Cells

Reynolds and Leies² discovered the photoresponse of CdS rectifiers. Reynolds^{7,364} measured the quantum yield of single crystal backwall cells which approached unity at wavelengths less than 600 nm. A special aspect of CdS cells is the considerable extrinsic photovoltaic response in the impurity dominated spectral region on the long wavelength side of the CdS absorption edge.

Backwall cells exhibit an extrinsic peak governed by Cu impurity centers in CdS and a shortwave cutoff below 520 nm due to the CdS absorption edge. The longwave onset of the photovoltaic response lies between 750 and 850 nm.^{6,10,82,171,270} Thin film backwall cells show the same general behavior as single crystal cells with a tendency for the maximum to shift to slightly longer wavelengths.^{5,78}

The response of frontwall CdS solar cells matches the more energetic portion of the solar spectrum, ranging from the ultraviolet at about 250 nm to the infrared at about 1 μm.³⁰ Most cells show a major peak at about 500 nm associated with the band edge and a second peak in the red at about 650–700 nm. Williams and Bube¹³ compared Cu-plated single crystal backwall and frontwall cells. They attributed the shortwave response of the frontwall cells to light absorbed in the metal layer followed by photoemission of electrons from Cu into CdS. Similar results were obtained by

TABLE XIV
SPECTRAL RESPONSE

Reference	CdS	Structure	Peaks (nm)	Cutoff	
				Short λ (nm)	Long λ (μm)
Reynolds ^{7,364}	single crystal	backwall	550,620		525
Hammond & Shirland ^{6,6}	single crystal	backwall	700	525	1.0
		frontwall	700	265	1.0
Woods & Champion ¹⁰	single crystal	backwall	510		1.1
		frontwall	700		
Moss ⁷⁸	thin film	backwall	570		
Bockemuehl ¹⁴	single crystal, insulating	backwall	520		
Williams & Bube ¹³	single crystal	backwall	520		
		frontwall	480		
Harshaw ⁶⁵	thin film	frontwall	520		1.0
Chamberlin & Skarman ^{89-91,112,113}	spray dep. film	backwall	700		1.0
		frontwall	495,580,700		
Drozdov ⁸⁵	thin film	backwall, Cu_2O	520,420		
Spakowski ^{336,337}	thin film	frontwall	480		1.0
Pastel ⁸⁷	thin film	backwall, thin Cu thick Cu	730 620		
Shirland ^{30,52}	thin film	frontwall	520,650-700	250	1.0
Balkanski ⁹²	thin film	frontwall	650	450	0.9
Pavelets ⁹³	sputtered film	frontwall, light In dope	520		
		heavy In dope	520,600		
Bernard ⁵⁵	thin film	frontwall	500-600		1.0
Potter & Schallia ^{338,339,365,366}	thin film	frontwall			
Myton ¹⁰⁰	thin film	frontwall	500		
Yefremenkova ¹¹¹ Egorova ¹⁰¹	sputtered film	frontwall	420,450-460,480, 490-500		
		backwall	580-650		
Shitaya & Sato ²²	single crystal	frontwall rearwall	420,450,490-500 480-600	510	0.8-0.85 0.8-0.85
Gill & Bube ^{279,285}	single crystal	frontwall before heat treatment after heat treatment	600,800 (shoulder)		1.1 0.75
Anehon ¹⁰³	thin film		500,580,900		
Miya ²³	single crystal	Cd plane S plane			1.1 0.85

Egorova¹⁰¹ with thin film cells. Spectral response determinations by different experimenters are listed in Table XIV.

b. *Long Wavelength Response*

It was discovered at Harshaw⁶⁵ that high efficiency frontwall cells show a response throughout the visible spectrum, whereas the response of low efficiency cells drops at 550 nm. Shirland⁶² attributed the broadening of the spectral response at higher wavelengths to copper trace impurities. Pavlevets and Fedorus⁹³ found that heavily doped cells exhibit a long wavelength peak as well as a short wavelength peak. Balkanski and Choné⁶² observed an increase in the maximum wavelength with illumination intensity due to the increasing ionization of traps resulting in the formation of a continuous band from localized levels.

Spakowski^{336,337} found the magnitude of the red response of the cells to be quite variable depending on the fabrication. He attributed the red response to excess Cd producing a deep impurity level in CdS at 1.2 eV below the conduction band. The red response is improved by the addition of excess Cd, also of In and Ag. Heat treatment lowers the red response. So does exposure to H₂S which removes the excess Cd.

c. *Thickness of Cuprous Sulfide Layer*

Mytton¹⁰⁰ measured the variation in spectral response of thin film solar cells as a function of the thickness of the Cu₂S layer. As the dip time is increased the short wavelength response goes through a maximum. The long wavelength response is independent of the dip time and is only a function of the solution concentration. Very long dip times produce a cell with no step in the response at the band edge of CdS and a decreasing overall response.

Egorova¹⁰¹ found that the width of the long wavelength sensitivity region decreases when the thickness of the Cu₂S layer is increased. The opposite effect was observed by Nakayama¹²² in ceramic cells. Cells with thin Cu₂S layers responded to wavelengths below 0.51 μ m. Prolonged electrochemical treatment caused the spectral response to shift toward higher wavelengths. Boer²⁵ observed a flat spectral response to 940 nm in electroplated cells.

d. *Effect of Other Process Variables*

Mytton¹⁰⁰ observed that the ratio of extrinsic to intrinsic response depends on the grain size of the CdS layer. A large grain size greater than 500 \AA is required to achieve a high extrinsic response.

The spectral response is sensitive to the temperature of the CuCl solution.¹⁰⁵ A drastic change in the spectral response occurs between 75° and 80°C. The longwave response is quenched by lower solution temperatures.

Williams and Bube¹⁸ found that cells made with CuCN and CuSO₄ plating solutions show different spectral response. Bube²¹ also showed that dipping in a cuprous sulfide and ammonia solution produces a substantially different spectral response which falls off rapidly at wavelengths above 500 nm.

Potter and Schalla^{338,339,365} observed the effect of lapping CdS single crystal surfaces before dipping. This produces a darker surface layer on the crystal of higher conductivity and containing excess Cd. This treatment increases the red response.

e. Spectral Response Changes on Heating

Spectral response changes on heating after junction formation have been observed by Williams and Bube,¹⁸ Hill and Keramidas,²⁷³ Mytton,¹⁰⁰ and Gill and Bube.^{26,279,285} On the other hand, Spakowski^{338,337} and Potter and Schalla^{338,339,365} found that heating in air at 250°C does not alter the spectral response significantly, suggesting that the red response occurs immediately after barrier formation. However, heat treatment does affect the magnitude of the red response relative to the blue response, since this ratio is very sensitive to surface treatment.

It appears that heat treatment in air increases the blue response at first, and subsequently decreases the overall response, particularly in the red. Simultaneous illumination with short wavelength light partially restores the long wavelength response.^{26,105,285}

f. Spectral Response Mechanism

Potter and Schalla^{338,339,365} considered the spectral response in the long wavelength region to be due to photoelectric emission from the chalcocite layer into CdS. The spectral response to shorter wavelengths is due to excitation across the CdS bandgap as well as photoelectric emission from the barrier layer. Nearly all the light is absorbed in the Cu₂S layer.

Shiozawa²⁸⁹ considered the longwave photoresponse to be caused by light absorption in the Cu₂S followed by electron collection by diffusion to the space charge region in CdS. Egorova¹⁰¹ considered the longwave sensitivity to be due to the Cu₂S layer and the shortwave response to be caused by the excitation of electron-hole pairs in CdS.

A dip in the spectral response corresponding to the CdS bandgap was reported by Chamberlin and Skarman,⁹⁰ Shiozawa,⁶⁰ and by Gill and

Bube.²⁸⁰ The large dip obtained by Chamberlin and Skarman is explained by their utilization of a digenite layer near the CdS. Shiozawa obtained the dip for thin Cu₂S layers only. Boer²⁴ considered the dip to be caused by the strain due to the Cu₂S:CdS lattice mismatch which produces an anomalous absorption near the band edge. The dip is seen for frontwall cells only; rearwall cells exhibit a sharper drop.

g. Spectral Response of Spray Deposited Cells

Chamberlin and Skarman^{39-91,112,113} prepared both the CdS and the cuprous sulfide layer by spray deposition. The latter was in the form of digenite, which might provide a different type of spectral response. The backwall cells showed a peak at 700 nm and a response up to 1 μm. Some frontwall cells showed a peak at 580 nm associated with the theoretical bandgap of Cu₂S. Some of the sprayed cells showed a very small extrinsic spectral response and had open circuit voltages around 1 V; see Section 18.

h. Enhancement and Quenching Effects by Secondary Illumination

Three different types of effects have been observed: the enhancement of the extrinsic red response by secondary illumination of energy greater than the CdS bandgap, enhancement by secondary infrared illumination, and the quenching of the primary signal by secondary illumination.

Woods and Champion¹⁰ reported the first published results on bias light measurements, in which the crystal was illuminated simultaneously by two separate monochromatic sources at 700 and 900 nm. The photogenerated current induced by 700 nm illumination was found to be greatly increased by illumination at 900 nm. The enhancement effect was ascribed to an increase in the lifetime of the free holes. This effect was also observed by Potter and Schalla,^{338,339,365,366} but only after heat treatment of the junction.

Duc Cuong and Blair¹⁹ observed an enhancement in the infrared spectral response by a factor of 200 on illumination by radiation with energy corresponding to the CdS bandgap. This was attributed to the depopulation of impurity levels by electron transitions resulting in additional minority carriers. Potter and Schalla^{338,339,365,366} found that the secondary illumination restored the extrinsic red response to its original level before the heat treatment. Shiozawa^{60,120,353} ascribed the effect to the reduction in the cell series resistance by the photoconductivity of a Cu doped CdS layer in the junction region.

Shirland³⁰ observed that secondary illumination had less effect on the response between 700 and 800 nm, and that the bias light seemed to quench

the cell output for this range. Gill and Bube^{26,285} observed a strong quenching of the primary signal at 800 nm. The photovoltaic effect was also quenched by secondary light at 0.8 and 1.1 eV when the primary light was sufficiently energetic to excite electrons from impurity levels.

13. STABILITY

Thin film CdS-Cu_xS solar cells have been beset with stability problems from the outset, and the long range prospects for their use as solar energy converters depend largely on the solution to this problem. The environmental effects of most concern are moisture, thermal cycling, elevated temperatures, and ion migration. The cells possess a high resistance to space radiation.

a. *Moisture*

It was discovered soon after the initial development of thin film solar cells that they are unstable unless protected against moisture.⁶ For a long time the cells were laminated using a hygroscopic nylon adhesive (see Section 2), and this caused a rapid initial deterioration of the cells.^{41,71,73,336,337,367,368} Chemiplated cells proved to be less susceptible than electroplated cells.

The cell output could be restored by heating in vacuum as long as the degradation was less than 50%.^{336,337,367,368} The deterioration was irreversible if the cell lost more than 50% of its power. The decrease in power is accompanied by an increase in series resistance and a deterioration in the diode characteristics. The degradation is caused by the diffusion of the moisture to the electrical junction and the formation of recombination centers. This degradation has been entirely eliminated by replacing the nylon adhesive by a transparent epoxy.⁴⁹

b. *Thermal Cycling*

The earlier thin film solar cell constructions with pressure contacts degraded on thermal cycling from -90° or -120° to +100°C due to the mismatch in the thermal expansion coefficients of the different layers.^{336,337,368,369} The cells on metal substrates short-circuited. The short circuit could be removed by relamination. Cells with electroplated grids were stable but had low outputs. Grids bonded with silver epoxy delaminated.³⁰ Cells on plastic substrates showed a much better performance than those on metal substrates.

The construction of cells on Kapton substrates with electroformed grids

that were attached by conducting epoxy showed a considerable improvement under thermal cycling. These cells were subjected to long term tests at NASA Lewis,^{370,371} the Boeing Corp.,³⁷²⁻³⁷⁴ and Lincoln Laboratory.^{283,375-377} The tests were made more representative of the space environment by cycling in vacuum for 60 min under illumination at 60°C followed by 30 min in darkness at -70°C. Long-term degradation of varying severity was seen, but the results were not easy to interpret, since the importance of keeping the output voltage constant throughout the experiment had not yet been discovered.

Cross-sectioning of degraded cells indicated lateral cracks in the CdS layer,³⁷⁵ and it was suspected that these were produced during thermal cycling due to the thermal mismatch with the substrate. It was shown by Bozek³⁷⁸ that these laminar cracks visible in cross-sectional photomicrographs were caused or aggravated by mounting or polishing techniques. Smithwick³⁷⁹ cycled cells between liquid nitrogen temperatures and 65°C. Under these severe conditions the Kapton cells split and delaminated resulting in a degradation of maximum power and short-circuit current proportional to the decrease in active area. There was no change in open-circuit voltage and fill factor.†

The following results were obtained in thermal cycling tests under controlled bias conditions: Tests at open-circuit voltage produced a severe loss in open-circuit voltage and fill factor due to copper nodule formation (see below). Long term tests under simulated space conditions showed a loss in short-circuit current: 7-12% after 5000 cycles, and a somewhat larger loss in fill factor.^{59,380,381} Thermal stresses were not the major cause of degradation, but delamination was observed along the edges in some cells.

It was found by a number of experimenters^{96,109,377,382} that exposure to illumination at high temperatures degrades the cells more than thermal cycling to the same maximum temperature. Mytton³⁸² attributed an improvement in the high temperature stability to a modification in the etching step before junction formation, which caused a decrease in the rate of loss of the fill factor.

c. *Diffusion*

At elevated temperatures above 100°C CdS photovoltaic cells show a steady loss of output and fill factor as well as an increase in the series resistance.³⁷⁰ There is also a change in the spectral response.³⁸³ These

† The fill factor is defined as the ratio of the maximum power to the product of the short-circuit current and the open-circuit voltage.

changes have been attributed to diffusion of ionic species, particularly copper, to ambient effects, and to phase transformations in the cuprous sulfide layer.

Hill and Keramidas²⁷²⁻²⁷⁴ postulated that CdS solar cells depend on an impurity concentration gradient. They observed marked changes in cell outputs and spectral response on heating and attributed this to changes in the impurity concentration gradient. They also observed a hysteresis effect on tracing current-voltage curves at room temperature which they attributed to ionic motion. The Clevite group^{30,51} considered this effect to be caused by the thermal emptying of trap levels. They were able to produce cells that were relatively stable at temperatures as high as 140°C and took this as evidence against the possibility of degradation by ion diffusion.

Shiozawa^{60,119,289,342} considered the increase in series resistance under high temperature storage to be caused by the diffusion of Cu from the Cu₂S surface layer into the CdS so as to increase the width of the insulating CdS layer. Copper diffusion is appreciable at 150°C. This effect could be reduced by doping the CdS base layer with In.

Martinuzzi *et al.*³⁸⁴ saw evidence of diffusion of Cu atoms into the CdS and of Cd diffusion into the Cu₂S layer by chemical analysis. The Zn from the ohmic contact to the CdS layer also diffuses into the cell. Palz *et al.*^{98,99} were able to reduce the Cu diffusion by doping and also by optimizing the CuCl dip. The fill factor deteriorates at high temperatures if the Cu₂S layer is too thick. Doping lowers the resistivity of the CdS layer and doubles the junction capacity. The doped cells were very stable under long term illumination at 60°C and showed no loss in fill factor. There was a slight decrease in the open circuit voltage. The efficiency was 6.5% at AMO. Konstantinova and Kanev¹²⁴ improved the high temperature stability of ceramic cells by means of Bi doping.

d. Phase Transformation in Cuprous Sulfide Layer

The various modifications of cuprous sulfide undergo phase transformations around 100°C; see Section 11. Reversible phase changes near 100°C in Cu_xS layers have been studied by TeVelde³⁸⁵ and by Boer.¹¹⁰

Prolonged heat treatment converts chalcocite, Cu₂S, into djurleite, Cu_{1.96}S.^{24,26,60,122} The Cu_{1.96}S layer grows until no photocurrent can penetrate under illumination of energy less than 1.8 eV. This causes an increase in series resistance and a loss in short-circuit current that is partly reversible under illumination. The absorption of intrinsic light in the Cu_{1.96}S layer causes neutral Cu vacancies to become effectively negatively charged. They then drift and diffuse out, thus converting the Cu_{1.96}S into Cu₂S.

Instabilities in the short-circuit current over the temperature range from 75° to 150°C and a sudden drop at 90°C have been attributed by Palz,⁹⁶ Coste,⁹⁷ and by Dunn²⁸⁴ to phase changes in the Cu₂S layer from the gamma low temperature phase to the beta phase which produces ionic conduction. Mytton³⁸² states that phase changes cannot be held responsible for cell degradation observed at 60°C.

Bogus and Mattes¹⁰⁶ were able to enhance the efficiency of thin film solar cells from 5 to 8% by evaporating a thin layer, 30–100 Å, of copper or silver over the cuprous sulfide layer, followed by heat treatment in air. The improvement was attributed to the conversion of the top surface of the cuprous sulfide layer from Cu_{1.96}S to Cu₂S. A similar effect was seen after glow discharge in hydrogen followed by heat treatment in air.

e. *Oxidation Effects*

Shiozawa^{60,121,326,386} showed that heating in air at 150°C produces a rapid degradation in the short-circuit current. The degradation could be partly removed by heating in vacuum. Single crystal cells were more resistant than undoped cells. A similar degradation mode was postulated by Mytton *et al.*³⁸² Experiments at the University of Delaware¹⁰⁹ indicated that cells degraded far more in oxygen and in air than in nitrogen.

Palz *et al.*^{98,99} noted a substantial loss in short-circuit current when thin film cells are exposed to oxidation by chlorine, bromine, iodine, or oxygen. The oxidation of the cuprous sulfide brings about a transformation from chalcocite to djurleite, which results in a marked decrease in the red response. The reaction in air increases with temperature and under ultraviolet illumination, which produces a photosensitized oxidation reaction. Doped stoichiometric cells are far more stable in an oxidizing environment. A Kapton cover affords some shielding of the ultraviolet. It is therefore extremely important that thin film cells should have no access to oxygen.

f. *Copper Nodule Formation*

Cell degradation due to copper ion electromigration was postulated by Shiozawa^{60,120} after observing a reversible loss in open-circuit voltage when cells were operated under forward bias conditions.

An examination of localized hot spots in degraded cells revealed the presence of pure copper nodules producing localized short-circuit paths.^{59,380,381,386–390} The formation of copper filaments is due to the electrochemical decomposition of Cu₂S with a threshold voltage between 0.35 and 0.40 V. The nodules have a copper taproot extending through the CdS layer to the substrate and cause hot spots on degraded cells when current is passed

from an external source. The pressure exerted on the nodules by newly created Cu atoms is very large; it exceeds the yield strength of the nodule and the plastic covers.^{386,391} Clark¹⁰⁷ studied the temperature dependence of the threshold voltage, which is 0.38 V at 22°C and decreases with increase in temperature.

Mathieu and Rickert^{392,393} measured the chemical potentials at the phase boundaries from 15° to 90°C using coulometric titration in a galvanic cell. They concluded that electrochemical decomposition of chalcocite may start at 0.265 V at 60°C, whereas the degradation in actual cells starts above 0.36 V. The electrochemical failure mechanism depends also on the stoichiometry and associated conductivity changes in the Cu₂S layer. The chalcocite layer limits the leakage current, so that the degradation threshold is shifted to higher voltages.

g. Other Degradation Modes

Haynos³⁹⁴ showed that the degradation depends on the illumination spectrum and is greater under illumination by longer wavelengths. Lindmayer and Revesz³⁹⁵ attributed this to electron trapping at interface states by infrared irradiation. The effect is reversed by short wavelength irradiation which causes hole injection.

Kanev, Fahrenbruch, and Bube²⁸⁶⁻²⁸⁸ observed a degradation due to electrochemical changes in the CdS depletion layer associated with undiffused Cu acceptors. Illumination can decrease the short-circuit current by two orders of magnitude in single crystal cells. The effect amounts to only 15% in thin film cells. The optical degradation process is thermally activated with an activation energy of 0.45 eV. Heat treatment above 100°C restores the cell. The activation energy for this process is 1.6 eV.

Hewig and Pfisterer³⁹⁶ carried out electron and light beam scanning of thin film solar cells. Degraded cells exhibited large inhomogeneous regions, whereas an improved stable construction by AEG-Telefunken¹⁰⁶ was homogeneous throughout.

h. Radiation Effects

Statler⁸⁷ subjected CdS solar cells to 1 MeV electron irradiation. The cells were not affected by a fluence of 10^{16} e/cm², though some damage was caused to the Mylar cover. CdS solar cells are therefore far more resistant to radiation than silicon cells.

Brandhorst and Hart³⁹⁷ observed no electron damage on cells with Kapton cover. At fluences greater than 4×10^{16} e/cm² there was some immediate damage, particularly in the blue region of the spectrum, which an-

TABLE XV
RADIATION EFFECTS

Reference	Cell Cover	Radiation	Energy	Fluence	Degradation Under Max. Fluence
Harshaw ^{28,67,70,71}	Mylar	e	1 MeV	10^{16} e/cm^2	Mylar cover 9 - 10%
		p	1.8, 3.0 MeV	$5 \times 10^{12} \text{ p/cm}^2$	I_{sc} 2% (1.8 MeV) 4% (3.0 MeV)
	Tedlar	$\text{Co}^{60}\gamma$		$1.4 \times 10^8 \text{ rad}$	I_{sc} 8%, Tedlar Cover
Brandhorst ³⁹⁷	Mylar	e	0.6 - 2.5 MeV	$10^{15}-10^{17} \text{ e/cm}^2$	
	Kapton	p	2 - 10 MeV	$10^{12}-3.6 \times 10^{14} \text{ p/cm}^2$	I_{sc} 8%, P_{max} 13%
Hui & Corra ⁸⁰	Bare	p	50 - 400 keV	10^{15} p/cm^2	I_{sc} = 80% (uncoated)
Brucker ³⁹⁸	Silicone	p	200,400 keV	10^{15} p/cm^2	I_{sc}, V_{oc} = 20% at 10^{13}
Loferski ³⁹⁹	Mylar, Kapton	e	425 MeV	10^{18} e/cm^2	none
Bernard ^{55,383}	Mylar,	e	450 keV	10^{17} e/cm^2	Plastic coating degrades
	Kapton, Tedlar	p	2 - 10 MeV	$6 \times 10^{14} \text{ p/cm}^2$	P_{max} 10%
Curtin ⁴⁰⁰	Kapton	p	250 keV - 50 MeV	10^{15} p/cm^2	
		e		10^{17} e/cm^2	
Van Aerschot ³⁴⁰	Bare	p	100 keV	$5 \times 10^{15} \text{ p/cm}^2$	I_{sc} = 25%

nealed out on overnight exposure to weak illumination. This was accompanied by a large increase in the red response that could not be explained by the authors. Proton irradiation resulted in some degradation above 10^{14} p/cm², see Table XV.

Hui³⁰ and Brucker³⁹⁸ irradiated bare cells with low energy protons. The degradation of the short-circuit current and open-circuit voltage was energy dependent with a maximum at a proton energy of 100 keV. The loss in open-circuit voltage depends on the distance from the front surface of the solar cell to the depletion region and the width of the depletion region. Maximum damage occurs when the protons come to rest in the depletion region which was 0.35 μ m below the surface. The open-circuit voltage of bare CdS cells is affected by low energy protons in the same way as silicon, but the critical fluence is 100 times as great. A 1 mil plastic cover prevents damage by low energy electrons up to fluences of 10^{18} e/cm². Bernard^{55,383} observed degradation at very high electron fluences, which caused an initial severe decrease in the short wavelength response due to darkening of the glue and plastic cover.

Bernard⁵⁵ and Curtin⁴⁰⁰ observed high energy proton damage at fluences above 10^{14} p/cm². Above this level there is a short-circuit current degradation due to a transmission loss in the Kapton cover which anneals out at room temperature. At a fluence of 10^{15} p/cm² the cell is damaged resulting in an increase in series resistance and a loss in short-circuit current, open circuit voltage, and maximum power. Similar results had previously been obtained by Brandhorst.³⁹⁷ Kapton covered cells did not degrade at electron fluences up to 10^{17} e/cm².

Further work with 100 keV protons was carried out by van Aerschot.³⁴⁰ The junction was located 0.16 μ m below the surface. The red response increased initially while the blue response decreased. The proton damage annealed out at 150°C in air. Van Aerschot concluded from the experiments that the junction depth is much deeper than the minority carrier diffusion length in Cu₂S.

14. OTHER PROPERTIES

a. Photovoltaic Cell Parameters

Low temperature current-voltage curves were extrapolated by Shiozawa^{60,120,289,342} to obtain a maximum open-circuit voltage at 0°K of 0.8–0.85 eV, which is equal to the barrier height. Measurements of capacitance as a function of the external voltage yielded an extrapolated value of the barrier height of 0.85 eV. The same value was also obtained for the extra-

polated value of the open-circuit voltage under intense illumination at room temperature.

The diode A factor in high quality thin film cells is 1.5 to 2; it is greater than 2 for poor quality cells.^{30,60,120,276} The A factor is greater in the dark than under illumination. Potter³⁶⁵ obtained a larger value under red light than under white light, but their A factors correspond to poor quality cells. Boer *et al.*¹¹⁰ state that the A factor is about 2 due to recombination at a center close to the maximum power point; at higher voltages A tends to 1.

Shiozawa¹²⁰ measured a reverse saturation current of 3×10^{-8} A/cm² in the dark and 1.3×10^{-7} A/cm² in light on ceramic cells. Values obtained by Potter³⁶⁵ on illuminated thin film cells were two orders of magnitude greater. Lindquist and Bube²⁷ obtained a value of 0.26 eV for the activation energy of the reverse saturation current in single crystal CdS. Lindmayer and Revesz³⁹⁵ obtained 0.2 eV for thin films. Boer¹¹⁰ states the activation energy is 0.45 eV.

b. Temperature Dependence

The first single crystal photovoltaic cells made by Reynolds¹ showed a drop in open-circuit voltage by 50% and a decrease of 80% in the short-circuit current on heating to 150°C. Hammond and Shirland^{4,6} observed a linear drop in open-circuit voltage which is 0.5 V at room temperature. Other measurements are shown in Table XVI.

The thermal properties of thin film photovoltaic cells were described by Shirland³⁰ and Liebert.²³³ The open-circuit voltage is constant at 0.65 V below 180°K. It decreases slowly up to -50°C and linearly at higher temperatures at 1.6 mV/°C. The short-circuit current is relatively temperature insensitive with a maximum at -40°C. The maximum power peaks at -80°C and drops rapidly at higher temperatures.

c. Light Intensity Effects

The open-circuit voltage increases with the light intensity and saturates at the highest intensity.^{30,92} The short-circuit current increases linearly with the light intensity.^{10,30,92} The power remains constant, since the shunt resistance decreases.³⁰

Middleton *et al.*⁵ observed a shift in the current-voltage curve with light intensity and a crossover of the light and dark curves as shown in Fig. 7, which they attributed to a shift in the barrier height. Shirland^{30,52} considered this phenomenon to be caused by a photoconductivity effect in

TABLE XVI
TEMPERATURE DEPENDENCE

Reference	Cell	Temperature Range	I_{sc}	V_{oc} (mV/°C)	P_{max} (mW/°C)	Efficiency
Reynolds ¹	single crystal	ambient - 150°C				
Hammond & Shirland ⁴⁻⁶	single crystal	-80 to +200°C				
Rappaport ^{9,401}	single crystal	0 ~ 400°C		-2		
Harshaw ⁶²	thin film, backwall	20 to 150°C 20 to 86°C 86 to 175°C	constant $\alpha T^{-1.385}$		-1.32	
Harshaw ⁷⁵	thin film			>1	$\frac{1}{P} \frac{dP}{dt} = 4 \times 10^{-3}/^{\circ}\text{K}$	
Shirland ³⁰	thin film	-180 to 150°C		1.6 above -50°C		
Liebert ²⁸³	thin film	110 to 330°K 0 to 60°C	-0.5 to +0.2 mA/°C	-1.5 to -1.8	-1.1 to -1.8	
Nakayama ¹²²	ceramic	-100 to +100°C	constant	-1.7	-3	$-3.6 \times 10^{-4}/^{\circ}\text{C}$

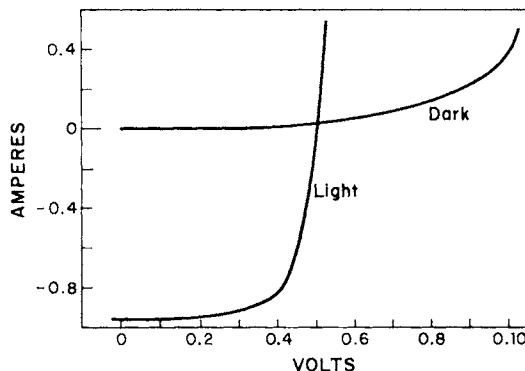


Fig. 7. Dark and light current-voltage characteristics. (From Middleton *et al.*⁵)

the depletion region which reduces the series resistance by nearly three orders of magnitude.

d. Transient Effects

Middleton *et al.*⁵ observed that the time lapse at each monochromator setting produced a shift in the longwave cutoff to shorter wavelengths, suggesting slow trapping states in the barrier region. Similar effects were reported by Shirland³⁰ and by Shiozawa.⁵⁶

Duc Cuong and Blair¹⁹ observed a transient on turning on the infrared illumination after the green light reached a steady state value. The relaxation time was 0.5–1 sec.

The photovoltaic response is rapid at low light levels; there are fast and slow components at high levels. The fast component comprises 85% of the total.³⁰ Shiozawa³²⁶ ascribed the slow transient effects to polarization induced by the copper ionic mobility.

Transient measurements by Gill and Bube^{26,286} indicated a fast response before heat treatment. After heat treatment there were slow and fast components, depending on the wavelength. The slow component showed an enhancement at short wavelengths through an increase in the density of trapped holes and a long wavelength quenching effect due to a decrease. The slow transients were on the order of minutes. The temperature dependence of the dark decay constant for the enhanced 0.8 μm photoresponse indicated thermal quenching due to the emptying of trapped holes from a 0.95 eV level above the valence band with a hole capture cross section of $2.5 \times 10^{-15} \text{ cm}^2$.

e. Other Properties of the Junction

Lindquist and Bube^{26,27,282,288,402} observed an increase in the junction capacitance on cooling and illumination by bandgap light. The effect persists on removing the photoexcitation in nonheat-treated cells. The photocapacitance is quenched by illumination in the 0.85 μm band. At 250°K there are two quenching bands at 0.9 and 1.35 μm . The photocapacitance is excited by intrinsic and extrinsic irradiation. It is quenched by forward biasing in the dark. The effect has been attributed to trapping of holes in deep acceptor centers in the CdS depletion region.

Gill and Bube^{279,280,285} observed a light induced junction breakdown, which they attributed to light absorption in the Cu₂S layer followed by electron diffusion to the interface and electron tunneling through conduction band spikes. The band-to-band tunneling or Zener breakdown occurs from the top of the Cu₂S valence band to the CdS conduction band. The effect is drastically reduced by widening the depletion layer by heat treatment after junction formation. Van Aerschot²⁷⁷ found this effect to have the same spectral response as the enhancement of the photocurrent by secondary illumination.

VI. Mechanisms of the CdS-Cu_xS Photovoltaic Cell

The operation of the CdS-Cu_xS photovoltaic cells is complex and has been the subject of many different interpretations. The proposed mechanisms have been extensively reviewed by Crossley³ and the more recent models by van Aerschot²⁴⁰. A table of different models is shown in Table XVII.

Reynolds¹ explained the extrinsic photovoltaic response by the presence of an impurity band in the forbidden zone into which a portion of the excited electrons could pass. Reynolds^{7,403} proposed that it would be necessary for this intermediate energy level to form a band rather than a set of spatially separated levels. Woods and Champion¹⁰ concluded that impurity band conduction was taking place by correlating measurements on photoconductivity and photovoltage in copper doped CdS.

Williams and Bube¹⁸ explained the extrinsic photovoltaic response by photoemission across a metal-semiconductor barrier. The extrinsic response increased with the thickness of the copper layer, indicating that the carriers were electrons photoemitted from the copper into the CdS. Photoemission was also supported by response time measurements of cells under pulsed illumination by Paritskii *et al.*¹⁵ Spitzer and Mead^{404,405} showed that

TABLE XVII
MECHANISMS

Reference	Mechanism	Recombina-tion Centers (eV)	Barrier Height (eV)
Reynolds ^{1,7,403}	Impurity band conduction		
Woods & Champion ¹⁰	Impurity band conduction		
Williams & Bube ¹³	Photoemission across Cu-CdS barrier		
Paritskii ¹⁵	Photoemission across Schottky barrier		
Bockemuehl ¹⁴	2 junctions produced by photocond. layer in CdS		
Fabricius ¹⁶	Schottky barrier, electron photoexcitation in CdS depletion region		
Grimmeiss & Memming ¹⁷	CdS p-n junction		
Mead & Spitzer ^{404,405}	Photoemission from Cu		
Cusano ²⁷¹	Cu_{2-x} -CdS heterojunction		
Keating ⁴⁰⁶	Cu_2S -CdS heterojunction		
Hill & Keramidas ^{273,274,75}	Cu_2S -CdS heterojunction, mobile ions		
Duc Cuong & Blair ¹⁹	Unspecified p-n junction	$E_v + 1.4$	
Balkanski & Choné ⁹²	CdS- Cu_xS heterojunction, light absorption at interface states		
Pavelets & Fedorus ⁹³	Cu_xS -CdS heterojunction, spectral response depends on barrier		
Spakowski, Potter ^{336-339,290}	CdS- Cu_2S heterojunction, light absorption in Cu_2S , photoemission from degenerate Cu_2S into CdS		0.85
Shiozawa ^{353,56}	i-n homojunction in CdS, light absorption in Cu_2S	$E_c - 1.4$	0.85
Shiozawa ^{276,120,289,60,326}	p-n heterojunction under illumination, light absorbed in Cu_2S , light modulates series resistance		0.85 in light 1.2 in dark
Shitaya & Sato ²²	Mott barrier layer, carriers excited from Cu levels in i-CdS layer		
Myton ¹⁰⁰	Heterojunction with extended junction region	$E_v + 1.0$	0.8
Gill, Lindquist, & Bube ^{279,285,402,26}	Electron tunneling through a conduction band spike at interface, illumination modulates depletion layer width	$E_v + 0.3$ $E_v + 1.1$	
Nakayama ¹²²	p ⁺ n heterojunction, impurity photovoltaic effect in CdS i-layer		
Boer ^{25,407}	Electron tunneling modified by electron recombination centers, compensated i-CdS layer	$E_c - 0.2$ $E_c - 0.65$	
Lindmayer & Revesz ³⁹⁵	p ⁺ n heterojunction, interface states and electron traps		0.95

the barrier height of copper contacts to vacuum cleaved CdS crystals was a function of the work function of the metal. This suggested that the junction was of the metal-semiconductor type and that the extrinsic response must arise from photoemission.

Bockemuehl *et al.*¹⁴ studied the properties of junctions formed by diffusing copper into photoconductive, dark insulating CdS crystals. The results indicated that in these junctions two barriers existed, one at the metal-semiconductor surface, the other in the semiconductor bulk. Fabricius¹⁶ showed by an optical technique that the generation of the photovoltage was localized in the depletion region, indicating that photoemission was not responsible.

Grimmeiss and Memming¹⁷ diffused copper into CdS and etched off the excess metal. In their model there is a junction between the normal n-type CdS base and a region of p-type CdS with an impurity band caused by the presence of a high density of levels in the middle of the CdS bandgap introduced by the copper dopant.

The concept of a Cu₂S-CdS heterojunction was first suggested by Cusano²⁷⁰ and supported by Keating.⁴⁰⁶ Hill and Keramidas²⁷³ determined that the cell contained a surface barrier region of nonstoichiometric degenerate cuprous sulfide in contact with the CdS. Hill *et al.*^{75,273,274} subsequently developed a model of a p-n heterojunction with a depletion region almost totally in the CdS. The impurity ions were assumed to be mobile under an applied electric field explaining room temperature instabilities.

Potter and Schalla^{338,339} advanced a model with the following features: a p-type barrier layer of highly degenerate chalcocite and photoemission of electrons from the Cu₂S valence band into the CdS conduction band over a 0.85 eV barrier. The efficiency of the photoemission is controlled by impurities in the CdS layer in the junction region. A similar model was proposed by Brandhorst.²⁹⁰

In the first model advanced by the Clevite group^{56,353} all light is absorbed in the Cu₂S layer in contact with an intrinsic CdS layer which is only slightly affected by illumination. This was changed,²⁷⁶ so that a p-n heterojunction was present under illumination. Illumination also changes the barrier height of the junction from 1.2 to 0.85 eV in agreement with the maximum open-circuit voltage at 0°K.¹²⁰ In the final model (shown in Fig. 8)^{60,289,326} light is absorbed in a highly nonplanar epitaxial surface layer, 0.3 μm thick.† Photoelectrons diffuse to the p-n heterojunction; their diffusion length is 0.2 μm. The change in the junction barrier height

† The thickness is variously stated as 0.2 and 0.3 μm in the different references, but this is well within the accuracy of the model.

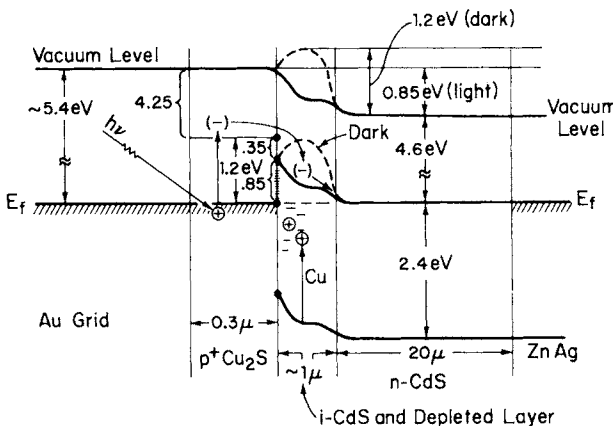


Fig. 8. Energy band diagram for Cu₂S-CdS solar cell, according to the Clevite model (Shiozawa *et al.*¹⁰).

under illumination is due to the photoconductivity induced in the 1 μm layer of copper doped CdS. A similar model was proposed by Mytton.¹⁰⁰

The Shiozawa model was criticized by Gill and Bube²⁶ and by van Aerschot.³⁴⁰ In this model the resistance of a photoconducting p-type CdS layer controls the photocurrent. This does not agree with the non-observed series resistance in the high forward current of the dark I - V characteristics, the increase in the short-circuit currents at relatively low levels of illumination, and the long persistence of photocurrent enhancement effects by secondary light.

Van Aerschot³⁴⁰ proposed a change in the barrier height of the interface state occupancy under illumination. Van Aerschot also pointed out that the Cu₂S layer cannot be degenerate since the diffusion length in a degenerate metal is less than 0.1 μm , whereas electron microscope measurements indicated a thickness of 0.2 μm .

In a model proposed by the Stanford group^{26,27,279,282,285,288,402} electrons diffusing across the junction must tunnel through a conduction band spike at the interface. After heat treatment the tunneling probability is controlled by the occupancy of deep lying levels in the CdS depletion region at 0.3 and 1.1 eV above the valence band. In the dark acceptor impurities widen the depletion layer, reducing the dark current. Illumination decreases the depletion width and restores the forward current. The band diagram for this model is shown in Fig. 9.

Boer^{25,407} attempted to combine the Shiozawa and the Stanford model. In his model the electron affinity of CdS is 0.35 eV larger than that of Cu₂S. Electron traps and recombination centers at the heterojunction

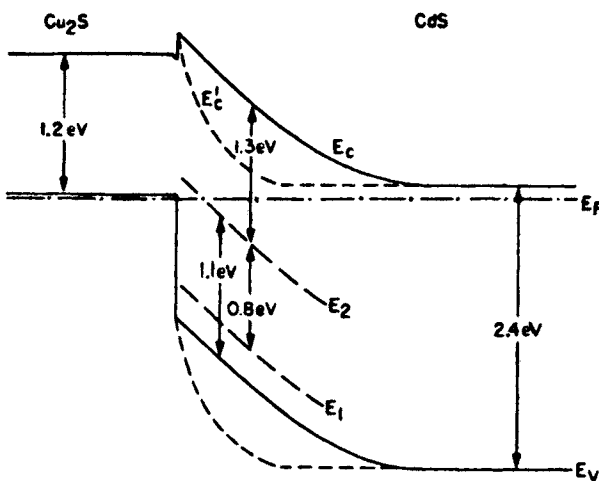


Fig. 9. Band diagram for the Stanford model (Gill *et al.* ^{26,27,279,285,402}). E_c' is the conduction band profile when energy levels E_2 are filled with holes.

interface affect the tunneling current at low forward bias, the cell fill factor, the open-circuit voltage, and its dependence on illumination.

VII. Other Photovoltaic Effects in CdS

15. CONTACT PHOTOVOLTAGE

In 1941 Goos⁴⁰⁸ observed a photo emf in a Cu doped CdS photoconductive powder on a glass plate with a transparent Pt barrier layer. A Au contact resulted in a smaller photo emf with a different spectral response. Broser and Warminsky⁴⁰⁹ produced a photovoltaic effect in CdS crystals with a Ag contact by irradiation with visible or ultraviolet light, also x and gamma rays, alpha particles, and electrons.

Reynolds¹ studied the spectral response of CdS crystals with Au, Ag, Cu, and Pt contacts. Grimmeiss and Memming¹⁷ diffused Cu, Ag, and Ni barrier metal into CdS single crystals at 600 to 700°C. They etched off the remainder to make frontwall photovoltaic cells. They achieved both backwall and frontwall sensitivity for CdS-Ag, with the same spectral response below the bandgap energy there was no response for backwall cells.

Nadjakov⁴¹⁰ was the first to study contact photovoltaic effects in thin film CdS layers deposited over a pair of Al and Au contacts. He obtained

photocurrents of 10^{-8} - 10^{-9} A. Table XVIII lists investigations of contact photovoltaic effects on CdS single crystals and sintered and thin film layers with a lateral and sandwich structure.

a. *Temperature Dependence*

Reynolds¹ found both the open-circuit voltage and the short-circuit current to decrease on increasing the temperature. Zyrianov¹⁹ also observed a decrease in the open-circuit voltage. Grimmelss and Memming¹⁷ describe a linear decrease in the open-circuit voltage with rise in temperature.

b. *Variation with Light Intensity*

Reynolds¹ states that the product of the short-circuit current and the open-circuit voltage increase linearly with the light intensity. Nadjakov¹⁰,¹⁵ describes a linear increase in the short-circuit current with light intensity, whereas the open-circuit voltage tends to approach the contact potential difference at high light intensity levels.

Bujatti and Muller¹⁹ find that at lower light levels the photovoltage depends linearly on the light intensity. At higher light intensities the photovoltage saturates at a value equal to the metal-semiconductor barrier height.⁴³ Bujatti⁴³² measured the saturation photovoltage for a number of different metals (see Table XVIII). The CdS-Au system did not saturate.

c. *Light Intensity Variation at Ohmic Contacts*

Ibuki *et al.*¹² observed a complex sign reversal of the photovoltage in In doped CdS as a function of light intensity and wavelength. The effect occurred only after heating the Cu contact. At low light intensities the polarity of the Cu contact changed from positive to negative.

A similar effect was observed by Ruppel^{422,423} on undoped CdS crystals with In contacts. At low light intensities the illuminated side became negative with respect to the crystal. At higher light levels the photovoltage underwent a sign reversal.

Ruppel⁴²³ observed a sign reversal as a function of wavelength on illuminating two lateral In and Au contacts. The photovoltage changed from positive to negative at the band edge reaching a minimum of 5100 Å. At wavelengths away from the band edge the photovoltage became positive for both shorter and longer wavelengths.

Ruppel⁴²³ explained these effects by an excess carrier generation at high light intensities which converts an electron accumulation layer into an

TABLE XVIII
CONTACT PHOTOVOLTAGE

Reference	CdS	Doping	Structure	Contacts		Temp. Range	Peak Wavelength (nm)	I_{sc}	V_{max} (V)
				Rectifying	Ohmic				
Goos ⁴⁰⁸	powder	Cu,Ni		transp. Pt,Au		-180 to +50°C	600 ~ 650	10 μA	
Broser ⁴⁰⁹	sgle. crystal			Ag	Al				
Veith ⁴¹¹ ,Wlérick ⁴¹²	thin film	Cu				220, 295°K			
Reynolds ¹	sgle. crystal	O ₂		Ag,Au,Cu,Pt	In	25 ~ 150°C	520, 680		
Liebson ^{413,414}	sgle. crystal			graphite					
Nadjakov ⁴¹⁵	sgle. crystal		lateral	Cu,Al,Fe,Pt	Zn			$10^{-9} - 10^{-10}$ A	
Nadjakov ^{410,187,416,417}	evap. film		lateral	Au	Al			$10^{-7} - 10^{-9}$ A	0.4 ~ 0.6
Nadjakov ⁴¹⁸	evap. film		lateral	Au	Al			100 ~ 200 μA	0.3
Zyrianov ⁴¹⁹	thin film	Cu		Pt		-180 to +250°C	487		
Gombay ²⁶⁶	sintered		lateral	Au,Cu	Al		480	1.6 μA	0.2
MacArthur ⁴²⁰	film		sandwich	Au,Al	Al				0.15
Cabannes ⁸¹	evap. film			Cu,Ag	In			27 μA	0.056
Kallmann ⁴²¹	sgle. crystal	Cu		jelly					0.2
Ibuki ¹²	sgle. crystal	In		Cu					0.5
Williams & Bube ¹³	sgle. crystal	I	frontwall/backwall	Cu			$2 \mu\text{A}/\text{cm}^2$	6.3	
				Fe			$0.08 \mu\text{A}/\text{cm}^2$	0.02	
				As			$0.02 \mu\text{A}/\text{cm}^2$	0.5	
				Au			$0.13 \mu\text{A}/\text{cm}^2$	0.3	
				Ag			$0.05 \mu\text{A}/\text{cm}^2$	0.02	
				Cu			$0.06 \mu\text{A}/\text{cm}^2$	very small	

Ruppel ^{422,423}	sgle. crystal		Au	In					
Grimmeiss ¹⁷	sgle. crystal	In,Ga	frontwall	Cu	Zn	-170 to 20°C	590,690,955	8.5 mA/cm ²	0.63
				Ag			540,590	0.5	0.45
				Ni			528	0.4	0.33
Fabricius ¹⁶	sgle. crystal			Cu,Au	In				
Lakshmanan ²³³	sputtered film		frontwall/ backwall	Cu,Au			550		
Moncrieff-Yeates ⁴²⁴	sgle. crystal			Ni,Cr,Pt					
Müller ⁴²⁵	sgle. crystal			Al,Au					
Mead & Spitzer ^{404,405}	cleaved sgle. crystal			Au,Cu	In				
Goodman ⁴²⁶	sgle. crystal			Ag,Cu,Pd,Au,Pt					
Palz & Ruppel ⁴²⁷⁻⁴²⁹	sgle. crystal	Cu,In	lateral & sandwich	Te,Au,Ag	In			0.49 μA	
Friedrich ⁴³⁰	sgle. crystal			Au	In	78°K, 300°K			
Bujatti ^{191,431,432}	thin film			Ag			< 500,850		0.02
				Cu					0.38, 0.45
				Au					>0.20
				Ni					0.52
				Te					0.63
Butendeich & Ruppel ⁴³³	vacuum cleared crystal			Ag					0.54
				Au					0.79
Okushi ⁴³⁴	thin film			Au,SnO ₂			480, 780		

electron depletion layer. The variation in wavelength varies the volume excitation of the electrons, and the sign reversal depends on the difference in electron excitation between volume and surface. There is a large generation of bulk carriers near the absorption edge.

Müller⁴²⁵ found that ohmic Al and Au contacts are negative under illumination due to the accumulation layer effect, whereas a rectifying Au contact is positive due to a barrier layer effect. In a barrier layer the short-circuit current varies linearly with the light intensity, but in an accumulation layer the intensity dependence is nonlinear.

d. *Light Intensity Variation of the Barrier Height in Photoconductive CdS*

Stirn, Boer, and Dussel⁴³⁵⁻⁴⁴¹ measured the barrier height in photoconductive CdS as a function of the light intensity. The barrier height ϕ_B was obtained from the carrier concentration n_c at the barrier:

$$n_c = N_c \exp(-\phi_B/kT).$$

n_c was derived from an analysis of the stationary high field domain^{437,442,443} adjacent to the cathode. The measurements were carried out over the temperature range from 155° to 300°K under bandgap illumination. The contact metals investigated were Au, Pt, Ag, Ni, Cu, and Sn. The CdS crystals were doped with Ag and Al; they were either air⁴³⁶ or vacuum cleaved.⁴³⁸ The same results were obtained with both types.

The effective barrier height under illumination was found to be independent of the metal work function, but decreased on increasing the light intensity. The following typical values were obtained for Au-CdS contacts: 155°K, 0.30 eV; 200°K, 0.38 to 0.48 eV; 300°K, 0.52 to 0.62 eV. The effective barrier height increases with the temperature and is 40-50% lower than for semiconducting CdS.

This lowering of the barrier height was originally attributed to the flux of holes into the barrier region. A more detailed analysis indicated that this is improbable.⁴⁴⁰ At low applied voltages thermal emission takes place at high temperatures and hole extraction at low temperatures. At high applied voltages there is tunneling through the barrier. The increase in the electric field is caused by space charge stored in native defects, due to donor levels 0.8 eV below the conduction band produced by cadmium interstitials or sulfur vacancies. This effect produces a space charge of 10^{18} cm^{-3} in the barrier region.

e. *Optical Enhancement of the Photovoltage*

Liebson^{413,414} observed an increase in the contact photovoltage by secondary infrared radiation. The enhancement in the photovoltage is coupled

to the quenching of the photoconductivity. The effect was studied in detail by Palz and Ruppel^{427-429,433} and by Friedrich.⁴³⁰ The maximum incremental photovoltage corresponds to the photoconductivity quenching maxima at 0.9 and 1.4 eV.

The increase in the photovoltage applies only if the light penetrates beyond the barrier layer. A reduction in photovoltage may take place depending on the wavelength and geometry, particularly in a lateral electrode arrangement. Zyrianov⁴¹⁹ reported quenching of the photovoltage by infrared illumination.

f. *Models of Contact Photovoltaic*

A number of different models have been advanced to explain the contact photovoltaic in CdS. Kallmann *et al.*⁴²¹ considered the photovoltages to be caused by inhomogeneous excitation due to a combination of electrode effects and the Dember⁴⁴⁸ effect. Müller⁴²⁵ showed that the Dember effect may be distinguished from other effects by a much longer time constant; the photovoltaic current risetime is less than 0.5 μ sec. An electrode effect was also proposed by Fabricius¹⁶ for a Au contact.

Nadjakov^{187,410,415-418,444} postulated a two-electrode photovoltaic effect when both contacts are illuminated in a lateral experimental arrangement. The photo emf corresponds to the value of the contact potential difference of the two electrodes. Two dissimilar metals are required to show a photovoltaic effect.

Williams and Bube,¹³ Mead and Spitzer,^{404,405} and Goodman⁴²⁶ have interpreted the contact photovoltaic as caused by electron emission at the metal contact. The variation of the photocurrent i_{sc} with the frequency of the light ν showed good agreement with the Fowler relation $i_{sc} \sim (h\nu - \phi_B)$, where ϕ_B is the barrier height. Williams and Bube¹³ showed that the photovoltaic current is strongly affected by light absorbed in metal layers not immediately adjacent to the CdS crystal, which they explained by the mean free path of the excited electrons in the metal.

Measurements by Palz and Ruppel^{428,429} indicated that the Fowler plot depends on doping the CdS and must therefore be explained by excitation within the CdS. Butendeich and Ruppel⁴³³ summarize the situation as follows. High conductivity CdS-metal junctions exhibit photoemission from the metal into CdS as postulated above. Low conductivity CdS-metal junctions show no photoresponse. Cu doped CdS-metal junctions exhibit impurity photovoltaic response, i.e., excitation of electrons into impurities. This mechanism was proposed by Palz and Ruppel^{427,428} and by Duc Cuong and Blair.¹⁹ The impurity photovoltage takes place entirely in the CdS and the metal just serves to separate the excited charge carriers.

Grimmeiss and Memming¹⁷ concluded that Cu, Ag, and Ni all form p-n junctions with CdS. Bujatti⁴⁴⁵ developed a Schottky barrier theory in which Bardeen's⁴⁴⁶ theory applies to low light levels. At high light intensities the photovoltage tends toward the potential barrier.

16. SURFACE PHOTOVOLTAGE

The surface photovoltage is the reduction in surface potential produced by light absorption. It was first measured in CdS by Schaaffs and Woelk.⁴⁴⁷ The photovoltage is due to a barrier layer photo effect caused by acceptor like charged surface states, but photovoltaic effects at the contacts and the Dember effect⁴⁴⁸ may also contribute. In highly conducting crystals the contribution of the latter is negligible.⁴⁴⁹

The effects of ambient changes and surface treatments on the surface photovoltage have been studied by Haas,⁴⁵⁰ Williams,⁴⁴⁹ Ludwig,⁴⁵¹ Many,⁴⁵²⁻⁴⁵⁴ Campbell,¹⁹⁶ Pamfilov,⁴⁵⁵ Steinrisser,^{456,457} and Gatos.⁴⁵⁸⁻⁴⁶² Campbell and Farnsworth¹⁹⁶ obtained a surface photovoltage of 20 to 60 mV for clean annealed (0001) Cd surfaces, whereas vacuum heated contaminated surfaces showed values less than 20 mV. Steinrisser and Hetrick^{456,457} obtained a relatively strong response to wavelengths longer than the bandgap after vacuum cleavage, which they attributed to excitation of electrons in intrinsic surface states or barrier states into the conduction band.

Williams^{211,449} and Many⁴⁵² obtained a surface photovoltage of 0.2 to 0.3 eV by the chemisorption of oxygen at atmospheric pressure due to the formation of charged acceptor states. The magnitude of the photovoltage increases logarithmically with oxygen pressure, light intensity, and exposure time.^{453,454} Ludwig⁴⁵¹ and Many⁴⁶⁴ observed saturation of the surface photovoltage at high illumination levels.

The photovoltage produced by absorbed electronegative gases is a measure of the absorption. Williams⁴⁴⁹ observed that iodine formed the largest photovoltage, followed by oxygen, air, and water vapor in that order. Neutral gases like helium, nitrogen, and also toluene or benzene had no effect. Balestra and Gatos⁴⁵⁸ observed a reduction in the surface photovoltage by water vapor. Williams⁴⁴⁹ found highly resistive CdS crystals to be independent of surface effects, whereas Ludwig⁴⁵¹ noted an oxygen dependence.

The spectral dependence of the surface photovoltage was studied by Nadzhakov^{463,464} and by Steinrisser and Hetrick.^{456,457} Lagowski, Balestra, and Gatos⁴⁵⁹⁻⁴⁶² developed photovoltage spectroscopy into a sophisticated tool for elucidating the parameters of the surface states of CdS. Nadzhakov

found that the surface photovoltage is generated primarily by light around 350–480 nm. Measurement of the photovoltage response near the absorption edge at 80°K by Steinrisser and Hetrick⁴⁵⁷ produced peaks corresponding to energies of maximum free exciton absorption.

Light of shorter wavelengths than the bandgap generates free carriers, and the surface photovoltage corresponds to changes in the surface barrier height. Longer wavelengths generate photostimulated emission or surface photovoltaic inversion. Photostimulated emission from surface states into the bulk decreases the barrier height and hence the contact potential difference.^{459–462} Illumination of subbandgap energy may also increase the surface barrier height by excitation of electrons at the valence band edge to unoccupied surface states, followed by hole trapping in the bulk. On illumination at certain wavelengths an initial depopulation of surface states due to photostimulated emission is followed by inversion resulting in a decrease in the contact potential difference. The initial rate of change of the surface barrier is a linear function of the illumination intensity.

Campbell and Farnsworth¹⁹⁶ measured an increase of 1.2 eV in the work function produced by one monolayer of oxygen photoabsorbed on a cleaved (0001) Cd surface. Approximately 0.2 eV of the work function change was interpreted as band bending at the surface, whereas the remaining change was attributed to an increase in electron affinity due to the formation of a dipole layer at the surface. Kanev⁴⁶⁵ determined the distribution of the surface potential of CdS crystals. He concluded that oxygen creates a barrier layer, and that the rectifying properties and hole injection intensity at the electrodes depend on differences in the adsorbed oxygen concentration.

17. OTHER PHOTOVOLTAIC DEVICES

a. *Other Heterojunctions*

A number of other heterojunction structures showing photovoltaic effects have been made in which one of the layers is composed of CdS; see Table XIX.

Kunioka and Sakai⁴⁶⁶ constructed a photovoltaic cell by evaporating CdS onto Se. The short-circuit current increased after heat treatment in air at 180°C. Okimura and Kondo^{471–473} obtained a heterojunction by evaporating CdS on Si crystals at 150° to 250°C. At lower temperatures a Schottky barrier was obtained. Cells on p-Si showed an excellent photovoltaic response with an efficiency of 5.5%. The CdS layer acts as a semi-transparent electrode. A high short-circuit current was obtained if the CdS

TABLE XIX
OTHER HETEROJUNCTION PHOTOVOLTAIC STRUCTURES

Reference	Contact	Base	Thin Film	Contact	I_{sc}	V_{oc} (V)	Efficiency	Max. Spectral Response (nm)
Kunioka & Sakai ⁴⁶⁶	metal	p-Se	evap. CdS	In		0.35-0.45		555
Kandilarov ⁴⁶⁷		CdS single crystal	evap. n-CdSe			0.3		
Pavlenko ⁴⁶⁸	In	CdS single crystal	p-CdTe	Pb-Sn		0.36	1%	650
Bonnet ^{469, 470}	In	CdS film	p-CdTe	Mo, Au			5-6%	
Okimura ⁴⁷¹⁻⁴⁷³	Au	p-Si n-Si	evap. CdS	Au			5.5%	
Adirovich ⁴⁷⁴	metal	CdS film	evap. CdTe					
Yoshikawa ⁴⁷⁵		n-GaAs	evap. CdS		2mA/cm ²	0.4		

layer was doped with chlorine. The structure resulted in photodiodes with excellent infrared response.

Kandilarov and Andreytchin⁴⁶⁷ developed n-n and n⁺-n heterojunctions by evaporating CdSe films on CdS single crystals. The sign and magnitude of the photovoltage is dependent on the doping. CdS-CdTe n-p heterojunctions were fabricated by Pavlenko⁴⁶⁸ and by Adirovich.⁴⁷⁴ Pavlenko made a photovoltaic cell with 1% efficiency. Adirovich *et al.* made photodiode networks in which a p-CdTe layer was sandwiched between two layers of n-CdS. Bonnet and Rabenhorst^{469,470} investigated CdS_xTe_{1-x} p-n junctions with a graded and abrupt energy gap on Mo foil substrates for solar cell applications.

b. *Ion Implantation*

Hou and Marley⁴⁷⁶ observed photovoltaic effects in CdS single crystals implanted with P⁺ ions. The polarity of the photovoltage indicated that the implanted layer was p-type. Lichtensteiger²²⁸ obtained photovoltaic effects by sputtering PH₃ doped CdS films onto high resistivity n-type CdS single crystals.

Photovoltaic effects were observed by Shiraki⁴⁷⁷ in p-n junctions formed by N ion implantation. After annealing the photovoltage peaked at 800 nm, indicating a level at 0.85 eV below the conduction band.

c. *Other Junctions*

Würfel and Ruppel⁴⁷⁸ evaporated CdS films onto barium titanate single crystals. Transient photocurrents were observed on illumination. The spontaneous polarization of the ferroelectric induces a photovoltage generated across a CdS space charge layer.

Nelson⁴⁷⁹ observed photovoltages on CdS separated from a metal contact by a layer of an organic dye.

d. *Becquerel Photovoltaic Effect*

Becquerel photovoltaic effects in CdS were first observed by Audubert and Stora.⁴⁸⁰ Electrolytes with a Cd anode and a CdS cathode showed a photovoltage with a maximum at 520 nm and a second maximum at 390 nm. The photovoltage was high in oxidizing solutions and very high in alkaline sulfides.

Williams⁴⁸¹ observed a photovoltaic effect produced by light incident at the interface of a Cl doped CdS crystal in a KCl solution. The photo emf was accompanied by a chemical reaction of the crystal in which Cd²⁺ ions go into solution and S²⁻ ions are left behind on the surface of the crystal.

Tell and Gibson⁴⁸² observed a photovoltage on immersing CdS crystals in KCl or K₂SO₄ electrolytes which increased at the CdS absorption edge. Ion implantation by Bi or Xe greatly reduced the photovoltage.

18. ANOMALOUS PHOTOVOLTAGES

Skarmian *et al.*⁴⁸³ observed larger than bandgap photovoltages up to 1.03 V in spray deposited Cu_xS-CdS solar cells. They were obtained by varying the spray parameters of CdS. The optimum substrate temperature was 575°F using a 0.03 molar solution at 1 liter/hr. A 2% conversion efficiency was obtained. The spectral response showed peaks at 495, 550 and 750 nm. The high voltage cells were affected more severely by heat treatment.

Brandhorst *et al.*^{483,484} observed anomalous photovoltages on high resistivity CdS films prepared by oblique deposition at 45° on quartz. The film thickness was 100–2000 Å. Photovoltages up to 17 V were obtained, though most were below 1 V at room temperature. The spectral response peaked at 0.5 μm but extended to 0.8 μm. The photovoltage was a maximum at –40 to –50°C and degraded in air. The photovoltage was attributed to a space charge created by a nonuniform distribution of trapped carriers. The decay showed traps at 0.08, 0.14, 0.26, and 0.41 eV below the conduction band in agreement with values obtained by thermally stimulated conductivity measurements.

Similar anomalous photovoltages were observed by Igras *et al.*⁴⁸⁵ in films deposited at 30° on hot glass substrates. The photovoltage was measured over the temperature range from –70° to 120°C and had an activation energy of 0.28 eV. The anomalous photovoltage was accompanied by a long risetime on the order of one minute, a long decay time, and an electret effect. Highly polycrystalline layers showed the highest photovoltages, which were attributed to structural defects at intercrystalline boundaries.

VIII. Conclusions

The development of the thin film CdS–Cu_xS photovoltaic cell has proceeded largely along empirical paths. In view of the potential of thin film solar cells for future solar energy conversion, a better understanding of the fundamental principles underlying cadmium sulfide thin film technology is needed.

Polycrystalline material of good quality can be deposited at substrate temperatures as low as 200°C, making it possible to utilize flexible organic

materials like polyimide as substrate. CdS crystallizes in the hexagonal system, so that the *c*-axis tends to align at right angles to the substrate even in polycrystalline material. This feature makes it possible to achieve efficiencies in polycrystalline material comparable to those in single crystals. The maximum achievable efficiency has been computed by Reynolds⁴⁸⁶ and by Shiozawa.^{60,120,326} For terrestrial applications (air mass one) this efficiency is 10%. Small area thin film cells with up to 8% efficiency have been constructed.

The present Clevite-Gould construction of the solar cell is far too expensive for use as a cheap photovoltaic converter for terrestrial use. To bring this about changes must be made in the deposition of the CdS film and in the metallic layers that serve as contacts and conductors. The CdS layer is now formed by vacuum deposition, but other methods listed in Section 5 could be considered for automation. However, a minimum thickness of about 25 μm is needed to form stable, high quality junctions by immersion in cuprous ion solutions. There is strong evidence that only this method of junction formation yields high efficiency photovoltaic cells (see Section 6) and that doping is required to produce a stable junction (Section 13). A difficult problem is the top conductor, which now consists of a gold-plated copper grid. Other materials have been tried without success.

Long-term degradation mechanisms present the most serious challenge to the use of thin film CdS solar cells. Many of these became apparent only after other, more rapid forms of degradation had been eliminated. Moisture and other surface effects have been removed by encapsulation. Catastrophic short circuits are produced by copper nodule formation, when the junction voltage is greater than 0.3 V, but this does not apply to normal operating conditions. Prolonged illumination at elevated temperatures, such as would be encountered in a desert environment, can produce significant degradation; see Section 13. From an understanding of the degradation mechanisms it should be possible to develop a design in which these effects are minimized.

Thin film CdS solar cells have been used to power balloons.^{54,99,487} They have also been utilized in experimental space flights, though showing significant degradation in output with time.^{54,275,284,488-490} Palz *et al.*⁹⁸ have predicted power outputs of up to 88 W/kg in lightweight arrays operating at 50°C. This compares favorably with silicon solar arrays, assuming that the cells can be stabilized.

Boer^{491,492} has made optimistic forecasts on the large scale use of low cost thin film arrays for terrestrial use. The present construction is to be modified by unspecified doping and proprietary treatments and encapsulated

between glass sheets. The cells have an expected lifetime of more than 10 years and an efficiency of 8% at air mass one. The cost is \$0.93/ft² for a continuous sheet or \$1.53/ft² for glass shingles to be used on rooftops. The projected generating cost of 1.2 to 4.2¢/kWh is comparable to the present cost of electricity.

REFERENCES

1. D. C. Reynolds, G. Leies, L. I. Antes, and R. E. Marburger, *Phys. Rev.* **96**, 533 (1954).
2. D. C. Reynolds and G. M. Leies, *Elec. Eng.* **73**, 734 (1954).
3. P. A. Crossley, G. T. Noel, and M. Wolf, Final Rep., Contract NASW-1427. RCA Astro-Electron. Div., Hightstown, New Jersey, 1968.
4. D. A. Hammond and F. A. Shirland, *Proc. Electron. Components Conf.*, 1959 p. 98 (1959).
5. A. E. Middleton, D. A. Gorski, and F. A. Shirland, *Progr. Astronaut. Rocketry* **3**, 275 (1961).
6. F. A. Shirland, ARL Tech. Rep. 60-293. Harshaw Chem. Co., 1960. †
7. D. C. Reynolds, "Encyclopedia of Chemical Technology," Suppl. 1, p. 667. Wiley (Interscience), New York, 1957.
8. D. C. Reynolds, U.S. Patents 2,844,640 (1958) and 2,981,777 (1961).
9. P. Rappaport, *RCA Rev.* **20**, 373 (1959).
10. J. Woods and J. A. Champion, *J. Electron. Contr.* **7**, 243 (1959).
11. M. Avinor, Ph.D. Dissertation, University of Amsterdam (1959).
12. S. Ibuki, H. Komiya, and H. Yamashita, *J. Phys. Soc. Jap.* **15**, 2356 (1960).
13. R. Williams and R. H. Bube, *J. Appl. Phys.* **31**, 968 (1960).
14. R. R. Bockemuehl, J. E. Kauppila, and D. S. Eddy, *J. Appl. Phys.* **32**, 1324 (1961).
15. L. G. Paritskii, A. A. Rogachev, and S. M. Ryvkin, *Fiz. Tverd. Tela* **3**, 1613 (1961); *Sov. Phys.—Solid State* **3**, 1170 (1961).
16. E. D. Fabricius, *J. Appl. Phys.* **33**, 1597 (1962).
17. H. G. Grimmeiss and R. Memming, *J. Appl. Phys.* **33**, 2217 (1962).
18. W. J. Deshotels, F. Augustine, and A. Carlson, 2nd Quart. Rep., Contract NAS7-203. Clevite Corp., 1963.
19. N. Duc Cuong and J. Blair, *J. Appl. Phys.* **37**, 1660 (1966).
20. B. Selle, W. Ludwig, and R. Mach, *Phys. Status Solidi* **24**, K149 (1967).
21. R. H. Bube, W. Gill, and P. Lindquist, Progr. Rep. No. 1, Grant NGR-05-020-214, Stanford University, (1967).
22. T. Shitaya and H. Sato, *Jap. J. Appl. Phys.* **7**, 1348 (1968).
23. N. Miya, *Jap. J. Appl. Phys.* **9**, 768 (1970).
24. K. W. Boer, Final Rep., Contract 952666. Jet Propulsion Lab., University of Delaware, Newark, 1970.
25. K. W. Boer, NASA-CR-129675, Grant NGR-08-001-028. University of Delaware, Newark, 1971.
26. W. D. Gill and R. H. Bube, *J. Appl. Phys.* **41**, 3731 (1970).
27. P. F. Lindquist and R. H. Bube, *J. Electrochem. Soc.* **119**, 936 (1972).
28. L. D. Massie, *Space/Aeronautics* p. 60 (1964).
29. F. A. Shirland, J. R. Hietanen, F. Augustine, and W. K. Bower, Final Rep., Contract NAS3-6461. Clevite Corp., 1965.

† The Clevite Corporation and the Harshaw Chemical Company are located in Cleveland, Ohio.

30. F. A. Shirland, *Advan. Energy Conv.* **6**, 201 (1966).
31. D. M. Perkins, *Advan. Energy Convers.* **7**, 265 (1968).
32. N. A. Komons, "Cadmium Sulfide, A History of Semiconductor Research at the Aerospace Research Laboratories." Off. Aerosp. Res., U.S. Air Force, 1964.
33. A. Carlson, "Research on Semiconductor Films," WADC Tech. Rep. 56-52. Clevite Corp., 1956.
34. A. E. Carlson, L. R. Shiozawa, and J. D. Finegan, U.S. Patent 2,820,841 (1958).
35. W. J. Deshotels, F. Augustine, and J. Koenig, 10th Mon. Sta. Rep., Contract NAS7-203 Clevite Corp. (1963).
36. W. J. Deshotels, F. Augustine, A. Carlson, J. Koenig, and M. P. Makowski, 3rd Quart. Rep., Contract NAS7-203. Clevite Corp., 1963.
37. W. J. Deshotels, F. Augustine, A. Carlson, and J. Koenig, 4th Quart. Rep., Contract NAS7-203. Clevite Corp., 1963.
38. W. J. Deshotels, F. Augustine, and J. Koenig, 1st Quart. Rep., Contract NAS3-2795. Clevite Corp., 1964.
39. W. J. Deshotels, F. Augustine, and J. Koenig, 2nd Quart. Rep., Contract NAS3-2795. NASA-CR-54065. Clevite Corp., 1964.
40. W. J. Deshotels and F. Augustine, 3rd Quart. Rep., Contract NAS3-2795, NASA-CR-54145. Clevite Corp., 1964.
41. W. J. Deshotels and F. Augustine, Final Rep., Contract NAS3-2795, NASA-CR-54343. Clevite Corp., 1964.
42. F. A. Shirland, F. Augustine, and W. Bower, 1st Quart. Rep., Contract NAS3-6461, NASA-CR-54302. Clevite Corp., 1965.
43. F. A. Shirland, F. Augustine, and W. K. Bower, 2nd Quart. Rep., Contract NAS3-6461, NASA-CR-54413. Clevite Corp., 1965.
44. F. A. Shirland, presented at Annu. Meet. Solar Energy Soc., 1965.
45. F. A. Shirland and J. R. Hietanen, *Proc. 19th Annu. Power Sources Conf.*, 1965 p. 177 (1965).
46. F. A. Shirland and J. R. Hietanen, *Proc. Photovoltaic Spec. Conf.*, 5th, 1965 Sect. IIC-3 (1966).
47. F. A. Shirland and F. Augustine, *Proc. Photovoltaic Spec. Conf.*, 5th, 1965 Sect. IIC-4 (1966).
48. F. A. Shirland, J. R. Hietanen, F. Augustine, and W. K. Bower, 3rd Quart. Rep., Contract NAS3-6461. Clevite Corp., 1965.
49. F. A. Shirland, J. R. Hietanen, F. Augustine, and W. K. Bower, 2nd Quart. Rep., Contract NAS3-8502. Clevite Corp., 1966.
50. F. A. Shirland, J. R. Hietanen, and W. K. Bower, 3rd Quart. Rep., Contract NAS3-8502. Clevite Corp., 1966.
51. F. A. Shirland, J. R. Hietanen, and W. K. Bower, Quart. Progr. Rep. and Final Rep., Contract NAS3-8502. Clevite Corp., 1966.
52. F. A. Shirland, Clevite Corp. Eng. Memo 66-17 (1966), presented at 2nd OAR Res. Appl. Conf., 1967.
53. J. R. Hietanen and F. A. Shirland, *Photovoltaic Spec. Conf. Rec.*, 6th, 1967 Vol. I, p. 179 IEEE (1967).
54. H. E. Nastelin, J. R. Hietanen, and F. A. Shirland, Final Rep., AF33(615)-3253. Clevite Corp., 1967.
55. J. Bernard, Tech. Note NT-02-2. Centre d'Études et de Recherches en Technologie Spatiale, 1967.
56. L. R. Shiozawa, G. A. Sullivan, F. Augustine, and J. M. Jost, Interim Tech. Rep., Contract AF33(615)-5224. Clevite Corp., 1967.

57. F. A. Shirland, W. K. Bower, and J. R. Green, Interim Tech. Rep., Contract NAS3-9434. Clevite Corp., 1968.
58. F. A. Shirland, presented at Hanover Electron. Conf., 1968.
59. F. A. Shirland, W. K. Bower, W. F. Dunn, and J. B. Green, Final Rep., NAS3-9434. Clevite Corp., 1969.
60. L. R. Shiozawa, F. Augustine, G. A. Sullivan, J. M. Smith, and W. R. Cook, Final Rep., Contract AF33(615)-5224. Clevite Corp., 1969.
61. F. A. Shirland and D. A. Gorski, 3rd Quart. Progr. Rep., Contract AF33(616)-6548. Harshaw Chem. Co., 1960.
62. F. A. Shirland, G. A. Wolff, and J. D. Nixon, ASD-TDR-62-69, Contract AF33(616)-7528. Harshaw Chem. Co., 1962.
63. J. D. Nixon and N. E. Heyerdahl, ARL-62-395, Contract AF33(616)-6548. Harshaw Chem. Co., 1962.
64. D. A. Gorski, U.S. Patent 3,186,874 (1965).
65. F. A. Shirland, G. A. Wolff, J. C. Schaefer, and G. H. Dierssen, ASD-TDR-62-69, Vol. II. Harshaw Chem. Co., 1962.
66. J. C. Schaefer, R. J. Humrick, E. R. Hill, and R. F. Belt, Final Rep., ASD-TDR-63-743. Harshaw Chem. Co., 1963.
67. J. C. Schaefer, *Proc. 3rd Photovoltaic Spec. Conf., 1963* Rep. No. PIC-SOL-209/3 (1963).
68. T. A. Griffin, R. W. Olmstead, and J. C. Schaefer, Final Rep., Contract NAS3-2493, NASA-CR-54108. Harshaw Chem. Co., 1962-1964.
69. T. A. Griffin and J. C. Schaefer, 3rd Quart. Progr. Rep., Contract NAS3-2493, NASA-CR-70370. Harshaw Chem. Co., 1963.
70. J. C. Schaefer and R. L. Statler, *Proc. Photovoltaic Spec. Conf., 4th, 1964* Vol. 2, p. A-6-1 (1966).
71. J. C. Schaefer, Tech. Rep. AFAPL-TR-65-1. Harshaw Chem. Co., 1965.
72. J. C. Schaefer, R. J. Humrick, and R. F. Belt, 2nd Quart. Tech. Progr. Rep., Contract AF33(615)-1248. Harshaw Chem. Co., 1964.
73. J. C. Schaefer, R. J. Humrick, and R. F. Belt, 1st Quart. Tech. Progr. Rep., Contract AF33(615)-1248. Harshaw Chem. Co., 1964.
74. T. A. Griffin, D. J. Krus, and J. C. Schaefer, Final Rep., Contract NAS3-4177. Harshaw Chem. Co., 1965.
75. J. C. Schaefer, E. R. Hill, and T. A. Griffin, Final Rep., Contract NAS3-7631. Harshaw Chem. Co., 1966.
76. J. C. Schaefer, J. Evans, and T. A. Griffin, Final Rep., Contract NAS3-8515. Harshaw Chem. Co., 1967.
77. H. I. Moss, *Proc. Nat. Aeronaut. Electron. Conf., 1960* p. 47 (1960).
78. H. I. Moss, *RCA Rev.* **22**, No. 1, 29 (1961).
79. R. R. Addiss *et al.*, Rep. No. ASD-TR-61-11. RCA Corp., Princeton, New Jersey, 1961.
80. W. L. C. Hui and J. P. Corra, *Proc. Photovoltaic Spec. Conf., 5th, 1965* Vol. II, C-5-1 (1966).
81. F. Cabannes, *C. R. Acad. Sci.*, **246**, 257 (1958).
82. L. E. Ravich, *Proc. U.N. Conf. New Sources Energy, Solar Energy, Wind, Power, Geothermal Energy, 1961*, Vol. 4, p. 258 (1964).
83. I. Abrahamsohn, U.S. Patent 3,376,163 (1968).
84. H. G. Grimmeiss and R. Memming, *J. Appl. Phys.* **33**, 3596 (1962).
85. V. A. Drozdov, Sh. D. Kurmashev, and A. L. Rvachev, *Radiotekh. Elektron.* **10**, 1358 (1965); *Radio Eng. Electron. Phys. (USSR)* **10**, 1172 (1965).

86. C. Pastel, *J. Phys.* **26**, 127 (1965).
87. C. Pastel, "Effect photovoltaïque dans les couches évaporées de sulfure de cadmium." Ph.D. Thesis, University of Paris, 1962.
88. B.A.R.A. Final Rep., Contract 64-34-375-00-480-75-01 (1965), Royal Aircraft Establishment Transl., 1966.
89. J. S. Skarman, A. B. Budinger, and R. R. Chamberlin, Summary Rep., Contract AF33(615)-1578. National Cash Register Co., Dayton, Ohio, 1965.
90. R. R. Chamberlin and J. S. Skarman, *Solid-State Electron.* **9**, 819 (1966).
91. R. R. Chamberlin and J. S. Skarman, *J. Electrochem. Soc.* **113**, 86 (1966).
92. M. Balkanski and B. Choné, *Rev. Phys. Appl.* **1**, 179 (1966).
93. S. Yu. Pavelets and G. A. Fedorus, *Ukr. Fiz. Zh.* **11**, 686 (1966).
94. K. R. Albrand, E. W. Justi, W. Möhle, G. H. A. Schneider, and D. Ullrich, *Coop. Med. Energ. Sol., Bull.* **13**, 5 (1967).
95. W. Palz, G. Cohen Solal, J. Vedel, J. Fremy, T. N. Duy, and J. Valerio, *Photovoltaic Spec. Conf., Rec., 7th, 1968* p. 54 IEEE (1968).
96. W. Palz, J. Besson, J. Fremy, T. N. Duy, and J. Vedel, *Photovoltaic Spec. Conf. Rec., 8th, 1970* p. 16, IEEE (1970).
97. G. Coste, J. Fremy, and T. N. Duy, *Proc. Int. Colloq. Solar Cells, 1970* p. 187 (1971).
98. W. Palz, J. Besson, T. N. Duy, and J. Vedel, *Photovoltaic Spec. Conf. Rec., 9th, 1972* p. 91, IEEE (1973).
99. W. Palz, J. Besson, T. N. Duy, and J. Vedel, *Photovoltaic Spec. Conf. Rec., 10th, 1973* p. 69, IEEE (1974).
100. R. J. Mytton, *Brit. J. Appl. Phys.* **1**, 721 (1968).
101. I. V. Egorova, *Fiz. Tekh. Poluprov.* **2**, 319 (1968), *Sov. Phys.—Semicond.* **2**, 266 (1968).
102. M. Daspet, J. Besson, and M. Lacroix, *Coop. Med. Energ. Solaire, Bull.* **14**, 117 (1968).
103. A. V. Anshon and I. A. Karpovich, *Fiz. Tekh. Poluprov.* **3**, No. 4, 503 (1969); *Sov. Phys.—Semicond.* **3**, No. 4, 503 (1969).
104. J. P. David, S. Martinuzzi, F. Cabane-Brouty, J. P. Sorbier, J. M. Mathieu, J. M. Roman, J. F. Bretzner, *Proc. Int. Colloq. Solar Cells, 1970*, p. 81 (1971).
105. K. Bogus, H. Fisher, S. Mattes, and N. Peters, *Proc. Int. Colloq. Solar Cells, 1970* p. 121 (1971).
106. K. Bogus and S. Mattes, *Photovoltaic Spec. Conf. Rec. 9th, 1972* p. 106, IEEE (1973).
107. L. Clark, R. Gale, K. Moore, R. J. Mytton, and R. S. Pinder, *Proc. Int. Colloq. Solar Cells, 1970* p. 241 (1971).
108. R. A. Mickelsen and D. D. Abbott, Final Rep., Contract NAS3-13232, NASA-CR-120812. Boeing Co., Seattle, Washington, 1971.
109. University of Delaware, Report NSF/RANN/SE/GI-34872/PR73/L (1973).
110. K. W. Boer *et al.*, *Photovoltaic Spec. Conf. Rec., 10th, 1973* p. 77, IEEE (1974).
111. V. M. Yefremenkova, I. V. Egorova, and V. E. Yurasova, *Izv. Akad. Nauk SSSR, Ser. Fiz.* **32**, No. 7, 1242 (1968).
112. R. R. Chamberlin and J. S. Skarman, ASD-TDR-63-223, Part II. National Cash Register Co., Dayton, Ohio, 1963.
113. R. R. Chamberlin, J. S. Skarman, D. E. Koopman, and L. E. Blakely, ASD-TDR-63-323, Part I. National Cash Register Co., Dayton, Ohio, 1963.

114. E. L. Lind, J. J. Loferski, L. Pensak, P. Rappaport, and S. M. Thomsen, 4th Interim Rep., Contract DA-36-039-SC-64643. RCA Corp., Princeton, New Jersey, 1956.
115. F. N. Nicoll, U.S. Patent 2,999,240 (1961).
116. S. Kanev, V. Sekerdzijski, and V. Stoyanov, *C. R. Acad. Bulg. Sci.* **16**, 685 (1961).
117. S. Kanev, V. Stoyanov, and V. Shekeredzhiyski, *Acta Phys. Pol.* **25**, 313 (1964).
118. S. Kanev, V. Stoyanov, and R. Stefanov, *C. R. Acad. Bulg. Sci.* **20**, 405 (1967); *Bull. Inst. Phys. Rech. At., Acad. Bulg. Sci.* **17**, 13 (1968).
119. L. R. Shiozawa, G. A. Sullivan, F. Augustine, and J. M. Jost, 6th Quart. Rep. Contract AF33(615)-5224. Clevite Corp., 1967.
120. L. R. Shiozawa *et al.*, 8th Quart. Progr. Rep., Contract AF33(615)-5224. Clevite Corp., 1968.
121. L. R. Shiozawa, F. Augustine, and W. R. Cook, 1st Quart. Progr. Rep., Contract F33615-68-C-1732. Clevite Corp., 1969.
122. N. Nakayama, *Jap. J. Appl. Phys.* **8**, 450 (1969).
123. *D. K. Newsletter* **3** (1969); N. Nakayama *et al.*, *Nat. Tech. Rep. (Matsushita Elec. Ind. Co., Osaka)* **15**, 154 (1969).
124. E. Konstantinova and S. Kanev, *J. Appl. Phys.* **42**, 5851 (1971).
125. S. Vojdani, A. Sharifnai, and M. Doroudian, *Electron. Lett.* **9**, 128 (1973).
126. T. S. TeVelde, *AGARD Conf. Proc. AGARD-CP-21*, 927 (1967).
127. T. S. TeVelde and G. W. M. T. van Helden, *Philips Tech. Rev.* **29**, 238 (1968).
128. R. E. Aitchison, *Nature (London)* **167**, 812 (1951).
129. M. G. Miksic, E. S. Schlig, and R. R. Haering, *Solid-State Electron.* **7**, 39 (1964).
130. D. M. Hughes and G. Carter, *Vacuum* **17**, 555 (1967).
131. J. Dresner and F. V. Shallcross, *Solid-State Electron.* **5**, 205 (1962).
132. R. Zuleeg and E. J. Senkovits, *Joint Symp. Thin Films Electron. Appl., Electro-chem. Soc.*, 1963 Extended Abstracts, p. 110 (1963).
133. J. de Klerk and E. F. Kelly, *Rev. Sci. Instrum.* **36**, 506 (1965).
134. J. de Klerk, in "Physical Acoustics" (W. P. Mason ed.), Vol. 4, Part A, Chapter 5. Academic Press, New York, 1966.
135. C. LeFloch, *Solid-State Electron.* **15**, 753 (1972).
136. W. Kahle and H. Berger, *Phys. Status Solidi A* **2**, 717 (1970).
137. F. V. Shallcross, *RCA Rev.* **28**, 569 (1967).
138. P. D. Fuchs and B. Lunn, *J. Appl. Phys.* **34**, 1762 (1963).
139. R. R. Addiss, *Nat. Symp. Vac. Tech. Trans.*, 10th, 1963 p. 354 (1963).
140. M. Bujatti, *J. Phys. D* [2] **1**, 983 (1968).
141. B. D. Galkin, N. V. Troitskaya, and R. D. Ivanov, *Kristallografiya* **12**, 878 (1967); *Sov. Phys.—Crystallogr.* **12**, No. 5, 766 (1968).
142. K. K. Muravyeva, I. P. Kalinkin, L. A. Sergeeva, V. B. Aleskovsky, and N. S. Bogomolov, *Izv. Akad. Nauk SSSR, Neorg. Mater.* **6**, 434 (1970); *Inorg. Mater. (USSR)* **6**, 381 (1971).
143. P. Hudock, *Trans. AIME* **239**, 338 (1967).
144. I. P. Kalinkin, K. K. Muravyeva, I. B. Yurgel, V. B. Aleskovsky, and I. N. Anikin, *Izv. Akad. Nauk SSSR, Neorg. Mater.* **6**, 1564 (1970); *Inorg. Mater. (USSR)* **6**, 1382 (1971).
145. K. K. Muravyeva, I. P. Kalinkin, V. B. Aleskovsky, and I. N. Anikin, *Thin Solid Films* **10**, 355 (1972).
146. G. A. Krasulin and A. V. Vanyukhov, *Izv. Akad. Nauk SSSR, Neorg. Mater.* **6**, 122 (1970); *Inorg. Mater. (USSR)* **6**, 101 (1970).
147. R. S. Spriggs and A. J. Learn, *Rev. Sci. Instrum.* **27**, 1539 (1966).

148. R. W. Hoffman, *Phys. Thin Films* **3**, 211 (1966).
149. C. A. Escoffery, *J. Appl. Phys.* **35**, 2273 (1964).
150. C. A. Escoffery, *Rev. Sci. Instrum.* **35**, 913 (1964).
151. M. Ohnishi, M. Yoshizawa, and S. Ibuki, *Jap. J. Appl. Phys.* **6**, 899 (1967).
152. M. Ohnishi, M. Yoshizawa, and S. Ibuki, *Jap. J. Appl. Phys.* **6**, 1020 (1967).
153. R. T. Galla, *Rev. Sci. Instrum.* **36**, 403 (1965).
154. F. E. Card and J. J. Galen, *Rev. Sci. Instrum.* **32**, 858 (1961).
155. A. Vecht, *Phys. Thin Films* **3**, 165 (1966).
156. C. E. Drumheller, *Nat. Symp. Vac. Tech. Trans.*, 7th, 1960, p. 306 (1961).
157. A. A. Aponick, Rep. ESL-R-229, MIT Proj. DSR 9948. M.I.T., Cambridge, Massachusetts, 1965.
158. R. J. Miller and C. H. Bachman, *J. Appl. Phys.* **29**, 1277 (1958).
159. W. C. Boesman and G. G. Avis, *Nat. Symp. Vac. Tech. Trans.*, 10th, 1963 p. 364 (1963).
160. L. E. Terry and E. E. Komarek, Tech. Memo SC-TM-64-1677. Sandia Corp., Albuquerque, New Mexico, 1964.
161. R. Weber, *Rev. Sci. Instrum.* **37**, 955 (1966).
162. R. Weber, *Proc. IEEE* **54**, 333 (1966).
163. J. P. Sorbier, J. P. Legre, and S. Martinuzzi, *Vide* **133**, 32 (1968).
164. D. W. Readey, *J. Amer. Ceram. Soc.* **49**, 681 (1966).
165. D. W. Readey, Rep. No. HDL-TR-1280. Harry Diamond Labs., Washington, 1965.
166. G. J. Mares, *Proc. IEEE* **54**, 1077 (1966).
167. G. G. Avis, W. C. Boesman, and D. W. Readey, Rep. No. TR-1297. Harry Diamond Labs., Washington, 1965.
168. R. Köhler, H. Lippmann, W. Kosak, E. Roll, and L. Waner, in "Proceedings of the 2nd Colloquium on Thin Films" (E. Hahn, ed.), p. 419. Vandenhoeck & Ruprecht, Göttingen, 1968.
169. G. O. Müller and H. Peibst, *Phys. Status Solidi* **8**, K51 (1965).
170. T. Avignon, J.-P. Sorbier, F. Cabane-Brouty, and S. Martinuzzi, *Vide* **141**, 196 (1969).
171. D. A. Cusano, in "Physics and Chemistry of II-VI Compounds" (M. Aven and J. S. Prener, eds.), Chapter 14. North-Holland Publ., Amsterdam, 1967.
172. L. S. Palatnik, M. N. Naboka, and N. T. Gladkikh, *Kristallografiya* **10**, 399 (1965); *Sov. Phys.—Crystallogr.* **10**, 320 (1965).
173. K. Günther, in "The Use of Thin Films in Physical Investigations" (J. C. Anderson, ed.), p. 213. Academic Press, New York, 1966.
174. D. J. Page, *Proc. Joint I.E.R.E. (Inst. Electron. Radio Eng.)-I.E.E. (Inst. Elec. Eng.) Conf. Appl. Thin Films Electron. Eng.*, 1966 p. 9-1 (1967).
175. D. Beecham, *Rev. Sci. Instrum.* **41**, 1654 (1970).
176. S. S. Aitkhozhin, A. D. Gingis, Yu. V. Gulyaev, A. M. Kmita, I. M. Kotelyanskii, A. V. Medved, A. I. Morozov, and B. A. Stankovskii, *Bull. Acad. Sci. USSR, Phys. Ser.* **35**, 852 (1971).
177. E. L. Lind, F. N. Lancia, and E. R. Hill, Rep. ASD-TDR-65-654. Harshaw Chemical Co., 1963.
178. N. F. Foster, *J. Appl. Phys.* **38**, 149 (1967).
179. N. F. Foster, *Proc. IEEE* **53**, 1400 (1965).
180. N. F. Foster, G. A. Coquin, G. A. Rozgonyi, and F. A. Vannatta, *IEEE Trans. Sonics Ultrason.* **15**, 28 (1968).

181. M. Aven and D. A. Cusano, *J. Appl. Phys.* **35**, 606 (1964).
182. F. A. Pizzarello, *J. Appl. Phys.* **35**, 2730 (1964).
183. J. de Klerk, *Phys. Rev.* **139**, A1635 (1965).
184. I. A. Karpovich and B. N. Zvonkov, *Fiz. Tverd. Tela* **6**, 3392 (1964); *Sov. Phys.—Solid State* **6**, 2714 (1965).
185. F. Gans, *Bull. Sci. AIM, Liege* **11**, 897 (1953).
186. A. J. Learn and J. A. Scott-Monck, *J. Phys. Chem. Solids* **29**, 2065 (1968).
187. G. Nadjakov, R. Andrejtschin, S. Balabanov, and J. Stanislavova, *C. R. Acad. Bulg. Sci.* **9**, 1 (1956).
188. W. J. Deshotels and F. Augustine, *Proc. Photovoltaic Spec. Conf., 4th, 1964* Vol. 2, p. A-4-1 (1964).
189. J. Schaefer, G. A. Wolff, and E. R. Hill, 2nd Quart. Tech. Progr. Rep., Contract AF33(657)-9975. Harshaw Chem. Co., 1963.
190. J. C. Schaefer, E. R. Hill, and T. A. Griffin, Rep. NASA-CR-54856. Harshaw Chem. Co., 1965.
191. M. Bujatti and R. S. Muller, *J. Electrochem. Soc.* **112**, 702 (1965).
192. J. A. Scott-Monck, R. E. Scott, H. T. Mann, and F. T. Snively, Rep. NASA-CR-72608. TRW Systems, Inc., Redondo Beach, 1970.
193. J. I. B. Wilson and J. Woods, *J. Phys. Chem. Solids* **34**, 171 (1973).
194. J. Gilles and J. van Cakenberghe, *Nature (London)* **182**, 862 (1958).
195. J. M. Gilles and J. van Cakenberghe, *Solid State Phys. Electron. Telecommun., Proc. Int. Conf., 1958* Vol. 2, Part 2, 900 (1960).
- 195a. R. H. Bube, *J. Appl. Phys.* **31**, 2239 (1960).
196. B. D. Campbell and H. E. Farnsworth, *Surface Sci.* **10**, 197 (1968).
197. F. H. Nicoll and B. Kazan, *J. Opt. Soc. Amer.* **45**, 647 (1955).
198. S. M. Thomsen and R. H. Bube, *Rev. Sci. Instrum.* **26**, 664 (1955).
199. F. H. Nicoll, *J. Electrochem. Soc.* **110**, 1165 (1963).
200. J. J. Hegyi, *Extended Abstr. Electron Div., Electrochem. Soc.* **13**, 72 (Abstract 150) (1964).
201. F. A. Kroger, H. J. Vink, and J. von den Boomgaard, *Z. Phys. Chem.* **203**, 1 (1954).
202. S. Ibuki, *J. Phys. Soc. Jap.* **14**, 1181 (1959).
203. S. Ibuki and K. Awazu, *J. Phys. Soc. Jap.* **11**, 1297 (1956).
204. P. D. Fuchs, *J. Appl. Phys.* **31**, 1733 (1960).
205. R. J. Caveney, *J. Cryst. Growth* **2**, 85 (1968).
206. J. Chikawa, *Appl. Phys. Lett.* **7**, 193 (1965).
207. J. C. Schaefer, E. R. Hill, and T. A. Griffin, Rep. NASA-CR-54932. Harshaw Chem. Co., 1965.
208. O. Igashiki, *J. Appl. Phys. Jap.* **8**, 642 (1969).
209. R. Nitsche and D. Richman, *Z. Elektrochem.* **66**, 709 (1962).
210. M. Weinstein and G. A. Wolff, *J. Phys. Chem. Solids, Suppl.* **1**, 537 (1967).
211. R. H. Bube, Rep. AFCRL-62-158. RCA Corp., Princeton, New Jersey, 1962.
212. R. Nitsche, H. U. Böhlsterli, and M. Lichtensteiger, *J. Phys. Chem. Solids* **21**, 199 (1961).
213. J. A. Beun, R. Nitsche, and H. U. Böhlsterli, *Physica (Utrecht)* **28**, 184 (1962).
214. R. Frerichs, *Phys. Rev.* **72**, 594 (1947).
215. F. Schossberger, *J. Electrochem. Soc.* **102**, 22 (1955).
216. A. I. Volkov and I. M. Kotelyanskii, *Izv. Akad. Nauk SSSR, Neorg. Mater.* **9**, 1109 (1973); *Inorg. Mater. (USSR)* **9**, 988 (1973).
217. J. E. Jacobs and C. W. Hart, *Proc. Nat. Electron. Conf.* **11**, 592 (1955).

218. L. Capella and J. C. Heyraud, *C. R. Acad. Sci.* **261**, 4053 (1965).
219. R. W. Berry, P. M. Hall, and M. T. Harris, "Thin Film Technology." Van Nostrand-Reinhold, Princeton, New Jersey, 1968.
220. L. I. Maisel, *Phys. Thin Films* **3**, 61 (1966).
221. G. K. Wehner, *Advan. Electron. Electron Phys.* **7**, 239 (1955).
222. G. Brincourt and S. Martinuzzi, *Vide* **22**, No. 131, 253 (1967).
223. V. M. Yefremenkova and V. Ye. Yurasova, *Izv. Akad. Nauk SSSR, Ser. Fiz.* **32**, 1056 (1968).
224. V. M. Efremenkova and V. E. Yurasova, *Bull. Acad. Sci. USSR, Phys. Ser.* **32**, 981 (1968).
225. V. Ye. Yurasova, L. N. Levykina, and V. M. Yefremenkova, *Fiz. Tverd. Tela* **7**, 2875 (1965); *Sov. Phys.—Solid State* **7**, 2332 (1966).
226. Yu. M. Gerasimov, G. I. Distler, V. M. Yefremenkova, and V. Ye. Yurasova, *Fiz. Tverd. Tela* **10**, 270 (1960); *Sov. Phys.—Solid State* **10**, 207 (1968).
227. I. Lagnado and M. Lichtensteiger, *J. Vac. Sci. Technol.* **7**, 318 (1970).
228. M. Lichtensteiger, I. Lagnado, and H. C. Gatos, *Appl. Phys. Lett.* **15**, 418 (1969).
229. M. Honda, *Trans. Inst. Elec. Commun. Eng. Jap.* **55-C**, 17 (1972).
230. W. H. Leighton, *J. Appl. Phys.* **44**, 5011 (1973).
231. D. B. Fraser and H. Melchior, *J. Appl. Phys.* **43**, 3120 (1972).
232. G. Helwig and H. König, *Z. Angew. Phys.* **7**, 323 (1955).
233. T. K. Lakshmanan and J. M. Mitchell, *Nat. Symp. Vac. Tech. Trans.*, *10th, 1963* p. 335 (1963).
234. J. Pompei, *Proc. Symp. Deposition Thin Films Sputtering*, *2nd, 1967* p. 127 (1967).
235. C. Weissmantel, G. Hecht, J. Herberger, and J. Tuphorn, *Proc. Colloq. Thin Films*, *2nd, 1967* p. 399 (1968).
236. G. Hecht and C. Weissmantel, presented at 2nd Conf. Thin Films, 1968.
237. R. Lawrance, *Brit. J. Appl. Phys.* **10**, 298 (1959).
238. J. S. Preston, *Proc. Roy. Soc., Ser. A* **202**, 449 (1950).
239. G. Helwig, *Z. Phys.* **132**, 621 (1952).
240. L. Holland and G. Siddal, *Vacuum* **11**, 375 (1953).
241. T. K. Lakshmanan, *J. Electrochem. Soc.* **110**, 548 (1963).
242. S. G. Mokrushin and Yu. D. Tkachev, *Kolloid. Zh.* **23**, 438 (1961); *Colloid J. USSR* **23**, 366 (1961).
243. G. A. Kitaev and A. A. Uritskaya, *Izv. Akad. Nauk SSSR, Neorg. Mater.* **2**, 1554 (1966).
244. G. A. Kitaev, A. A. Uritskaya, and S. G. Mokrushin, *Russ. J. Phys. Chem.* **39**, 1101 (1965).
245. G. A. Kitaev, S. G. Mokrushin, and A. A. Uritskaya, *Kolloid. Zh.* **27**, 51 (1965); *Colloid J. USSR* **27**, 38 (1965).
246. G. A. Kitaev, A. A. Uritskaya, and S. G. Mokrushin, *Kolloid. Zh.* **27**, 379 (1965); *Colloid J. USSR* **27**, 317 (1965).
247. A. A. Uritskaya, G. A. Kitaev, and S. G. Mokrushin, *Kolloid. Zh.* **27**, 767 (1965); *Colloid J. USSR* **27**, 654 (1965).
248. M. Nagao and S. Watanabe, *J. Appl. Phys. Jap.* **7**, 684 (1968).
249. N. Pavaskar and C. Menezes, *J. Appl. Phys. Jap.* **7**, 743 (1968).
250. F. B. Micheletti and P. Mark, *Appl. Phys. Lett.* **10**, 136 (1967).
251. F. B. Micheletti, Ph.D Dissertation, Princeton University, Princeton, New Jersey (1968).
252. R. R. Chamberlin, *Bull. Amer. Ceram. Soc.* **45**, 698 (1966).

253. C. Wu, R. S. Feigelson, and R. H. Bube, *J. Appl. Phys.* **43**, 756 (1972).
254. S. M. Thomsen, U.S. Patent 2,765,385 (1956).
255. C. P. Hadley and E. Fisher, *RCA Rev.* **20**, 635 (1959).
256. M. J. B. Thomas and E. J. Zdanuk, *J. Electrochem. Soc.* **106**, 964 (1959).
257. R. R. Billups, W. L. Gardner, and M. D. Zimmerman, Tech. Rep. No. 200. M.I.T. Lincoln Laboratory, Lexington, Massachusetts, 1959.
258. S. Kitamura, *J. Phys. Soc. Jap.* **15**, 2343 (1960).
259. S. Kitamura, T. Kubo, T. Yamashita, and Y. Amano, *Jap. J. Appl. Phys.* **29**, 636 (1960).
260. S. Kitamura *et al.*, *Nat. Tech. Rep. (Matsushita Elec. Ind. Co., Osaka)* **35**, 11 (1961).
261. Y. T. Sihvonen, S. G. Parker, and D. R. Boyd, *J. Electrochem. Soc.* **114**, 96 (1967).
262. E. Hill, Final Rep., Contract NAS5-5884. Harshaw Chem. Co., 1964-1965.
263. F. B. Micheletti and P. Mark, *J. Appl. Phys.* **39**, 5274 (1968).
264. S. Yoshimatsu, C. Kanzaki, S. Ibuki, and N. Murai, *J. Phys. Soc. Jap.* **10**, 493 (1955).
265. N. A. deGier, W. van Gool, and J. G. van Santen, *Philips Tech. Rev.* **20**, 277 (1958/1959).
266. L. Gombay, J. Gyulai, and I. Hevesi, *Acta Phys. Chem.* **4**, 30 (1958).
267. L. Gombay, J. Lang, and J. Kispéter, *Acta Phys. Chem.* **10**, 23 (1964).
268. P. H. Wendland, *Rev. Sci. Instrum.* **33**, 337 (1962).
269. D. A. Hammond and F. A. Shirland, Tech. Rep., WADC TR57-770. Harshaw Chem. Co., 1957.
270. D. A. Cusano, *Solid-State Electron.* **6**, 217 (1963).
271. F. A. Shirland, U.S. Patent 3,146,158 (1964).
272. E. R. Hill and B. G. Keramidas, *Proc. Photovoltaic Spec. Conf., 5th, 1965* PIC-SOL 209/6.1, Sect. C-6-NASA-CR-70169 (1966).
273. E. R. Hill and B. G. Keramidas, *Rev. Phys. Appl.* **1**, 189 (1966); *IEEE Trans. Electron. Devices* **14**, 22 (1967).
274. E. R. Hill, B. G. Keramidas, and D. J. Krus, *Photovoltaic Spec. Conf. Rec. 6th, 1967*, Vol. I, p. 35, IEEE (1967).
275. W. F. Dunn and H. E. Nastelin, Rep. ARL70-0036. Clevite Corp., 1970.
276. L. R. Shiozawa, G. A. Sullivan, F. Augustine, and J. M. Jost, 5th Quart. Rep., Contract AF33(615)-5224. Clevite Corp., 1967.
277. A. E. van Aerschot, J. J. Capart, K. H. David, M. Fabbricotti, K. H. Heffels, J. J. Loferski, and K. K. Reinhartz, *Photovoltaic Spec. Conf. Rec., 7th, 1968* p. 22, IEEE (1968).
278. M. Fabbricotti, A. van Aerschot, J. J. Loferski, K. K. Reinhartz, A. P. von Rosenstiel, and A. P. Voskamp, *Proc. Int. Conf. X-Ray Opt. Microanal.*, **5th**, 1968 p. 447 (1969).
279. W. D. Gill, P. F. Lindquist, and R. H. Bube, *Photovoltaic Spec. Conf. Rec., 7th, 1968* p. 47, IEEE (1968).
280. W. D. Gill and R. H. Bube, *J. Appl. Phys.* **41**, 1694 (1970).
281. A. E. van Aerschot and K. K. Reinhartz, *Proc. Int. Colloq. Solar Cells*, 1970 p. 95 (1971).
282. P. F. Lindquist and R. H. Bube, *J. Appl. Phys.* **43**, 2839 (1972).
283. A. F. Forestieri, A. E. Spakowski, and H. W. Brandhorst, eds., NASA Tech. Memo NASA TMX-52579. NASA, Washington, D.C., 1968.
284. W. F. Dunn, Rep. ARL 71-0015. Clevite Corp., 1971.
285. W. D. Gill and R. H. Bube, *Proc. Int. Conf. Photocond.*, **3rd**, 1969 p. 395 (1971).

286. S. K. Kanev, A. L. Fahrenbruch, and R. H. Bube, *Appl. Phys. Lett.* **19**, 459 (1971).
287. A. L. Fahrenbruch and R. H. Bube, *Photovoltaic Spec. Conf. Rec.*, 9th, 1972 p. 118, IEEE (1973).
288. A. L. Fahrenbruch and R. H. Bube, *Photovoltaic Spec. Conf. Rec.*, 10th, 1973 p. 85, IEEE (1974).
- 288a. M. P. Prince, *J. Appl. Phys.* **26**, 534 (1955).
289. L. R. Shiozawa, G. A. Sullivan, and F. Augustine, *Photovoltaic Spec. Conf. Rec.*, 7th, 1968 p. 39, IEEE (1968).
290. H. W. Brandhorst, *Photovoltaic Spec. Conf. Rec.*, 7th, 1968 p. 33, IEEE (1968).
291. J. C. Schaefer and E. R. Hill, Rep. NASA-CR-54965. Harshaw Chem. Co., 1965.
292. K. V. Shalimova, A. F. Andrushko, V. A. Dmitriev, and L. P. Pavlov, *Kristallo-grafiya* **8**, 774 (1963); *Sov. Phys.—Crystallogr.* **8**, 618 (1964).
293. A. F. Andrushko, *Fiz. Tverd. Tela* **4**, 582 (1962); *Sov. Phys.—Solid State* **4**, 424 (1962).
294. P. Wendland, *J. Opt. Soc. Amer.* **52**, 581 (1962).
295. K. V. Shalimova, A. F. Andrushko, V. A. Dmitriev, and L. P. Pavlov, *Kristallo-grafiya* **9**, 418 (1964); *Sov. Phys.—Crystallogr.* **9**, 340 (1964).
296. L. S. Palatnik, M. N. Naboka, and V. E. Marincheva, *Izv. Akad. Nauk SSSR, Neorg. Mater.* **6**, 1526 (1970); *Inorg. Mater. (USSR)* **6**, 1344 (1971).
297. M. Bujatti, *Phys. Lett. A* **24**, 36 (1967).
298. L. L. Kazmerski, W. B. Berry, and C. W. Allen, *Photovoltaic Spec. Conf. Rec.*, 8th, 1970 p. 9, IEEE (1970).
299. L. L. Kazmerski, W. B. Berry, and C. W. Allen, *Proc. Int. Colloq. Solar Cells*, 1970 p. 141 (1971).
300. L. L. Kazmerski, W. B. Berry, and C. W. Allen, *J. Appl. Phys.* **43**, 3515 and 3521 (1972).
301. F. V. Shallcross, *Trans. AIME* **236**, 309 (1966).
302. L. S. Palatnik and M. N. Naboka, *Izv. Akad. Nauk SSSR, Neorg. Mater.* **6**, 1779 (1970); *Inorg. Mater. (USSR)* **6**, 1565 (1970).
303. L. S. Palatnik, M. N. Naboka, and O. A. Obolyaninova, *Izv. Akad. Nauk SSSR, Neorg. Mater.* **6**, 1922 (1970); *Inorg. Mater. (USSR)* **6**, 1689 (1971).
304. H. Mayer, "Physik dünner Schichten," Part II. Wiss. Verlagsges., Stuttgart, 1955.
305. D. M. Evans and H. Wilman, *Acta Crystallogr.* **5**, 731 (1952).
306. D. C. Reynolds and L. C. Greene, *J. Appl. Phys.* **29**, 559 (1958).
307. D. C. Reynolds and S. J. Czyzak, *J. Appl. Phys.* **31**, 94 (1960).
308. G. A. Rozgonyi and N. F. Foster, *J. Appl. Phys.* **38**, 5172 (1967).
309. A. Vecht, W. Grindle, and R. Mears, *J. Appl. Phys.* **36**, 2935 (1966); **37**, 3321 (1966).
310. A. Doi and T. Ogawa, *Jap. J. Appl. Phys.* **9**, 723 (1970).
311. Y. Terasaki, T. Murakami, and H. Toyoda, *Rev. Elec. Commun. Lab.* **14**, 425 (1966).
312. M. L. Conrigan and R. S. Muller, *Solid-State Electron.* **8**, 830 (1965).
313. W. Kahle and A. Berger, *Phys. Status Solidi* **14**, K201 (1966).
314. K. V. Shalimova, L. P. Pavlov, and I. A. Karetnikov, *Izv. Uch. Zarednyi, Fiz.* **9**, 132 (1966) (NASA TT F-10, 260).
315. J. Dresner and F. V. Shallcross, *J. Appl. Phys.* **34**, 2390 (1963).
316. A. Vecht and A. Apling, *Phys. Status Solidi* **3**, 1238 (1963).
317. A. J. Behringer and L. Corrsin, *J. Electrochem. Soc.* **110**, 1083 (1963).
318. K. W. Boer, A. S. Esbitt, and W. M. Kaufman, *J. Appl. Phys.* **37**, 2664 (1966).

319. K. W. Boer, J. W. Feitknecht, D. G. Kannenberg, *Phys. Status Solidi* **16**, 697 (1966).
320. E. F. Gross, B. S. Razbirin, and V. N. Safarov, *Fiz. Tverd. Tela* **2**, 2945 (1960); *Sov. Phys.—Solid State* **2**, 2617 (1960).
321. K. L. Chopra, *J. Appl. Phys.* **37**, 2249 (1966).
322. K. L. Chopra, *J. Appl. Phys.* **37**, 3405 (1966).
323. K. Heime, *Solid-State Electron.* **10**, 732 (1967).
324. R. R. Chamberlin and J. S. Skarman, 4th Quart. Rep., Contract AF33(657)7919. National Cash Register Co., Dayton, Ohio, 1963.
325. N. Pavaskar, *Jap. J. Appl. Phys.* **9**, 212 (1970).
326. L. R. Shiozawa, F. Augustine, and W. R. Cook, Jr. Final Rep., Contract F33(615)-69-C-1732. Clevite Corp., 1970.
327. W. R. Cook, Jr., L. Shiozawa, and F. Augustine, *J. Appl. Phys.* **41**, 3058 (1970).
328. P. Rahlfs, *Z. Phys. Chem.* **31**, 157 (1936).
329. M. J. Buerger and N. W. Buerger, *Amer. Mineral.* **29**, 55 (1944).
330. S. Djurle, *Acta Chem. Scand.* **12**, 1415 (1958).
331. J. Singer and P. A. Faeth, *Appl. Phys. Lett.* **11**, 130 (1967).
332. E. H. Roseboom, *Econ. Geol.* **61**, 641 (1966).
333. E. Posnjak, E. T. Allen, and H. E. Merwin, *Econ. Geol.* **10**, 491 (1915).
334. W. Jost and P. Kubaschewski, *Nachr. Akad. Wiss. Goettingen, Math.-Phys. Kl.*, **2** p. 201 (1967).
335. H. Rau, *J. Phys. Chem. Solids* **28**, 903 (1967).
336. A. E. Spakowski, A. E. Potter, and R. L. Schalla, *Proc. Photovoltaic Spec. Conf., 5th, 1965 PIC-SOL 209/6.1 Sect. C-7* (1966).
337. A. E. Spakowski, A. E. Potter, and R. L. Schalla, *NASA Tech. Memo NASA TM X-52144* (1965).
338. A. E. Potter and R. L. Schalla, *Photovoltaic Spec. Conf. Rec., 6th, 1967* p. 24 IEEE (1967).
339. A. E. Potter and R. L. Schalla, *NASA Tech. Note NASA TN D-3849* (1967).
340. A. E. van Aerschot, J. J. Capart, K. H. David, M. Fabbricotti, K. H. Heffels, J. J. Loferski, and K. K. Reinhartz, *IEEE Trans. Electron Devices* **18**, 471 (1971).
341. L. R. Shiozawa, G. A. Sullivan, F. Augustine, and J. M. Jost, 7th Quart. Progr. Rep., Contract AF33(615)-5224. Clevite Corp., 1968.
342. L. R. Shiozawa, G. A. Sullivan, and F. Augustine, 9th Quart. Progr. Rep., Contract AF33(616)-5224. Clevite Corp., 1968.
343. L. Eisenmann, *Ann. Phys. (Leipzig)* [6] **10**, 129 (1952).
344. R. H. Bube, E. L. Lind, and A. B. Dreeben, *Phys. Rev.* **128**, 532 (1962).
345. R. Marshall and S. S. Mitra, *J. Appl. Phys.* **36**, 3882 (1965).
346. G. P. Sorokin, Yu. M. Papshev, and P. T. Oush, *Fiz. Tverd. Tela* **7**, 2244 (1965); *Sov. Phys.—Solid-State* **7**, 1810 (1966).
347. S. G. Ellis, *J. Appl. Phys.* **38**, 2906 (1967).
348. V. P. Kryzhanovskii, *Opt. Spektrosk.* **24**, 149 (1968); *Opt. Spectrosc. (USSR)* **24**, 135 (1968).
349. B. Selle and J. Maege, *Phys. Status Solidi* **30**, K153 (1968).
350. N. Nakayama, *J. Phys. Soc. Jap.* **25**, 290 (1968).
351. M. Ramoin, J.-P. Sorbier, J.-F. Bretzner, and S. Martinuzzi, *C. R. Acad. Sci.* **268**, 1097 (1969).
352. F. Gustavino, H. Luquet, and J. Bougnat, *C. R. Acad. Sci.* **269**, 831 (1969).
353. L. R. Shiozawa, G. A. Sullivan, F. Augustine, and J. M. Jost, 2nd Quart. Progr. Rep., Contract AF33(615)-5224. Clevite Corp., 1968.

354. E. Hirahara, *J. Phys. Soc. Jap.* **2**, 211 (1947).
355. E. Hirahara, *Proc. Phys. Soc. Jap.* **4**, 10 and 12 (1949).
356. E. Hirahara, *J. Phys. Soc. Jap.* **6**, 422 (1951).
357. E. Hirahara, *J. Phys. Soc. Jap.* **6**, 428 (1951).
358. C. Tubandt, S. Eggert, and G. Schiebbe, *Z. Anorg. Allg. Chem.* **117**, 1 (1921).
359. A. B. Abdullaev, Z. A. Aliyarova, E. H. Zamanova, and G. A. Asadov, *Phys. Status Solidi* **26**, 65 (1968).
360. S. Martinuzzi, *Phys. Status Solidi A* **2**, K9 (1970).
361. J. Bougnat, F. Gustavino, H. Luquet, and D. Sodini, *Phys. Status Solidi A* **8**, K93 (1971).
362. B. J. Mulder, *Proc. Int. Colloq. Solar Cells, 1970* p. 131 (1971).
363. M. Neuberger, "Cuprous Sulfide and Cuprous Sulfide-Cadmium Sulfide Heterojunctions," R-69. Electron. Properties Inform. Cent., Hughes Aircraft Co., Culver City, 1970.
364. R. E. Marburger, D. C. Reynolds, L. L. Antes, and R. S. Hogan, *J. Chem. Phys.* **23**, 2448 (1955).
365. A. E. Potter, *NASA, Tech. Note NASA TN D-4333* (1967).
366. A. E. Potter, R. L. Schalla, H. W. Brandhorst, and L. Rosenblum, *Photovoltaic Spec. Conf. Rec., 7th, 1968* p. 62 IEEE (1968).
367. A. E. Spakowski, F. L. Acampora, and R. E. Hart, Jr., *NASA, Tech. Note NASA TN D-3663* (1966).
368. A. E. Spakowski, *IEEE Trans. Electron Devices* **14**, 18 (1967).
369. A. E. Spakowski and J. G. Ewashinka, *NASA Tech. Note NASA TN D-3556* (1966).
370. F. A. Shirland, A. F. Forestieri, and A. E. Spakowski, *Intersoc. Energy Conv. Eng. Conf., 1968* Vol. 1, p. 112 (1968).
371. A. F. Ratajczak, T. M. Klucher, and C. K. Swartz, *NASA, Tech. Memo NASA TM X-1884* (1969).
372. K. L. Kennerud, Rep. T2-113518-1. Boeing Corp., Seattle, 1967.
373. K. L. Kennerud, "A Summary of Work Completed in Phase I and II," Contract NAS3-6008. Boeing Corp., Seattle, 1967.
374. K. L. Kennerud, Rep. D2-121002-1, NASA CR-72507. Boeing Corp., Seattle, 1969.
375. A. G. Stanley, Tech. Note 1967-52. M.I.T. Lincoln Laboratory, Lexington, Massachusetts, 1967.
376. A. G. Stanley, *Proc. IEEE* **57**, 692 (1969).
377. A. G. Stanley, Tech. Note 1970-33. M.I.T. Lincoln Laboratory, Lexington, Massachusetts, 1970.
378. J. M. Bozek, *NASA, Tech. Memo NASA TM X 1722* (1969).
379. J. J. Smithwick, *NASA, Tech. Memo NASA TM X 1819* (1969).
380. H. W. Brandhorst, Jr., R. L. Schalla, A. E. Potter, Jr., and L. Rosenblum, *NASA, Tech. Note NASA TN D-5521* (1970).
381. H. W. Brandhorst, Jr. and D. T. Bernatowicz, *Proc. Int. Colloq. Solar Cells, 1970* p. 215 (1971).
382. R. J. Myton, L. Clark, R. W. Gale, and K. Moore, *Photovoltaic Spec. Conf. Rec., 9th, 1972* p. 133 IEEE (1973).
383. J. Bernard, J. Berry, J.-P. Buisson, and A. Paillous, *Proc. Int. Colloq. Solar Cells, 1970* p. 229 (1971).
384. S. Martinuzzi, F. Cabane-Brouty, and J.-F. Bretzner, *Photovoltaic Spec. Conf. Rec., 9th, 1972* p. 111 IEEE (1973).
385. T. TeVelde, *Photovoltaic Spec. Conf. Rec., 8th, 1970* p. 372 IEEE (1970).

386. L. R. Shiozawa, F. Augustine, and W. R. Cook, Jr., 3rd Quart. Progr. Rep., Contract F33(615)-69-C-1732. Clevite Corp., 1970.
387. D. T. Bernatowicz and H. W. Brandhorst, *Photovoltaic Spec. Conf. Rec.*, 8th, 1970 p. 24 IEEE (1970).
388. A. F. Forestieri, ed., *NASA, Tech. Memo NASA TM X-52920* (1970).
389. L. R. Scudder, M. P. Godlewski, and T. M. Klucher, *NASA, Tech. Memo NASA TM X-52668* (1969).
390. M. P. Godlewski, J. M. Bozek, and L. R. Scudder, *NASA, Tech. Memo NASA TM X-52697* (1969).
391. L. R. Shiozawa, F. Augustine, and G. A. Sullivan, 10th Quart. Progr. Rep., Contract AF33(615)-5224 Clevite Corp., (1969).
392. H. J. Mathieu and H. Rickert, *Z. Phys. Chem.* **79**, 315 (1972).
393. H. J. Mathieu, K. K. Reinhartz, and H. Rickert, *Photovoltaic Spec. Conf. Rec.*, 10th, 1973 p. 93 IEEE (1974).
394. J. G. Haynos, *Photovoltaic Spec. Conf. Rec.*, 8th, 1970 p. 184 IEEE (1970).
395. J. Lindmayer and A. G. Revesz, *Solid-State Electron.* **14**, 647 (1971).
396. G. H. Hewig and F. Pfisterer, *Photovoltaic Spec. Conf. Rec.* 9th, 1972 p. 138 IEEE (1973).
397. H. W. Brandhorst and R. E. Hart, *NASA, Tech. Note NASA TN D-2932* (1965).
398. G. J. Brucker, W. L. C. Hui, and G. T. Noel, *Proc. IEEE* **54**, 895 (1966).
399. J. J. Loferski, *Rev. Phys. Appl.* **1**, 221 (1966).
400. D. J. Curtin, *Tech. Memo. CL-23-68*. COMSAT Corp., 1968.
401. J. J. Wysocki and P. Rappaport, *J. Appl. Phys.* **31**, 571 (1960).
402. P. F. Lindquist and R. H. Bube, *Photovoltaic Spec. Conf. Rec.*, 8th, 1970 p. 1 IEEE (1970).
403. D. C. Reynolds and S. J. Czyzak, *Phys. Rev.* **96**, 1705 (1954).
404. C. A. Mead and W. G. Spitzer, *Appl. Phys. Lett.* **2**, 74 (1963).
405. W. G. Spitzer and C. A. Mead, *J. Appl. Phys.* **34**, 3061 (1963).
406. P. N. Keating, *J. Appl. Phys.* **36**, 564 (1965).
407. K. W. Boer and J. Phillips, *Photovoltaic Spec. Conf. Rec.*, 9th, 1972 p. 125 IEEE (1973).
408. F. Goos, *Ann. Phys. (Leipzig)* [5] **39**, 281 (1941).
409. J. Broser and R. Warminsky, *Z. Naturforsch. A* **5**, 62 (1950).
410. G. Nadjakov, R. Andreitchine, and M. Borissov, *C. R. Acad. Bulg. Sci.* **7**, 17 (1954); *Bulg. Akad. Nauk* **4**, 11 (1954).
411. W. Veith and G. Wlérick, *C. R. Acad. Sci.* **233**, 1097 (1951).
412. G. Wlerick, *Physica (Utrecht)* **20**, 1099 (1954).
413. S. H. Liebson, *J. Electrochem. Soc.* **101**, 359 (1954).
414. S. H. Liebson, *J. Electrochem. Soc.* **102**, 529 (1955).
415. G. Nadjakov and R. Andreitchine, *C. R. Acad. Bulg. Sci.* **7**, 13 (1954); *Izv. Bulgar. Akad. Nauk* **4**, 3 (1954).
416. G. Nadjakov, R. Andreitschin, S. Balabanov, and J. Stanislavova, *C. R. Acad. Bulg. Sci.* **10**, 277 (1957).
417. G. Nadjakov and R. Andrejtschin, *C. R. Acad. Bulg. Sci.* **13**, 19 (1960).
418. G. Nadjakov, R. Andrejtschin, S. Balabanov, and J. Stanislavova, *C. R. Acad. Bulg. Sci.* **13**, 15 (1960).
419. G. K. Zyrianov, *Zh. Tekh. Fiz.* **28**, 2657 (1958); *Sov. Phys.—Tech. Phys.* **3**, 2429 (1958).

420. J. W. MacArthur, Rep. 7848-7849-R-4, M.I.T. Servomechanisms Lab., Cambridge, Massachusetts, 1958.
421. H. Kallmann, B. Kramer, J. Shain, and G. M. Spruch, *Phys. Rev.* **117**, 1482 (1960).
422. W. Ruppel, *Helv. Phys. Acta* **34**, 790 (1961).
423. W. Ruppel, *Helv. Phys. Acta* **36**, 458 (1963).
424. A. J. Moncrieff-Yeates, U.S. Patent 3,104,188 (1963).
425. G. O. Müller, *Phys. Status Solidi* **3**, 523 (1963).
426. A. M. Goodman, *J. Appl. Phys.* **35**, 573 (1964).
427. W. Palz and W. Ruppel, *Phys. Status Solidi* **6**, K161 (1964).
428. W. Palz and W. Ruppel, *Phys. Status Solidi* **15**, 649 (1966).
429. W. Palz and W. Ruppel, *Phys. Status Solidi* **15**, 665 (1966).
430. H. Friedrich, *Phys. Status Solidi* **12**, 149 (1965).
431. M. Bujatti, *Proc. IEEE* **55**, 1634 (1967).
432. M. Bujatti, *Brit. J. Appl. Phys.* [2] **1**, 581 (1968).
433. R. Butendieck and W. Ruppel, *Proc. Int. Colloq. Solar Cells*, 1970 p. 111 (1971).
434. H. Okushi, A. Matsuda, M. Saito, M. Kikuchi, and Y. Hirai, *Solid State Commun.* **11**, 287 (1972).
435. R. J. Stirn and K. W. Boer, *Bull. Amer. Phys. Soc.* [2] **13**, 1476 (1968).
436. K. W. Boer, G. A. Dussel, and P. Voss, *Phys. Rev.* **179**, 703 (1969).
437. K. W. Boer, G. A. Dussel, and P. Voss, in "Ohmic Contacts to Semiconductors" (B. Schwartz, ed.), p. 82. Electrochem. Soc., Electron. Div., New York, 1969.
438. R. J. Stirn, K. W. Boer, G. A. Dussel, and P. Voss, *Proc. Int. Conf. Photocond.*, 3rd, 1969 p. 389 (1971).
439. R. J. Stirn, *JPL Space Program Sum.* **37-58**, No. III, 138 (1969).
440. G. A. Dussel, K. W. Boer, and R. J. Stirn, *Phys. Rev. B* **7**, 1443 (1973).
441. R. J. Stirn, K. W. Boer, and G. A. Dussel, *Phys. Rev. B* **7**, 1433 (1973).
442. K. W. Boer, G. Döhler, G. A. Dussell, and P. Voss, *Phys. Rev.* **169**, 700 (1967).
443. K. W. Boer and P. Voss, *Phys. Rev.* **171**, 899 (1968).
444. G. Nadjakov and R. Andrejtschin, *C. R. Acad. Bulg. Sci.* **13**, 135 (1960).
445. M. Bujatti, *Proc. IEEE* **53**, 397 (1965).
446. J. Bardeen, *Bell Syst. Tech. J.* **29**, 469 (1950).
447. W. Schaaffs and H. Woelk, *Z. Angew. Phys.* **10**, 456 (1958).
448. W. van Roosbroeck, *Phys. Rev.* **101**, 1716 (1956); H. Dember, *Z. Phys.* **32**, 554 and 856 (1931); **33**, 207 (1932).
449. R. Williams, *J. Phys. Chem. Solids* **23**, 1057 (1962).
450. K. J. Haas, D. C. Fox, and M. J. Katz, *J. Phys. Chem. Solids* **26**, 1779 (1965).
451. W. Ludwig, *Phys. Status Solidi* **3**, 1738 (1963).
452. A. Many and A. Katzir, *Surface Sci.* **6**, 279 (1967).
453. J. Shappir and A. Many, *Surface Sci.* **14**, 169 (1969).
454. A. Many, J. Shappir, and U. Shaked, in "Molecular Processes in Solid Surfaces" (E. Drauglis *et al.*, eds.), p. 199. McGraw-Hill, New York, 1969.
455. A. V. Pamfilov, Ya. S. Mazurkevich, and S. Yu. Mukhlya, *Russ. J. Phys. Chem.* **44**, 958 (1970).
456. F. Steinrisser and R. E. Hetrick, *Surface Sci.* **28**, 607 (1971).
457. F. Steinrisser and R. E. Hetrick, *Rev. Sci. Instrum.* **42**, 304 (1971).
458. C. L. Balestra and H. C. Gatos, *Surface Sci.* **28**, 563 (1971).
459. C. L. Balestra, J. Lagowski, and H. C. Gatos, *Surface Sci.* **26**, 317 (1971).
460. J. Lagowski, C. L. Balestra, and H. C. Gatos, *Surface Sci.* **27**, 547 (1971).

461. J. Lagowski, C. L. Balestra, and H. C. Gatos, *Surface Sci.* **29**, 203 (1972).
462. J. Lagowski, C. L. Balestra, and H. C. Gatos, *Surface Sci.* **29**, 213 (1972).—
463. G. Nadzhakov, and S. Balabanov, *Fiz. Tverd. Tela* **7**, 1193 (1965); *Sov. Phys.—Solid-State* **7**, 957 (1965).
464. G. Nadzhakov, S. Balabanov, E. Nikolova, and S. Simov, *Proc. Int. Conf. Phys. Semiconduct.*, 1968 p. 510 (1969).
465. St. Kynev, R. Pirinchieva, and K. Marinova, *Fiz. Tverd. Tela* **5**, 291 (1963); *Sov. Phys.—Solid State* **5**, 212 (1963).
466. A. Kunioka and Y. Sakai, *Solid State Electron.* **8**, 961 (1965).
467. B. Kandilarov and R. Andreytchin, *Phys. Status Solidi* **8**, 897 (1965).
468. A. A. Pavlenko, E. A. Muzalevskii, and I. D. Konozenko, *Izv. Akad. Nauk SSSR, Neorg. Mater.* **3**, 1139 (1967); *Inorg. Mater. (USSR)* **3**, 1007 (1967).
469. D. Bonnet and H. Rabenhorst, *Proc. Int. Colloq. Solar Cells*, 1970 p. 155 (1971).
470. D. Bonnet and H. Rabenhorst, *Photovoltaic Spec. Conf. Rec.*, 9th, 1972 p. 129 IEEE (1973).
471. H. Okimura, M. Kawakami, and Y. Sakai, *Jap. J. Appl. Phys.* **6**, 908 (1967).
472. H. Okimura and R. Kondo, *Jap. J. Appl. Phys.* **9**, 274 (1970).
473. R. Kondo, H. Okimura, and Y. Sakai, *Jap. J. Appl. Phys.* **10**, 1547 (1971).
474. E. I. Adirovich, Yu. M. Yuabov, and G. R. Yagudaev, *Dokl. Akad. Nauk SSSR* **208**, 325 (1973); *Sov. Phys.—Dokl.* **18**, 70 (1973).
475. A. Yoshikawa, R. Kondo, and Y. Sakai, *Jap. J. Appl. Phys.* **12**, 1096 (1973).
476. S. L. Hou and J. A. Marley, *App. Phys. Lett.* **16**, 467 (1970).
477. Y. Shiraki, T. Shimada, and K. F. Komatsubara, *J. Appl. Phys.* **43**, 710 (1972).
478. P. Würfel and W. Ruppel, *Proc. Int. Colloq. Solar Cells*, 1970 p. 1165 (1971).
479. R. C. Nelson, *J. Opt. Soc. Amer.* **46**, 13 (1956).
480. R. Audubert and C. Stora, *C. R. Acad. Sci.* **194**, 1124 (1932).
481. R. Williams, *J. Chem. Phys.* **32**, 1505 (1960).
482. B. Tell and W. M. Gibson, *J. Appl. Phys.* **40**, 5320 (1969).
483. H. W. Brandhorst, F. L. Acampora, and A. E. Potter, *NASA, Tech. Note NASA TN D-3417* (1966).
484. H. W. Brandhorst, F. L. Acampora, and A. E. Potter, *J. Appl. Phys.* **39**, 6071 (1968).
485. E. Igras, W. Plesiewicz, and B. Orlowski, *Acta Phys. Pol.* **31**, 581 (1967).
486. D. C. Reynolds, presented at AGARD Conf. Liege (1967).
487. F. A. Shirland, presented at 23rd Annu. Conf. Instrum. Soc. Amer., 1968.
488. F. W. Sarles, Jr., A. G. Stanley, and C. Burrows, *Photovoltaic Spec. Conf. Rec.*, 7th, 1968 p. 262 IEEE (1968).
489. F. W. Sarles, Jr. and A. G. Stanley, *Photovoltaic Spec. Conf. Rec.*, 8th, 1970 p. 214 IEEE (1970).
490. F. W. Sarles, Jr. and A. G. Stanley, *Photovoltaic Spec. Conf. Rec.*, 9th, 1972 p. 331, IEEE (1973).
491. K. W. Boer, *Photovoltaic Spec. Conf. Rec.*, 9th, 1972 p. 351 IEEE (1973).
492. K. W. Boer, *J. Environ. Sci.* **17**, 8 (1974).